BEILSTEIN JOURNAL OF ORGANIC CHEMISTRY

Reactive intermediates part I: radicals

Edited by Tehshik P. Yoon

Imprint

Beilstein Journal of Organic Chemistry
www.bjoc.org
ISSN 1860-5397
Email: journals-support@beilstein-institut.de

The *Beilstein Journal of Organic Chemistry* is published by the Beilstein-Institut zur Förderung der Chemischen Wissenschaften.

Beilstein-Institut zur Förderung der Chemischen Wissenschaften
Trakehner Straße 7–9
60487 Frankfurt am Main
Germany
www.beilstein-institut.de

BEILSTEIN JOURNAL OF ORGANIC CHEMISTRY

Photocatalyic Appel reaction enabled by copper-based complexes in continuous flow

Clémentine Minozzi, Jean-Christophe Grenier-Petel, Shawn Parisien-Collette and Shawn K. Collins*

Letter

Open Access

Address:
Department of Chemistry and Centre for Green Chemistry and Catalysis, Université de Montréal, CP 6128 Station Downtown, Montréal, Québec, H3C 3J7, Canada

Email:
Shawn K. Collins* - shawn.collins@umontreal.ca

* Corresponding author

Keywords:
Appel; continuous flow; copper; halides; photocatalysis

Beilstein J. Org. Chem. **2018,** *14,* 2730–2736.
doi:10.3762/bjoc.14.251

Received: 09 July 2018
Accepted: 12 October 2018
Published: 30 October 2018

This article is part of the thematic issue "Reactive intermediates part I: radicals".

Guest Editor: T. P. Yoon

Abstract

A copper-based photocatalyst, Cu(tmp)(BINAP)BF_4, was found to be active in a photoredox Appel-type conversion of alcohols to bromides. The catalyst was identified from a screening of 50 complexes and promoted the transformation of primary and secondary alcohols to their corresponding bromides and carboxylic acids to their anhydrides. The protocol was also amendable and optimized under continuous flow conditions.

Introduction

Synthetic photochemistry and photocatalysis continues to influence molecular synthesis [1-4]. In exploring photochemical reactivity manifolds, there exists the potential to discover new methods to construct important molecular fragments, as well as revamp traditional chemical transformations. One such process is the Appel reaction [5], which employs PPh_3 and an electrophilic halogen source to promote the formation of an organic halide from the corresponding alcohol (Figure 1) [6,7]. The Appel reaction is representative of a host of transformations that require stoichiometric reagents to effect a functional group change of an alcohol. In 2011, Stephenson and co-workers reported that photocatalysis could be used to promote the alcohol→halide conversion using low catalyst loadings of a ruthenium-based catalyst ($Ru(bpy)_3Cl_2$, 1 mol %) in the absence of PPh_3 as a reductant (Figure 1) [8]. The method possesses numerous advantages (wide functional group tolerance, no formation of oxidized phosphine byproducts [9-14], mild reaction conditions and visible-light irradiation), which should be easily embraced by the synthetic community. To further develop the photochemical alcohol→halide transformation, the use of alternative photocatalysts based upon more abundant metals was envisioned [15-18]. Specifically, our group has demon-

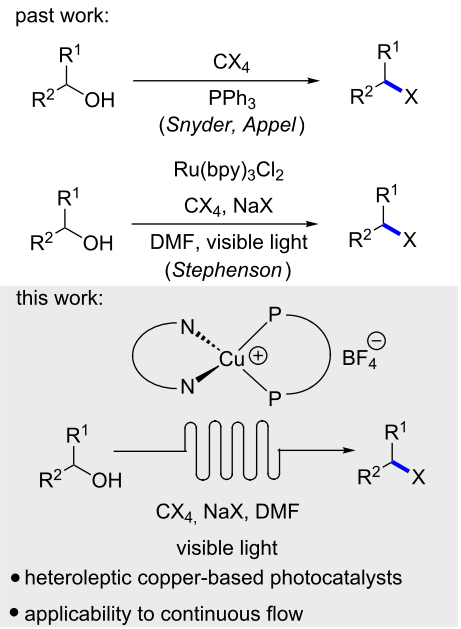

Figure 1: Alcohol→bromide functional group transformations.

strated that heteroleptic Cu(I) complexes [19-21] have significant potential as photocatalysts that can promote a variety of mechanistically distinct photochemical transformations including single electron transfer (SET), energy transfer (ET), and proton-coupled electron transfer (PCET) reactions [22-26]. Herein, the evaluation of Cu(I)-complexes for photocatalytic Appel reactions and demonstration in continuous flow is described.

Results and Discussion

The first step in identifying a heteroleptic diamine/bisphosphine Cu(I)-based photocatalyst for the conversion of an alcohol to bromide involved screening a wide variety of structurally varied complexes. Our group has previously demonstrated that the nature of each ligand influences the physical and photophysical properties as well as catalytic activity of the resulting catalyst (Figure 2) [27].

A library of 50 different catalysts was evaluated in the conversion of alcohol **1** to bromide **2** (Figure 2 and Figure 3). Several homoleptic complexes were not evaluated due to problematic

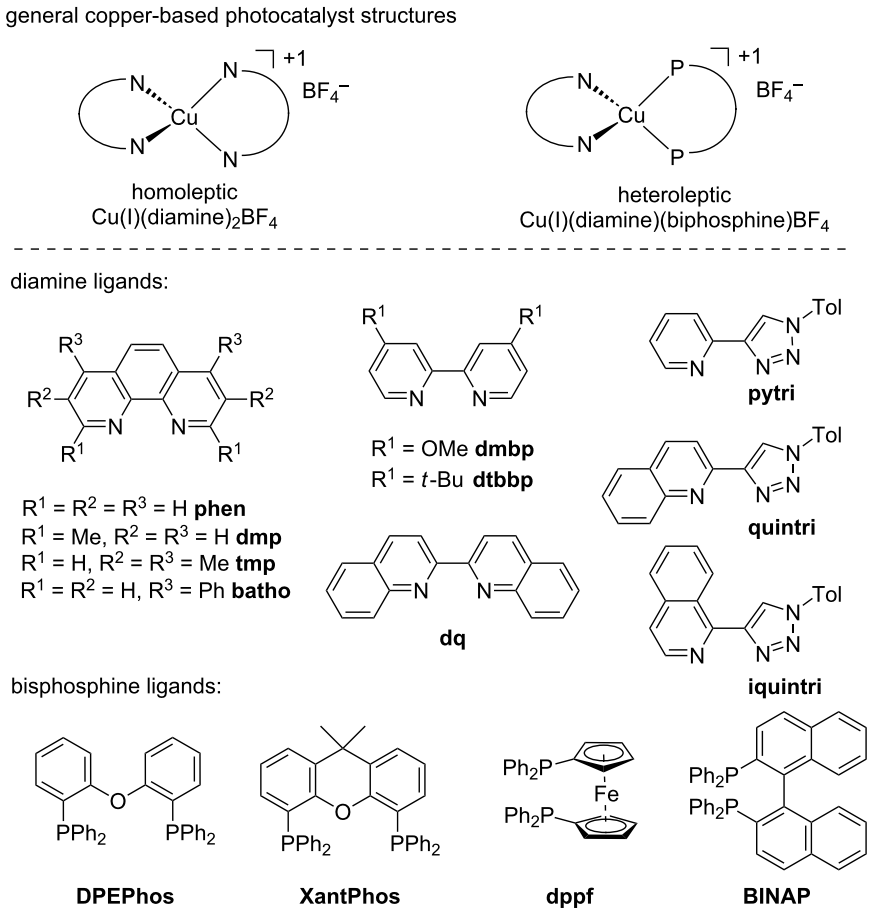

Figure 2: Ligands used in the library generation of heteroleptic copper(I)-based complexes for photocatalysis.

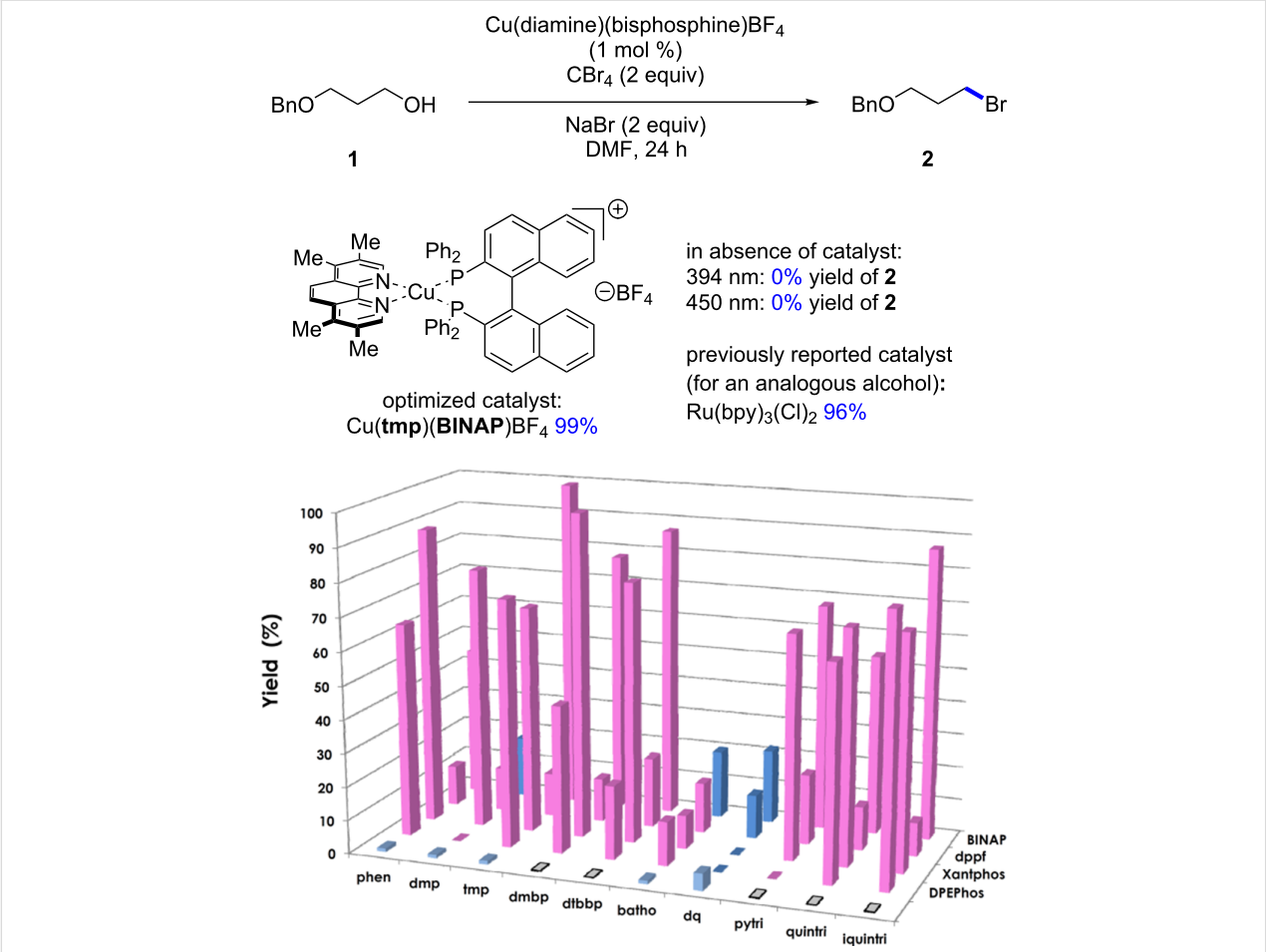

Figure 3: Evaluation of the library of copper-based complexes in photocatalytic alcohol→bromide conversion. Reactions irradiated with 394 nm light (pink) or 450 nm (blue). Front entries without an indicated phosphine ligand pertain to homoleptic Cu(diamine)$_2$BF$_4$ complexes and are colored in lighter blue. Entries without a color indicate reactions which could not be performed due to solubility or overoxidation of the complex.

oxidation or low solubility. Reactions were irradiated at either 394 nm (purple LEDs) or 450 nm (blue LEDs), depending on the UV–vis absorption characteristics of the photocatalysts [28]. Stephenson and co-workers had previously reported that a primary alcohol structurally similar to **1** underwent conversion to the corresponding bromide in 96% yield upon irradiation in the presence of Ru(bpy)$_3$Cl$_2$ (1 mol %). The screening for a suitable copper-based catalyst was performed under identical reaction conditions whereby the Ru-based photocatalyst was substituted for the Cu-based complex. Control reactions performed in the absence of light or in the absence of catalyst at either 394 or 450 nm revealed no conversion to the bromide. From the results, none of the homoleptic complexes promoted the alcohol-to-halide conversion (**1**→**2**, see the light blue entries in the front row of Figure 3). While many of the heteroleptic complexes promoted the reaction, some trends were apparent. In general, amongst the phosphines the dppf-based complexes were poor catalysts, while when considering the diamine ligands the dq and bathophenthroline catalysts provided poor to modest yields. Also, BINAP and Xantphos-based catalysts tended to afford higher yields of **2**, while amongst the diamines, the triazole-based complexes were almost all efficient at providing **2** (54–87% yield, not including dppf-based complexes). Interestingly, the best catalyst for the transformation (Cu(tmp)(BINAP)BF$_4$, 99% of **2**) was a poor catalyst for a previously reported photoredox reaction [27]. It should be noted that Cu(tmp)(BINAP)$^+$ possesses an excited state reduction potential of −1.93 V vs. SCE, much greater than that of Ru(bpy)$_3^{+2}$ (−0.81 V vs SCE), albeit the copper complex has a much shorter excited state lifetime (≈4 ns vs ≈1100 ns for Ru(bpy)$_3^{+2}$). The excited state reduction potential should match favorably with CBr$_4$ ($E_{½}$ = 0.30 V vs SCE) in DMF [29]. Note that many of the corresponding homoleptic copper-based sensitizers were ineffective at promoting the Appel-type reaction.

With conditions in hand for the formation of the bromides, different alcohols were converted to their corresponding halides

(Table 1). As shown previously, a benzyl-protected alcohol **1** could be transformed to the corresponding bromide **2** in 99% yield, respectively (Table 1, entry 1). The corresponding bromide of citronellol (**4**) was also formed in high yield (91%, Table 1, entry 2). A long chain methyl ester **5** was also tolerated under the reaction conditions (98% of the bromide, Table 1, entry 3). The corresponding dibromide could be formed from 1,9-nonadiol (**6**) in quantitative yield (99%, Table 1, entry 4). A sulfur-containing alcohol **7** was smoothly converted to its bromide in 99% yield (Table 1, entry 5). An allylic alcohol **8** having a *cis*-olefin underwent alcohol-to-halide conversion in 89% yield and was isolated as a 1:1 mixture of *cis* and *trans* isomers (Table 1, entry 6). Finally, a racemic secondary alcohol **9** was easily transformed to the corresponding racemic bromide (99%, Table 1, entry 7).

Following the optimization of the catalyst structure and exploration of scope, the batch reaction conditions were then transferred to continuous flow (Table 2). Initially, an experimental set-up using a previously reported reactor for purple LEDs was selected for the reaction [30,31]. Following injection of the reaction mixture with a target residence time of 60 min, only traces of the desired bromide **2** were observed. Extending the residence time to 120 or 240 min increased the yield to 32–53%, but significant quantities of the starting alcohol **1** and the corresponding formate ester **3** were observed. Using tetra-*n*-butylammonium bromide (TBAB) as the halide source did not improve the yield, but resulted in larger amount of the formy-

Table 1: Photocatalytic conversion of alcohols to bromides in batch.

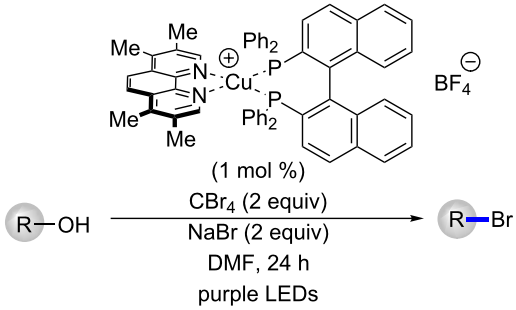

entry	alcohol		yield (%)[a]
1	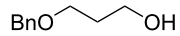	**1**	99
2	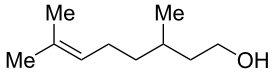	**4**	91
3	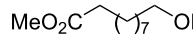	**5**	98
4	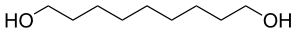	**6**	99
5	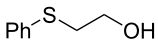	**7**	99
6	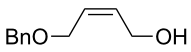	**8**	89[b]
7	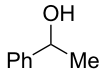	**9**	99

[a]Yield determined by isolation via chromatography. [b]Isolated as a 1:1 mixture of *cis* and *trans* isomers.

Table 2: Photocatalytic conversion of alcohol **1** to bromide **2** in continuous flow.

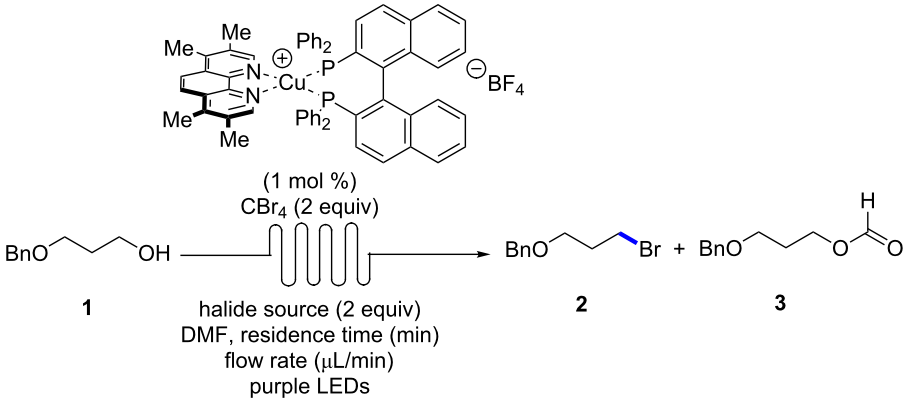

entry	halide source	T_{res} (min)	flow rate (μL/min)	recovered **1** (%)[a]	yield **2** (%)[a]	yield **3** (%)[a]
1	NaBr	60	216	89	<5	<5
2	NaBr	120	110	47	53	–
3	NaBr	240	54.2	45	32	23
4	TBAB	240	110	–	21	63
5	NaBr	240	110	–	91(83)[b]	–

[a]Yield determined by analysis of ^{1}H NMR. [b]Yield determined by isolation via chromatography.

lated product **3** (Table 2, entry 4). A possible explanation for the increased yield of **3** when using TBAB could be due to slower displacement of leaving group by the "bulkier" source of bromide. In attempting to extend the residence time, the flow rate of the reaction mixture was decreased. Knowing that faster flow rates can improve mixing and reaction rates [32], an additional reactor was placed in line and the residence time of 240 min was repeated but with an increased flow rate (110 μL/min, Figure 4 and Table 2 entry 5). Gratifyingly, the desired bromide **2** was isolated in 91% yield.

With optimized flow conditions in hand for the formation of bromides in continuous flow, five different alcohols were converted to their corresponding halides (Table 3). The benzyl-protected alcohol **1** could be transformed to the bromide in 83% yield (Table 3, entry 1), as was citronellol (**4**, 83% yield, Table 3, entry 2). A methyl ester **5**, allylic alcohol **8** and racemic secondary alcohol **9** could all undergo conversion to their corresponding bromides in 240 min using the continuous flow protocol (Table 3, entries 3 to 5).

The continuous flow protocol was also applicable to the synthesis of anhydrides, which has also been previously reported by Stephenson and co-workers [33]. The carboxylic acid **10** was submitted to a flow protocol using the optimized Cu(tmp)(BINAP)BF_4 catalyst, CBr_4 (1 equiv) and 2,6-lutidine as base with a residence time of 20 min (Scheme 1). The anhydride derived from *p*-methoxybenzoic acid was isolated in 90% yield.

Table 3: Photocatalytic conversion of alcohols to bromides in continuous flow.

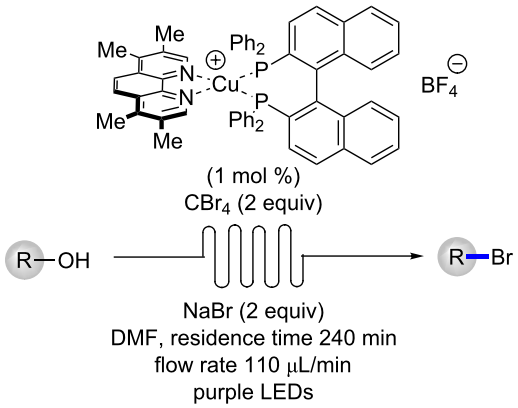

entry	alcohol		yield (%)[a]
1	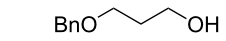	**1**	83
2	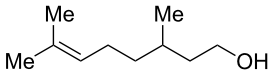	**4**	83
3	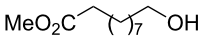	**5**	85
4		**8**	86
5	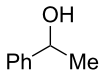	**9**	86

[a]Yield determined by isolation via chromatography.

Figure 4: Experimental set-up for the photocatalytic conversion of alcohols to bromides. PFA tubing is wrapped around purple LEDs (394 nm) and fans are placed underneath reactors to maintain cooling.

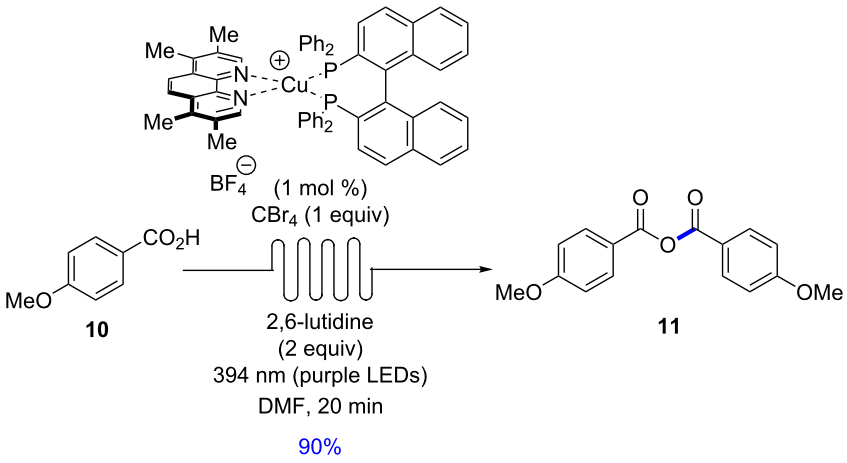

Scheme 1: Copper-based photocatalysis for photocatalytic synthesis of an anhydride.

Conclusion

In summary, a heteroleptic copper-based photocatalyst Cu(tmp)(BINAP)BF_4 was discovered for the photochemical Appel-type conversion of alcohols to bromides, as well as carboxylic acids to their anhydrides. The protocol was highly efficient and could be adapted to continuous flow using purple LED reactors. The batch and continuous flow processes were all made possible due to the ability to screen highly modular copper-based complexes for photocatalysis.

Supporting Information

Supporting Information File 1

Experimental details and compound characterization.
[https://www.beilstein-journals.org/bjoc/content/supplementary/1860-5397-14-251-S1.pdf]

Acknowledgements

The authors acknowledge the Natural Sciences and Engineering Research Council of Canada (NSERC), the NSERC CREATE program in Continuous Flow Science, the Canadian Foundation for Innovation for financial support for continuous flow infrastructure and the Centre in Green Chemistry and Catalysis (CGCC) for funding. Ms. Vanessa Kairouz is thanked for assistance with the continuous flow infrastructure.

ORCID® iDs

Shawn K. Collins - https://orcid.org/0000-0001-9206-5538

References

1. Stephenson, C. R. J.; Yoon, T. P.; MacMillan, D. W. C., Eds. *Visible Light Photocatalysis in Organic Chemistry;* Wiley-VCH: Hoboken, New Jersey, 2018.
2. Albini, A.; Fagnoni, M., Eds. *Handbook of Synthetic Photochemistry;* Wiley-VCH: Germany, 2010.
3. Rackl, D.; Kreitmeier, P.; Reiser, O. *Green Chem.* **2016,** *18,* 214–219. doi:10.1039/C5GC01792K
4. Lima, C. G. S.; de M. Lima, T.; Duarte, M.; Jurberg, I. D.; Paixão, M. W. *ACS Catal.* **2016,** *6,* 1389–1407. doi:10.1021/acscatal.5b02386
5. Appel, R. *Angew. Chem., Int. Ed. Engl.* **1975,** *14,* 801–811. doi:10.1002/anie.197508011
6. Weiss, R. G.; Snyder, E. I. *Chem. Commun.* **1968,** 1358–1359. doi:10.1039/C19680001358
7. Weiss, R. G.; Snyder, E. I. *J. Org. Chem.* **1971,** *36,* 403–406. doi:10.1021/jo00802a009
8. Dai, C.; Narayanam, J. M. R.; Stephenson, C. R. J. *Nat. Chem.* **2011,** *3,* 140–145. doi:10.1038/nchem.949
9. Larock, R. C. *Comprehensive Organic Transformations,* 2nd ed.; John Wiley & Sons, 1999; p 689.
10. Fujisawa, T.; Iida, S.; Sato, T. *Chem. Lett.* **1984,** *13,* 1173–1174. doi:10.1246/cl.1984.1173
11. Mukaiyama, T.; Shoda, S.-i.; Watanabe, Y. *Chem. Lett.* **1977,** *6,* 383–386. doi:10.1246/cl.1977.383
12. Benazza, T.; Uzan, R.; Beaupère, D.; Demailly, G. *Tetrahedron Lett.* **1992,** *33,* 4901–4904. doi:10.1016/S0040-4039(00)61228-5
13. Benazza, T.; Uzan, R.; Beaupère, D.; Demailly, G. *Tetrahedron Lett.* **1992,** *33,* 3129–3132. doi:10.1016/S0040-4039(00)79831-5
14. Kelly, B. D.; Lambert, T. H. *J. Am. Chem. Soc.* **2009,** *131,* 13930–13931. doi:10.1021/ja906520p
15. Zhao, Y.; Antonietti, M. *ChemPhotoChem* **2018,** *2,* 720–724. doi:10.1002/cptc.201800084
See for an alternative route to convert alcohols to iodides in the absence of catalyst.
16. Reiser, O.; Kachkovskyi, G.; Kais, V.; Kohls, P.; Paria, S.; Pirtsch, M.; Rackl, D.; Seo, H. *Chem. Photocatal.* **2013,** 139–150. doi:10.1515/9783110269246.139
17. Higgins, R. F.; Fatur, S. M.; Shepard, S. G.; Stevenson, S. M.; Boston, D. J.; Ferreira, E. M.; Damrauer, N. H.; Rappé, A. K.; Shores, M. P. *J. Am. Chem. Soc.* **2016,** *138,* 5451–5464. doi:10.1021/jacs.6b02723
18. Ruhl, K. E.; Rovis, T. *J. Am. Chem. Soc.* **2016,** *138,* 15527–15530. doi:10.1021/jacs.6b08792

19. Hernandez-Perez, A. C.; Collins, S. K. *Acc. Chem. Res.* **2016,** *49,* 1557–1565. doi:10.1021/acs.accounts.6b00250
20. Hernandez-Perez, A. C.; Collins, S. K. *Angew. Chem., Int. Ed.* **2013,** *52,* 12696–12700. doi:10.1002/anie.201306920
21. Knorn, M.; Rawner, T.; Czerwieniec, R.; Reiser, O. *ACS Catal.* **2015,** *5,* 5186–5193. doi:10.1021/acscatal.5b01071
22. Beatty, J. W.; Stephenson, C. R. J. *Acc. Chem. Res.* **2015,** *48,* 1474–1484. doi:10.1021/acs.accounts.5b00068
23. Prier, C. K.; Rankic, D. A.; MacMillan, D. W. C. *Chem. Rev.* **2013,** *113,* 5322–5363. doi:10.1021/cr300503r
24. Shaw, M. H.; Twilton, J.; MacMillan, D. W. C. *J. Org. Chem.* **2016,** *81,* 6898–6926. doi:10.1021/acs.joc.6b01449
25. Arias-Rotondo, D. M.; McCusker, J. K. *Chem. Soc. Rev.* **2016,** *45,* 5803–5820. doi:10.1039/C6CS00526H
See for energy transfer.
26. Gentry, E. C.; Knowles, R. R. *Acc. Chem. Res.* **2016,** *49,* 1546–1556. doi:10.1021/acs.accounts.6b00272
See for proton-coupled electron transfer.
27. Minozzi, C.; Caron, A.; Grenier-Petel, J.-C.; Santandrea, J.; Collins, S. K. *Angew. Chem., Int. Ed.* **2018,** *57,* 5477–5481. doi:10.1002/anie.201800144
28. See Supporting Information File 1 for tabular data on reaction yields.
29. Fukui, K.; Morokuma, K.; Kato, H.; Yonezawa, T. *Bull. Chem. Soc. Jpn.* **1963,** *36,* 217–222. doi:10.1246/bcsj.36.217
30. Parisien-Collette, S.; Cruché, C.; Abel-Snape, X.; Collins, S. K. *Green Chem.* **2017,** *19,* 4798–4803. doi:10.1039/C7GC02261A
31. Parisien-Collette, S.; Collins, S. K. *ChemPhotoChem* **2018,** *2,* 855–859. doi:10.1002/cptc.201800096
32. Cambié, D.; Bottecchia, C.; Straathof, N. J. W.; Hessel, V.; Noël, T. *Chem. Rev.* **2016,** *116,* 10276–10341. doi:10.1021/acs.chemrev.5b00707
33. Konieczynska, M. D.; Dai, C.; Stephenson, C. R. J. *Org. Biomol. Chem.* **2012,** *10,* 4509–4511. doi:10.1039/c2ob25463h

License and Terms

BEILSTEIN JOURNAL OF ORGANIC CHEMISTRY

Copper(I)-catalyzed tandem reaction: synthesis of 1,4-disubstituted 1,2,3-triazoles from alkyl diacyl peroxides, azidotrimethylsilane, and alkynes

Muhammad Israr[1,2], Changqing Ye[1,2], Munira Taj Muhammad[1], Yajun Li[1] and Hongli Bao[*1,2]

Full Research Paper

Open Access

Address:
[1]Key Laboratory of Coal to Ethylene Glycol and Its Related Technology, State Key Laboratory of Structural Chemistry, Fujian Institute of Research on the Structure of Matter, Center for Excellence in Molecular Synthesis, Chinese Academy of Sciences, 155 Yangqiao Road West, Fuzhou, Fujian 350002, P. R. China and [2]University of Chinese academy of Science (UCAS), Beijing 100190, P. R. China

Email:
Hongli Bao[*] - hlbao@fjirsm.ac.cn

* Corresponding author

Keywords:
alkyl diacyl peroxides; azidotrimethylsilane; click reaction; copper catalysis; radical; 1,2,3-triazoles

Beilstein J. Org. Chem. **2018,** *14,* 2916–2922.
doi:10.3762/bjoc.14.270

Received: 01 September 2018
Accepted: 07 November 2018
Published: 23 November 2018

This article is part of the thematic issue "Reactive intermediates part I: radicals".

Guest Editor: T. P. Yoon

Abstract

A copper-catalyzed azide–alkyne cycloaddition (CuAAC) reaction for the synthesis of 1,4-disubstituted 1,2,3-triazoles from alkyl diacyl peroxides, azidotrimethylsilane, and terminal alkynes is reported. The alkyl carboxylic acids is for the first time being used as the alkyl azide precursors in the form of alkyl diacyl peroxides. This method avoids the necessity to handle organic azides, as they are generated in situ, making this protocol operationally simple. The Cu(I) catalyst not only participates in the alkyl diacyl peroxides decomposition to afford alkyl azides but also catalyzes the subsequent CuAAC reaction to produce the 1,2,3-triazoles.

Introduction

The “click chemistry”, coined by K. B. Sharpless in 2001 [1], is a powerful chemical transformation that has rapidly orthogonalized traditional disciplinary boundaries. With the discovery of “click chemistry”, new fields have been opened for the research and synthesis of functionalized compounds that have applications in medicinal chemistry, drug discovery, materials chemistry, and as well as in bioconjugates [2-12].

The copper-catalyzed azide–alkyne cycloaddition (CuAAC) reaction [13-21], derived from the Huisgen’s 1,3-dipolar cycloaddition of azides and alkynes [22], has conceivably emerged as the premier example of click chemistry. Generally, organic azides are used as the azido source in most of the CuAAC reactions (Scheme 1a) [23]. However, the organic azides with low molecular weight are considered to be unstable moieties that

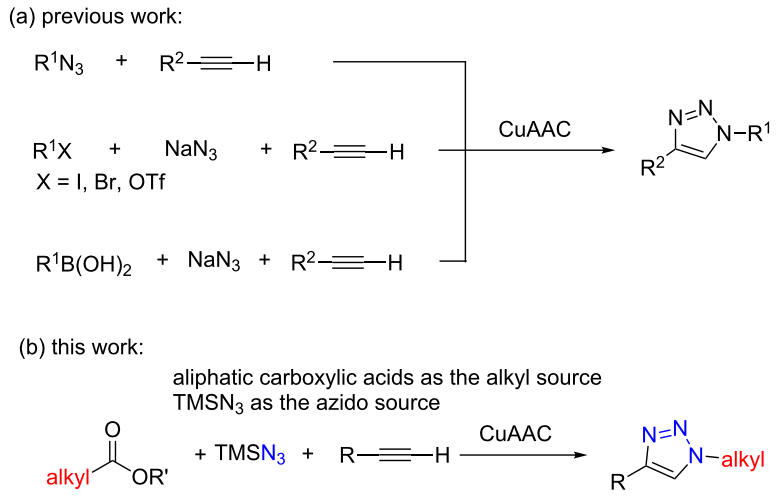

Scheme 1: General methods for the synthesis of triazoles.

can decompose spontaneously, with which the reactions are difficult or dangerous to handle [16]. Thus, a one-pot two-step process for the in situ generation of organic azides is highly required. A frequently used method to in situ generate organic azides is the azidation of organic halides, such as aliphatic halides, vinyl halides, or aromatic halides with sodium azide [24-27]. Organic triflates [28] and organic boronic acids [29-31] can also be used as alternative precursors for organic azides, when reacted with sodium azide.

However, sodium azide is a highly toxic compound and has the potential to explode. Azidotrimethylsilane ($TMSN_3$) has been considered as a safer azide source, which actually has been successfully used in the CuAAC reaction directly [32-35], but rarely been used as an azido precursor to enrich the functionality of organic azide source. Moreover, as one of the most commonly appearing compounds in nature, carboxylic acids have rarely been directly used as the organic azide precursors for CuAAC reactions, considering the frequent involvement of organic halides. Thus, new methods with non or less toxic reagents and enriched organic azide sources for CuAAC reaction are still highly required.

Herein, we report a novel CuAAC reaction, using aliphatic carboxylic acids as the alkyl source [36], and $TMSN_3$ as the azide source (Scheme 1b). Because $TMSN_3$ can react with alkynes to form the CuAAC reaction product [32-35], there is one significant challenge of this method that need to be emphasized: how to control the reaction to generate the alkyl azides from aliphatic carboxylic acids and $TMSN_3$, before $TMSN_3$ directly reacting with alkynes.

Results and Discussion

Based on our unpublished work, we found that alkyl azide has always appeared as a side product when the reaction involved $TMSN_3$ and alkyl diacyl peroxide, easily available compounds derived from aliphatic carboxylic acids. With this information in mind, initially, we started our investigation with phenylacetylene (**1a**), commercially available lauroyl peroxide (**2a**), and $TMSN_3$ (Table 1). In a preliminary experiment, the reaction of **1a** with **2a** in the presence of 10 mol % of CuCl in THF at 50 °C afforded 1,4-disubstituted 1,2,3-triazole **3a** in 65% isolated yield (Table 1, entry 1). Surprisingly, under these conditions no CuAAC product between $TMSN_3$ and phenylacetylene was detected. This result encouraged us to further exploit the optimization of the reaction conditions. Afterwards, the effect of the solvent was also investigated (Table 1, entries 2−8). Dichloromethane could afford the best result and the yield of the desired product **3a** could be as high as 97% (Table 1, entry 2). Other metal salts of copper, such as $Cu(OAc)_2$, CuI, and CuBr were then examined and they showed lower catalytic efficiencies than that of CuCl (Table 1, entries 9−11). Moreover, a reduced amount of the catalyst loading leads to lower yields of product **3a** (Table 1, entries 12–14).

With the optimized reaction conditions in hand, the scope of the terminal alkynes was screened and the results are depicted in Scheme 2. First, the reactivity of various substituted terminal arylalkynes was examined. Only 1,4-regioisomeric products were formed with good to excellent yields. Phenylacetylene with an electron-withdrawing bromo-, chloro-, or fluoro substituent afforded the corresponding products **3h**–**n** in up to 92% yield, while phenylacetylenes with electron-donating

Table 1: Optimization of the reaction conditions[a].

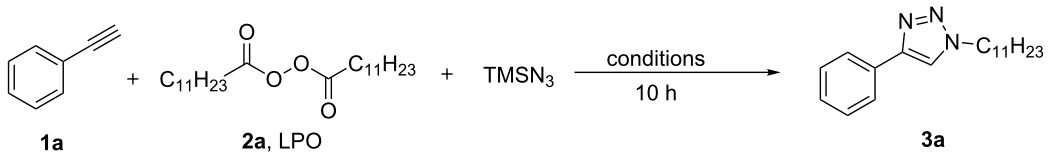

1a **2a**, LPO **3a**

entry	catalyst (mol %)	solvent	yield (%)[b]
1	CuCl (10)	THF	(65)[c]
2	CuCl (10)	CH_2Cl_2	96 (97)[c]
3	CuCl (10)	EtOH	53
4	CuCl (10)	DMF	13
5	CuCl (10)	MeOH	7
6	CuCl (10)	1,4-dioxane	trace
7	CuCl (10)	MeCN	trace
8	CuCl (10)	acetone	trace
9	CuI (10)	CH_2Cl_2	52
10	CuBr (10)	CH_2Cl_2	48
11	$Cu(OAc)_2$ (10)	CH_2Cl_2	64
12	CuCl (7.5)	CH_2Cl_2	84
13	CuCl (5)	CH_2Cl_2	70
14	CuCl (2)	CH_2Cl_2	54

[a]Reaction conditions: **1a** (0.5 mmol), **2a** (0.75 mmol), $TMSN_3$ (0.75 mmol), catalyst (mol %), solvent (2 mL), 50 °C, 10 h. [b]Yield was determined by ^1H NMR analysis. [c]Isolated yield in parentheses.

groups gave the corresponding products **3b**–**g** and **3o**–**q** in up to 86% yield. Instead of a six-membered ring, five-membered heteroaromatics (ethynylthiophenes) have also been used, and afforded the desired products **3s** and **3t** in up to 76% yield. Terminal aliphatic alkynes were then examined and it was found that they could smoothly deliver the corresponding 1,2,3-triazoles **3u**–**z** with high yields.

Furthermore, the scope of the alkyl diacyl peroxides was then studied (Scheme 3). The alkyl diacyl peroxides **2** were synthesized from the corresponding aliphatic carboxylic acids in a single step by DCC-mediated dehydrative condensation with hydrogen peroxide, and were used directly after simple filtration without further treatment; see Supporting Information File 1 for details [37]. The alkyl diacyl peroxides with long-chain alkyl groups and methyl-substituted long-chain alkyl groups afforded the corresponding 1,4-disubstituted 1,2,3-triazoles with good to excellent yields (**3aa**, **3bb**, **3dd**, **3ff**, **3hh**, **3ii**, and **3ll**). Remarkably, the chlorodiacyl peroxide also tolerated the reaction conditions to afford chloro-substituted triazole **3ee** with good yield. Moreover, alkyl diacyl peroxides bearing a phenyl group, cyclopentyl group, or a cyclohexyl group also afforded good yields (**3cc**, **3mm**, and **3nn**). Significantly, diacyl peroxides with cyclic secondary alkanyl and alkenyl groups can also gave the corresponding 1,2,3-triazoles **3gg**, **3jj**, and **3kk**. Tertiary alkyl diacyl peroxides are relatively more reactive than primary and secondary alkyl diacyl peroxides, but they are not stable enough for the simple filtration separation at room temperature. Thus, we have not tried the reactions with tertiary alkyl diacyl peroxides.

In order to understand the mechanism of this reaction, we performed a set of experiments (Scheme 4). Firstly a radical capturing reaction was carried out with the addition of a radical trapping reagent (tetramethylpiperdinyloxy, TEMPO) [38,39] to the standard reaction system, no product **3a** was obtained; only the radical trapped product **4** was detected by GC–MS (Scheme 4a).

To further investigate this phenomenon, we synthesized a substrate bearing a cyclopropylmethyl moiety, diacyl peroxide **2p**, which is a radical-clock [40,41]. The reaction of phenylacetylene with the diacyl peroxide **2p** afforded a ring-opened product **3pp** in 88% yield. This result suggested the engagement of radical species in the reaction (Scheme 4b).

Based on the previous literature [16,42,43] and the above experimental findings, a possible reaction mechanism is suggested as shown in Scheme 5. In the presence of the Cu(I) catalyst, alkyl diacyl peroxide decomposes into an alkyl radical, CO_2, and

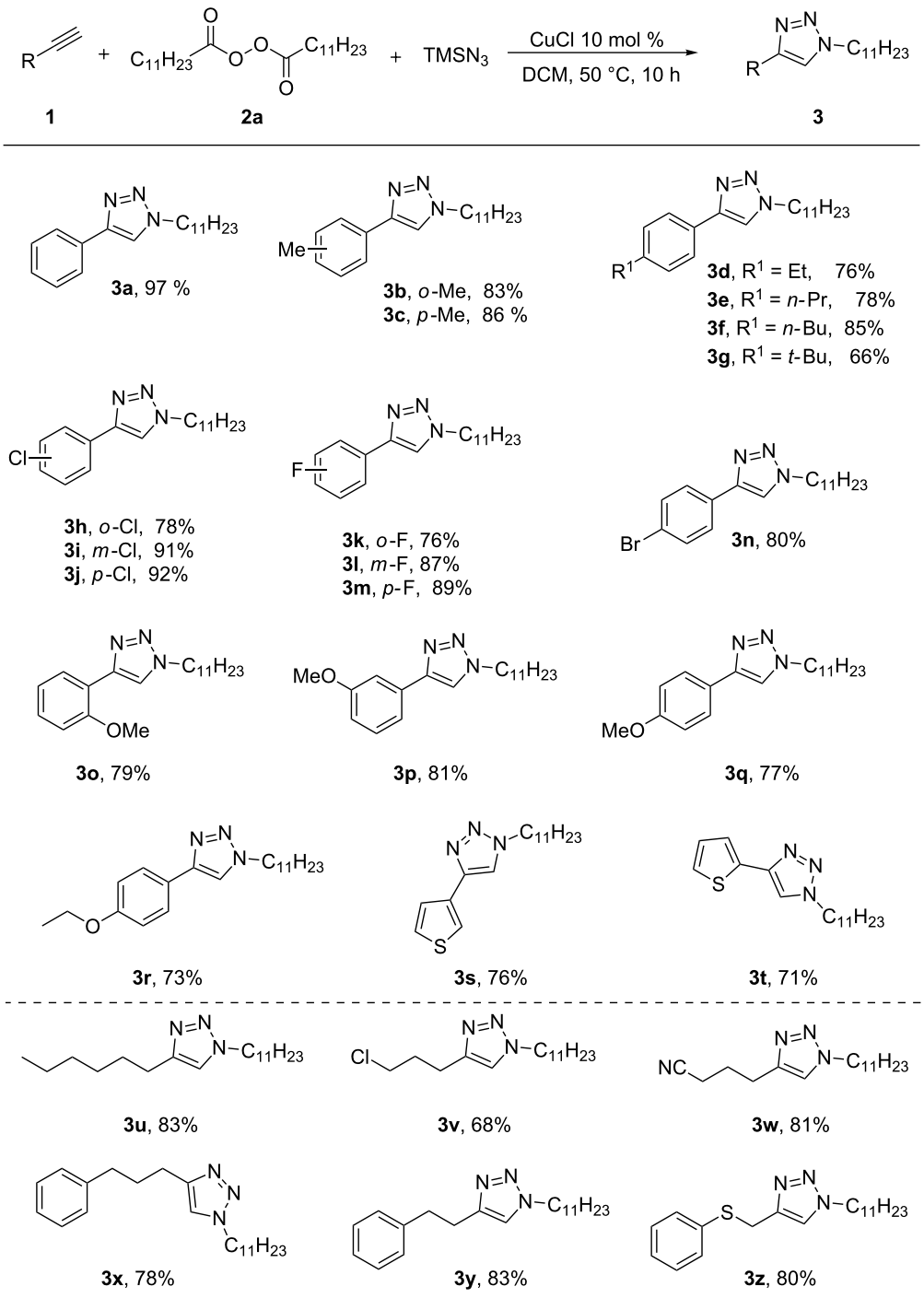

Scheme 2: Substrate scope of the terminal alkynes. Conditions: **1** (0.5 mmol), **2a** (0.75 mmol), $TMSN_3$ (0.75 mmol), CuCl (10 mol %), DCM (2 mL), 50 °C, 10 h. Yields of the isolated products are given.

releases a carboxyl–Cu(II) complex, which undergoes a ligand exchange with azidomethylsilane to form azido–Cu(II) species. The alkyl radical then abstracts the azido moiety from the azido–Cu(II) species to afford an alkyl azide and the regenerated Cu(I) catalyst. Then, a conventional CuAAC process delivers the desired cycloaddition product **3**.

Conclusion

In summary, we have established an efficient, ligand- and additive-free CuAAC reaction for the synthesis of 1,4-disubstituted 1,2,3-triazoles directly from a variety of readily accessible substrates such as alkyl diacyl peroxides, azidotrimethylsilane, and terminal alkynes. The alkyl carboxylic acids are for the first

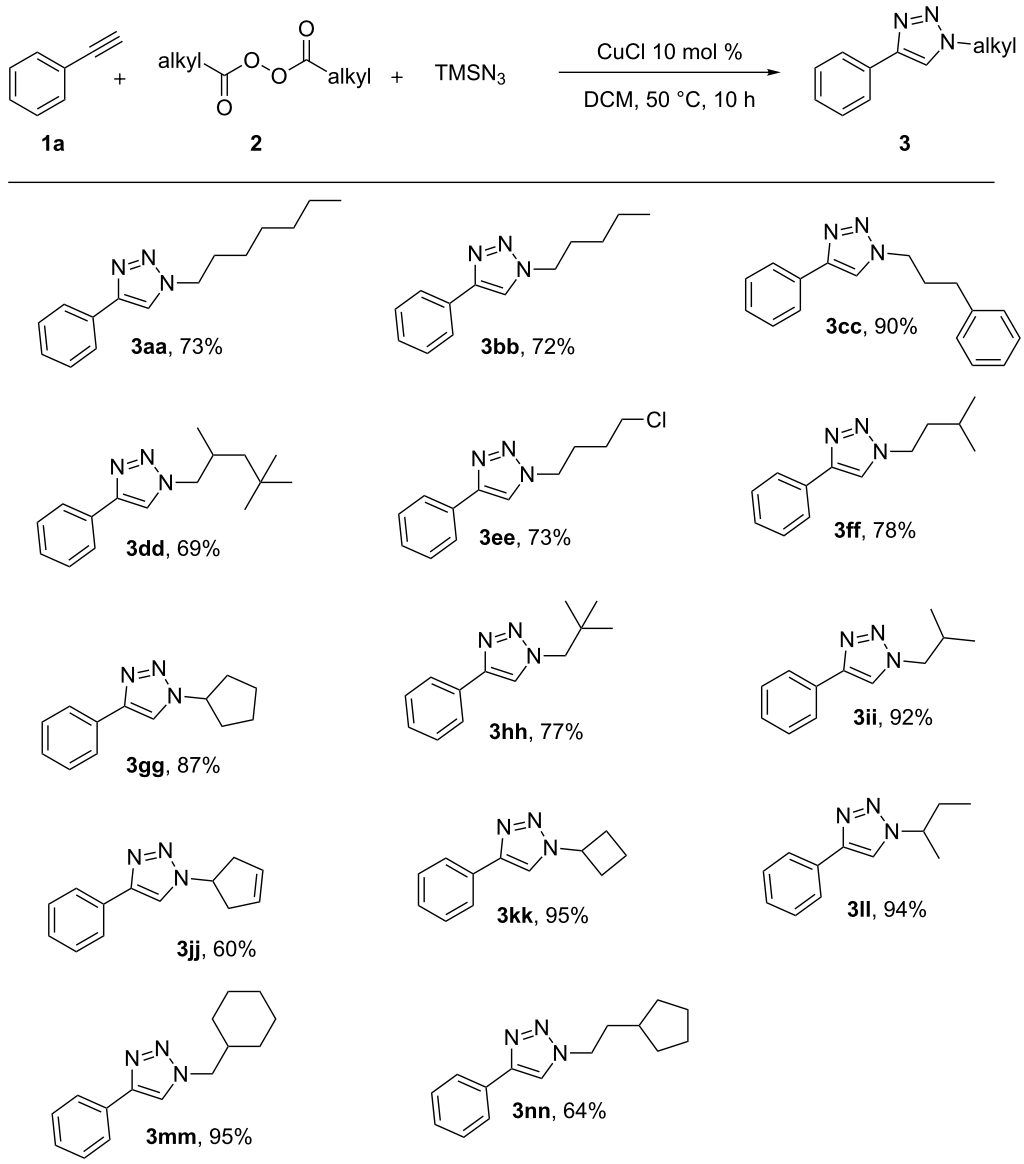

Scheme 3: Substrate scope of the alkyl diacyl peroxides. Conditions: **1a** (0.5 mmol), **2** (0.75 mmol), $TMSN_3$ (0.75 mmol), CuCl (10 mol %), DCM (2 mL), 50 °C, 10 h. Yields of the isolated products are given.

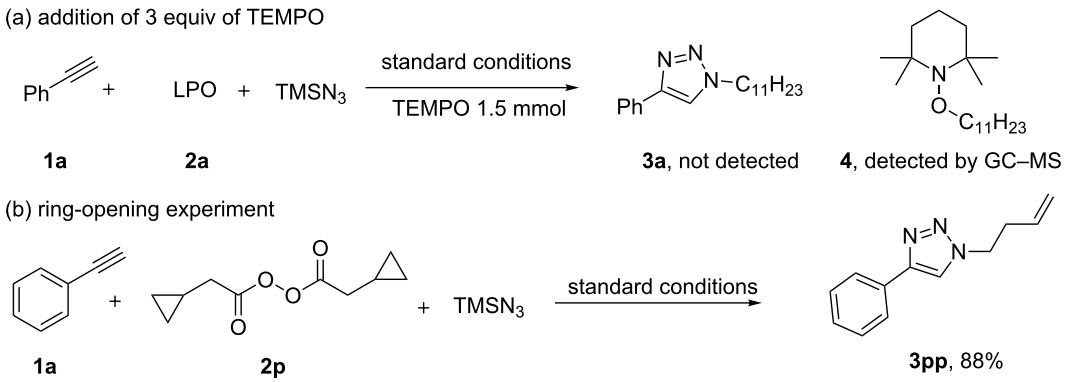

Scheme 4: Preliminary mechanistic studies.

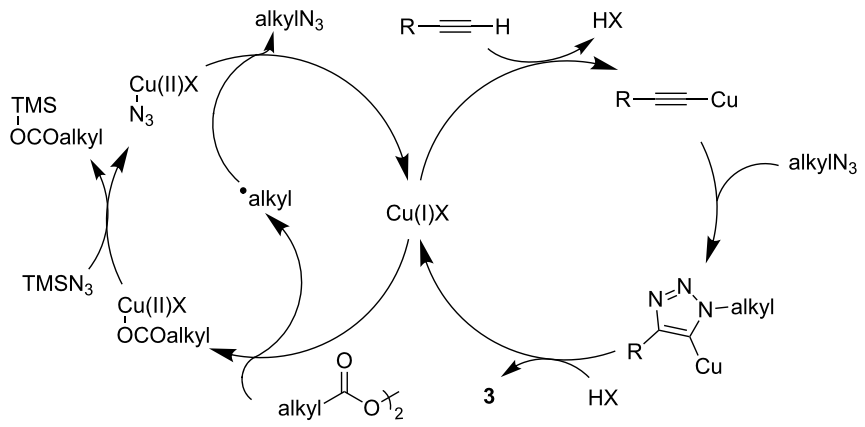

Scheme 5: Plausible reaction mechanism.

time being used as the alkyl azide precursors in the form of alkyl diacyl peroxides. This method avoids the necessity to handle organic azides, as they are generated in situ, making this protocol operationally simple. This reaction features a wide substrate scope, good functional group tolerance, high yields, and excellent regioselectivity. Most of all, the Cu(I) catalyst plays two roles in the reaction: decomposes the alkyl diacyl peroxides to afford the alkyl azides and catalyzes the subsequent CuAAC reaction to produce the 1,2,3-triazoles.

Experimental

General procedure: To a flame-dried Schlenk tube containing a magnetic stirring bar, terminal alkyne **1** (0.5 mmol), diacyl peroxide **2** (0.75 mmol), $TMSN_3$ (90.4 mg, 0.75 mmol), CuCl (4.9 mg, 0.05 mmol) and CH_2Cl_2 (2 mL) were added, respectively. The reaction mixture was stirred vigorously for 10 h at 50 °C. Then, the reaction mixture was cooled to room temperature, poured into saturated sodium bicarbonate solution (25 mL) and extracted with CH_2Cl_2 (3 × 25 mL). After drying over $MgSO_4$, the solvent was removed under reduced pressure in a rotary evaporator; the residue was purified by column chromatography on silica gel (PE/EA) to afford **3**.

Supporting Information

Supporting Information File 1

Detailed experimental procedures and characterization data for all new compounds.
[https://www.beilstein-journals.org/bjoc/content/supplementary/1860-5397-14-270-S1.pdf]

Acknowledgements

We thank the National Key R&D Program of China (Grant No. 2017YFA0700103), the NSFC (Grant Nos. 21502191, 21672213), the Strategic Priority Research Program of the Chinese Academy of Sciences (Grant No. XDB20000000), the Haixi Institute of CAS (Grant No. CXZX-2017-P01) and CAS-TWAS president program of the UCAS for financial support.

References

1. Kolb, H. C.; Finn, M. G.; Sharpless, K. B. *Angew. Chem., Int. Ed.* **2001,** *40,* 2004–2021. doi:10.1002/1521-3773(20010601)40:11<2004::aid-anie2004>3.0.co;2-5
2. Wang, Q.; Chan, T. R.; Hilgraf, R.; Fokin, V. V.; Sharpless, K. B.; Finn, M. G. *J. Am. Chem. Soc.* **2003,** *125,* 3192–3193. doi:10.1021/ja021381e
3. Ustinov, A. V.; Stepanova, I. A.; Dubnyakova, V. V.; Zatsepin, T. S.; Nozhevnikova, E. V.; Korshun, V. A. *Russ. J. Bioorg. Chem.* **2010,** *36,* 401–445. doi:10.1134/s1068162010040011
4. Speers, A. E.; Adam, G. C.; Cravatt, B. F. *J. Am. Chem. Soc.* **2003,** *125,* 4686–4687. doi:10.1021/ja034490h
5. Nair, D. P.; Podgórski, M.; Chatani, S.; Gong, T.; Xi, W.; Fenoli, C. R.; Bowman, C. N. *Chem. Mater.* **2014,** *26,* 724–744. doi:10.1021/cm402180t
6. Moses, J. E.; Moorhouse, A. D. *Chem. Soc. Rev.* **2007,** *36,* 1249–1262. doi:10.1039/b613014n
7. Link, A. J.; Tirrell, D. A. *J. Am. Chem. Soc.* **2003,** *125,* 11164–11165. doi:10.1021/ja036765z
8. Kolb, H. C.; Sharpless, K. B. *Drug Discovery Today* **2003,** *8,* 1128–1137. doi:10.1016/s1359-6446(03)02933-7
9. Hein, C. D.; Liu, X.-M.; Wang, D. *Pharm. Res.* **2008,** *25,* 2216–2230. doi:10.1007/s11095-008-9616-1
10. El-Sagheer, A. H.; Brown, T. *Chem. Soc. Rev.* **2010,** *39,* 1388–1405. doi:10.1039/b901971p
11. Deiters, A.; Cropp, T. A.; Mukherji, M.; Chin, J. W.; Anderson, J. C.; Schultz, P. G. *J. Am. Chem. Soc.* **2003,** *125,* 11782–11783. doi:10.1021/ja0370037
12. Amblard, F.; Cho, J. H.; Schinazi, R. F. *Chem. Rev.* **2009,** *109,* 4207–4220. doi:10.1021/cr9001462
13. Tornøe, C. W.; Christensen, C.; Meldal, M. *J. Org. Chem.* **2002,** *67,* 3057–3064. doi:10.1021/jo011148j

14. Rostovtsev, V. V.; Green, L. G.; Fokin, V. V.; Sharpless, K. B. *Angew. Chem., Int. Ed.* **2002,** *41,* 2596–2599. doi:10.1002/1521-3773(20020715)41:14<2596::aid-anie2596>3.0.co;2-4
15. Meldal, M.; Tornøe, C. W. *Chem. Rev.* **2008,** *108,* 2952–3015. doi:10.1021/cr0783479
16. Hein, J. E.; Fokin, V. V. *Chem. Soc. Rev.* **2010,** *39,* 1302–1315. doi:10.1039/b904091a
17. Liang, L.; Astruc, D. *Coord. Chem. Rev.* **2011,** *255,* 2933–2945. doi:10.1016/j.ccr.2011.06.028
18. Sokolova, N. V.; Nenajdenko, V. G. *RSC Adv.* **2013,** *3,* 16212. doi:10.1039/c3ra42482k
19. Haldón, E.; Nicasio, M. C.; Pérez, P. J. *Org. Biomol. Chem.* **2015,** *13,* 9528–9550. doi:10.1039/c5ob01457c
20. Wei, F.; Wang, W.; Ma, Y.; Tung, C.-H.; Xu, Z. *Chem. Commun.* **2016,** *52,* 14188–14199. doi:10.1039/c6cc06194j
21. Johansson, J. R.; Beke-Somfai, T.; Said Stålsmeden, A.; Kann, N. *Chem. Rev.* **2016,** *116,* 14726–14768. doi:10.1021/acs.chemrev.6b00466
22. Huisgen, R. Chapter 1. In *1,3-Dipolar Cycloaddition Chemistry;* Padwa, A., Ed.; Wiley: New York, 1984; pp 1–176.
23. Bräse, S.; Banert, K. *Organic Azides: Syntheses and Applications;* John Wiley & Sons: Chichester, 2010.
24. Odlo, K.; Høydahl, E. A.; Hansen, T. V. *Tetrahedron Lett.* **2007,** *48,* 2097–2099. doi:10.1016/j.tetlet.2007.01.130
25. Liang, X.; Andersen, J.; Bolvig, S. *Synlett* **2005,** 2941–2947. doi:10.1055/s-2005-921887
26. Kacprzak, K. *Synlett* **2005,** 0943–0946. doi:10.1055/s-2005-864809
27. Feldman, A. K.; Colasson, B.; Fokin, V. V. *Org. Lett.* **2004,** *6,* 3897–3899. doi:10.1021/ol048859z
28. Quan, Z.-J.; Xu, Q.; Zhang, Z.; Da, Y.-X.; Wang, X.-C. *J. Heterocycl. Chem.* **2015,** *52,* 1584–1588. doi:10.1002/jhet.2219
29. Tao, C.-Z.; Cui, X.; Li, J.; Liu, A.-X.; Liu, L.; Guo, Q.-X. *Tetrahedron Lett.* **2007,** *48,* 3525–3529. doi:10.1016/j.tetlet.2007.03.107
30. Hao, C.; Zhou, C.; Xie, J.; Zhang, J.; Liu, P.; Dai, B. *Chin. J. Chem.* **2015,** *33,* 1317–1320. doi:10.1002/cjoc.201500643
31. Chen, B.; Yang, D.; Fu, N.; Liu, Z.; Li, Y. *Synlett* **2007,** 0278–0282. doi:10.1055/s-2007-968007
32. Partyka, D. V.; Updegraff, J. B.; Zeller, M.; Hunter, A. D.; Gray, T. G. *Organometallics* **2007,** *26,* 183–186. doi:10.1021/om0607200
33. Taherpour, A. A.; Kheradmand, K. *J. Heterocycl. Chem.* **2009,** *46,* 131–133. doi:10.1002/jhet.36
34. Saha, S.; Kaur, M.; Bera, J. K. *Organometallics* **2015,** *34,* 3047–3054. doi:10.1021/acs.organomet.5b00348
35. Carmona, A. T.; Carrión-Jiménez, S.; Pingitore, V.; Moreno-Clavijo, E.; Robina, I.; Moreno-Vargas, A. J. *Eur. J. Med. Chem.* **2018,** *151,* 765–776. doi:10.1016/j.ejmech.2018.04.008
36. Kolarovič, A.; Schnürch, M.; Mihovilovic, M. D. *J. Org. Chem.* **2011,** *76,* 2613–2618. doi:10.1021/jo1024927
37. Li, Y.; Han, Y.; Xiong, H.; Zhu, N.; Qian, B.; Ye, C.; Kantchev, E. A. B.; Bao, H. *Org. Lett.* **2016,** *18,* 392–395. doi:10.1021/acs.orglett.5b03399
38. Moad, G.; Rizzardo, E.; Solomon, D. H. *Aust. J. Chem.* **1983,** *36,* 1573–1588. doi:10.1071/ch9831573
39. Dong, X.; Han, Y.; Yan, F.; Liu, Q.; Wang, P.; Chen, K.; Li, Y.; Zhao, Z.; Dong, Y.; Liu, H. *Org. Lett.* **2016,** *18,* 3774–3777. doi:10.1021/acs.orglett.6b01787
40. Ge, L.; Li, Y.; Jian, W.; Bao, H. *Chem. – Eur. J.* **2017,** *23,* 11767–11770. doi:10.1002/chem.201702385
41. Ye, C.; Li, Y.; Bao, H. *Adv. Synth. Catal.* **2017,** *359,* 3720–3724. doi:10.1002/adsc.201700798
42. Zhou, H.; Jian, W.; Qian, B.; Ye, C.; Li, D.; Zhou, J.; Bao, H. *Org. Lett.* **2017,** *19,* 6120–6123. doi:10.1021/acs.orglett.7b02982
43. Yuan, Y.-A.; Lu, D.-F.; Chen, Y.-R.; Xu, H. *Angew. Chem., Int. Ed.* **2016,** *55,* 534–538. doi:10.1002/anie.201507550

License and Terms

BEILSTEIN JOURNAL OF ORGANIC CHEMISTRY

Degenerative xanthate transfer to olefins under visible-light photocatalysis

Atsushi Kaga, Xiangyang Wu, Joel Yi Jie Lim, Hirohito Hayashi, Yunpeng Lu, Edwin K. L. Yeow* and Shunsuke Chiba*

Full Research Paper

Open Access

Address:
Division of Chemistry and Biological Chemistry, School of Physical and Mathematical Sciences, Nanyang Technological University, Singapore 637371, Singapore

Email:
Edwin K. L. Yeow* - edwinyeow@ntu.edu.sg; Shunsuke Chiba* - shunsuke@ntu.edu.sg

* Corresponding author

Keywords:
energy transfer; olefin; photocatalysis; radical; xanthate

Beilstein J. Org. Chem. **2018,** *14,* 3047–3058.
doi:10.3762/bjoc.14.283

Received: 28 September 2018
Accepted: 28 November 2018
Published: 13 December 2018

This article is part of the thematic issue "Reactive intermediates part I: radicals".

Guest Editor: T. P. Yoon

Abstract

The degenerative transfer of xanthates to olefins is enabled by the iridium-based photocatalyst [Ir{dF(CF$_3$)ppy}$_2$(dtbbpy)](PF$_6$) under blue LED light irradiation. Detailed mechanistic investigations through kinetics and photophysical studies revealed that the process operates under a radical chain mechanism, which is initiated through triplet-sensitization of xanthates by the long-lived triplet state of the iridium-based photocatalyst.

Introduction

A degenerative radical transfer of xanthates to olefins has been developed as a robust synthetic tool to create new C–C and C–S bonds in a single operation [1-13]. The method is featured by not only its capability of introducing a wide range of carbon substituents but also the ability of the installed xanthyl group in being transformed into a variety of functionalities [1-14]. This concept has also been of particular importance in the field of polymer science, known as reversible addition–fragmentation chain transfer (RAFT) polymerization [15,16]. Mechanistically, the degenerative transfer of xanthates **1** to olefins **2** proceeds through a radical chain mechanism, and thus requires an initial formation of carbon radicals **A** that add onto olefins **2**. The subsequent reaction of the resulting alkyl radicals **B** with xanthates **1** provides xanthate adducts **3** with generation of carbon radicals **A** that maintain the radical chain (Scheme 1A). Peroxide initiators such as dilauroyl peroxide (DLP) are commonly utilized [1-14], while decomposition of DLP needs a high reaction temperature and inevitably generates considerable amounts of byproducts derived from DLP that sometimes require tedious purification of the desired products. A combination of triethylborane (Et$_3$B) and molecular oxygen can also initiate the reaction at lower temperature (e.g., room tempera-

ture), while the employment of Et_3B is hampered due to its pyrophoric nature under aerobic conditions as well as undesired Et_3B-mediated dexanthylation of α-xanthyl ketones [17-21]. As an alternative strategy, a light-driven approach has been developed [22-26], since the first degenerative transfer of xanthates using *S*-benzoyl *O*-ethyl xanthate as a photo-cleavable initiator under tungsten lamp irradiation was reported by Zard [25,26] (Scheme 1B). However, these protocols have thus far adopted energy intensive light sources. Therefore, there is still ample room for establishing new protocols to realize the degenerative transfer of xanthates onto olefins under user-friendly and milder reaction conditions. Herein, we report a photocatalytic degenerative radical transfer of xanthates to olefins using an iridium-based photocatalyst under blue LED irradiation (Scheme 1C). A series of mechanistic investigations identified that the process involves a triplet-sensitization of the xanthates by the long-lived triplet state of the iridium-based photocatalyst that triggers the radical chain process [27].

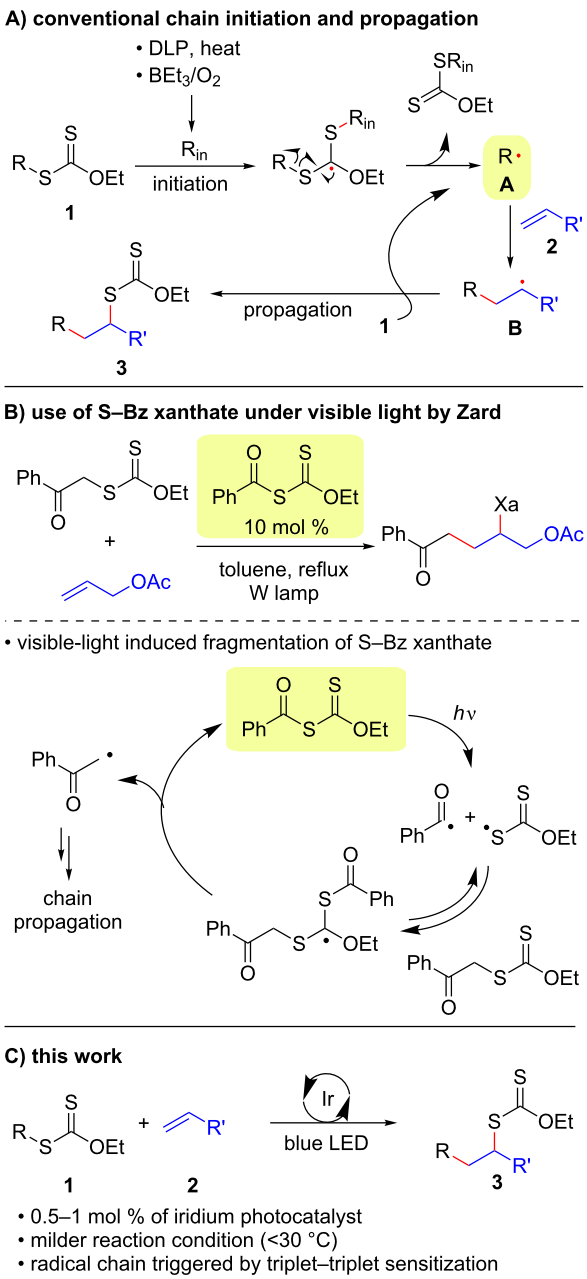

Scheme 1: Degenerative radical transfer of xanthates to olefins.

Results and Discussion

Over the last decade, there has been a remarkable advance in synthetic chemistry that takes advantage of various chromophores (either metallic or organic) having visible-light charge transfer absorption [28-37]. In the area of polymer synthesis, visible-light-induced RAFT polymerization of xanthates with vinyl monomers under blue LED (light-emitting diode) irradiation has been reported [38-41]. Visible-light-induced single unit monomer insertion of the thiocarbonylthio compounds has also been developed for the synthesis of the sequence-controlled oligomers [41-45]. For example, the group of Boyer and Xu developed *fac*-Ir(ppy)$_3$ (**6**)-catalyzed polymerization of xanthate **4** with various vinyl monomers such as vinyl acetate, providing polymers of type **5** having a high molecular weight with a narrow molecular weight distribution. It was proposed that the polymerization is initiated by single-electron reduction of xanthate **4** by the highly reducing photo-excited state of *fac*-Ir(ppy)$_3$ (**6**) [46], although the details were not elucidated (Scheme 2) [39,40].

Based on these backgrounds, we wondered if the degenerative transfer of xanthates onto olefins could be facilitated by visible-light photocatalysis under milder reaction conditions. We therefore commenced our investigation with the reaction of ethyl ethoxycarbonylmethyl xanthate (**1a**) and 1-octene (**2a**) using *fac*-Ir(ppy)$_3$ (**6**) in DMSO under blue LED irradiation (λ_{max} = 469 nm, Table 1, entry 1). As expected, the desired xanthate transfer was observed, while the process efficiency was not very high, forming **3aa** in only 58% yield with incomplete conversion even after stirring for 20 h. Interestingly, we found that the employment of the less reducing Ir catalysts **7** [46] and **8** [47] also worked for the process (Table 1, entries 2 and 3). Especially, the rather oxidizing [Ir{dF(CF$_3$)ppy}$_2$(dtbpy)](PF$_6$) (**8**) resulted in full conversion of **1a**, affording **3aa** in 89% yield (Table 1, entry 3). Other photocatalysts, such as Ru(bpy)$_3$Cl$_2$ (**9**) [46], fluorescein (**10**) [48], and phenoxazine **11** [49], were not optimal for the present transformation (Table 1, entries 4–6). It should be noted that the reaction without the photocatalyst under visible light- and halogen lamp irradiation resulted in poorer conversion with formation of **3aa** in only 10% and 30% yield, respectively, suggesting that the photocatalyst was important for the degenerative transfer of xanthate **1a** (Table 1,

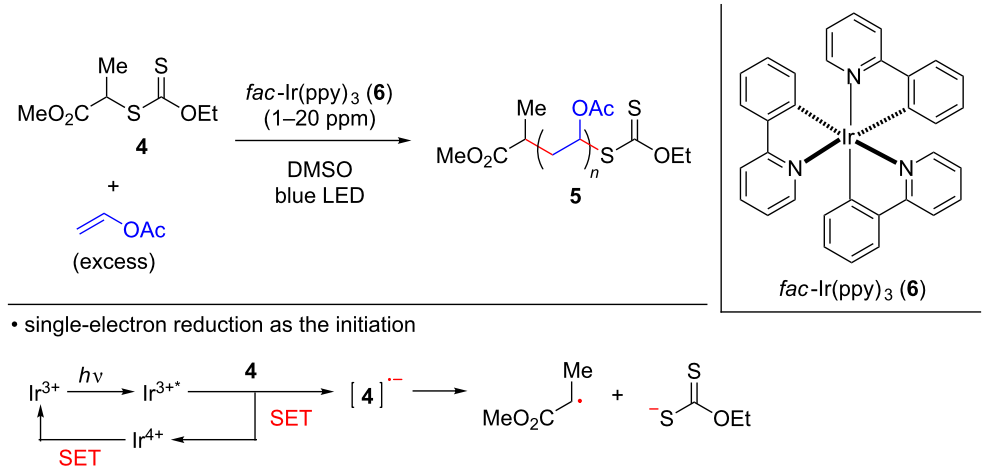

Scheme 2: Photocatalytic RAFT polymerization of xanthate **4**.

entries 7 and 8). On the other hand, the employment of a 365 nm UV lamp in place of the blue LED gave **3aa** in 75% yield, although a slower reaction rate was observed compared to the optimal reaction conditions (Table 1, entry 9).

In principle, visible-light-mediated photocatalysis can serve for electron transfer (for either oxidation or reduction) and/or for energy transfer. We found that the reduction potential $E_{p/2}$ of xanthate **1a** is −1.78 V vs SCE, which is not sufficient to be reduced by the photoexcited states of Ir catalysts **6**–**8** ($E_{1/2}$ of **6***, **7*** and **8*** = −1.73, −1.28, and −0.89 V vs SCE, respectively [46,47]). Apparently, photoinduced single-electron reduction of xanthate **1a** by the photoexcited state of the optimal catalyst **8** is not feasible. In contrast, the triplet energy E_T of xanthate **1a** was estimated as 57.5 kcal/mol by DFT calculation, that is close to those of photocatalysts **7** and **8** (E_T = 60.1 kcal/mol [50]), indicating that the process could be initiated by the triplet sensitization pathway [51,52]. This assumption is in agreement with the lower process efficiency (Table 1, entry 1) observed in the reaction with *fac*-Ir(ppy)$_3$ (**6**) that possesses a lower triplet energy (E_T = 55.2 kcal/mol [50]). The optimal photocatalyst **8** [47] has a longer excited state lifetime than **7** does [46], suggesting that the lifetime of the excited state of the photocatalyst is a key factor for the energy transfer mechanism.

To obtain a detailed mechanistic insight, steady-state photoluminescence (PL) quenching of photocatalyst **8** was examined using xanthate **1a** and 1-octene (**2a**) as potential quenchers (Figure 1). The intensity of the PL peak of photocatalyst **8** (concentration of **8** was fixed as 25 μM solution in degassed DMSO for all the samples; for details see Supporting Information File 1) at 480 nm, arising from the radiative emission of the ^{3}MLCT state of the photocatalyst, was measured using 410 nm light excitation. When the concentration of xanthate **1a** was gradually increased, a reduction in the PL intensity (I) of photocatalyst **8** was observed (Figure 1A). The Stern–Volmer plot of the ratio I_0/I, where I_0 is the initial PL intensity in the absence of quencher, versus concentration of **1a** showed a linear relationship with a quenching rate $k_q = 1.25 \times 10^7$ M^{-1}s^{-1} (see Supporting Information File 1). On the other hand, the addition of 1-octene (**2a**, 40 mM), in place of xanthate **1a**, resulted in only a small PL quenching of photocatalyst **8** (<8%, Figure 1B).

The time-resolved PL lifetime decay profiles of photocatalyst **8** (25 μM solution in degassed DMSO, 410 nm pulse excitation and monitoring emission at 480 nm) were recorded in the absence of a quencher, and in the presence of xanthate **1a** and 1-octene (**2a**, 40 mM, Figure 1C). The lifetime profiles were described using a mono-exponential decay function with a lifetime of 1.40 μs in the absence of a quencher, and 1.03 and 1.37 μs in the presence of xanthate **1a** and 1-octene (**2a**), respectively. The decrease in the PL lifetime of photocatalyst **8** in the presence of xanthate **1a** suggests that they are interacting with each other. On the other hand, only a very weak interaction exists between 1-octene (**2a**) and the photocatalyst **8** as demonstrated by the insignificant PL quenching of the photocatalyst [53].

The ns-transient absorption (TA) spectra of photocatalyst **8** (25 μM solution in degassed DMSO) obtained using 355 nm pulse excitation and recorded at different delay times are shown in Figure 2A. The band between 450 nm and 600 nm is attributed to the excited ^{3}MLCT state of the photocatalyst [53-55]. The positive ΔOD feature in the UV region (<400 nm) is also ascribed to the excited ^{3}MLCT state [55]. The transient kinetic profile probed at 480 nm decays mono-exponentially with a

Table 1: Optimization of reaction conditions.[a]

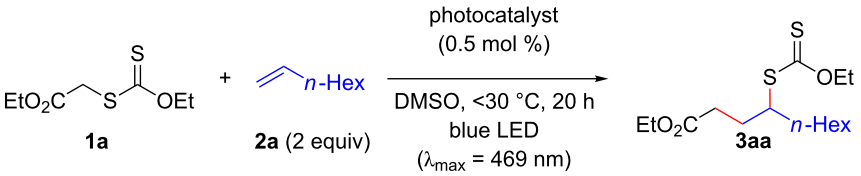

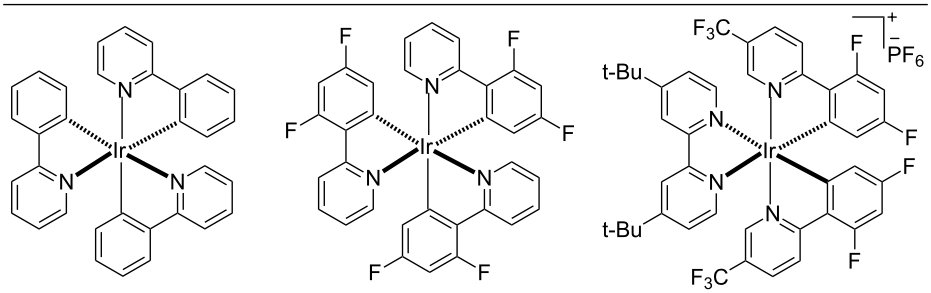

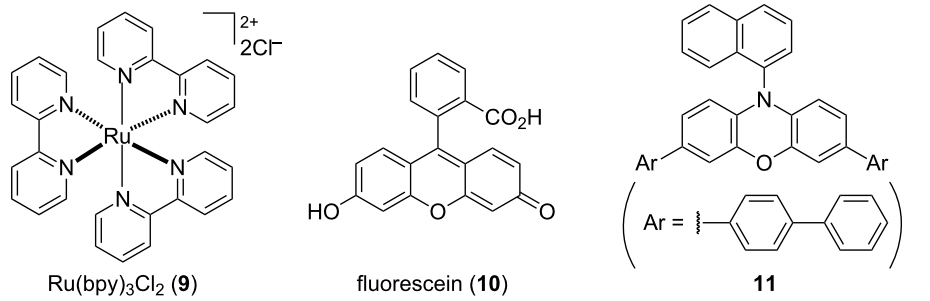

Entry	Photocat.	$E_{1/2(M+/M^*)}$ [V vs SCE][b]	E_T [kcal/mol][b]	Conv. [%][c]	Yield [%][c]
1	**6**	–1.73	55.2	64	58
2	**7**	–1.28	60.1	38	34
3	**8**	–0.89	60.1	>99	90 (89)[d]
4	**9**	–0.81	46.5	13	13
5	**10**	–1.42	44.7	34	31
6	**11**	–1.80	56.5	9	9
7	none	–	–	10	10
8[e,f]	none	–	–	39	30
9[g]	none	–	–	84	75

[a]The reactions were conducted using 0.3–0.5 mmol of xanthate **1a**, 1-octene (**2a**, 2 equiv) and a photocatalyst in DMSO (1 M) at <30 °C with irradiation of a blue LED strip (λ_{max} = 469 nm, 15 W/m, 1.5 m) under an argon atmosphere. [b]The values were obtained from references [46-50]. [c]NMR yields using 1,1,2,2-tetrachloroethane as an internal standard. [d]Isolated yield is stated in parentheses. [e]Halogen lamp (300 W) was used in place of blue LED. [f]Reaction was conducted at 40 °C. [g]365 nm UV lamp (100 W) was used in place of blue LED.

lifetime of 1.73 µs (Figure 2B); close to the lifetime of the excited ^{3}MLCT state of photocatalyst **8** measured in Figure 1C. The ns-TA spectra of xanthate **1a** in degassed DMSO, measured using 355 nm pulse excitation, at various delay times show a broad band centered at ≈620 nm (Figure 2C). This band has previously been ascribed to the absorption of the xanthic acid radical formed plausibly from homolytic C–S bond cleavage of the short-lived triplet state of xanthate **1a** [22].

The ns-TA spectra of photocatalyst **8** (25 µM) in the presence of xanthate **1a** (40 mM) in degassed DMSO at various delay times are shown in Figure 2D. The kinetic profile at 480 nm is described using a mono-exponential decay function with a quenched lifetime of 1.27 µs. The ca. 37% decrease in the lifetime of the excited ^{3}MLCT state of photocatalyst **8** observed in the PL lifetime decay measurement (Figure 1C) and ns-TA kinetic measurement (Figure 2B) can be rationalized using

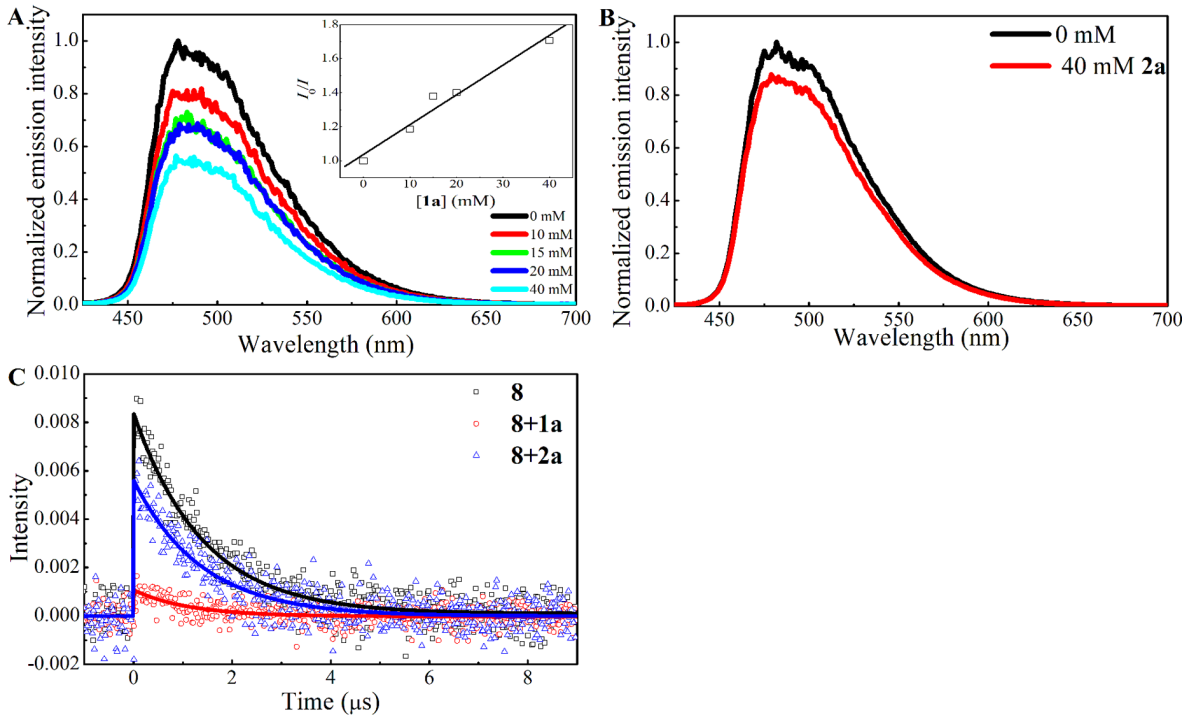

Figure 1: Photoluminescence (PL) spectra of the ^{3}MLCT state of **8** in degassed DMSO solvent with (A) various concentrations of xanthate **1a** added and (B) 40 mM of 1-octene (**2a**) added. The inset of (A) gives the Stern–Volmer plot of the corrected PL quenching at 480 nm. (C) Time-resolved PL lifetime decay profiles of photocatalyst **8** in degassed DMSO in the absence of quencher (square), presence of xanthate **1a** (circle) and presence of 1-octene (**2a**, triangle). The mono-exponential decay fits are provided.

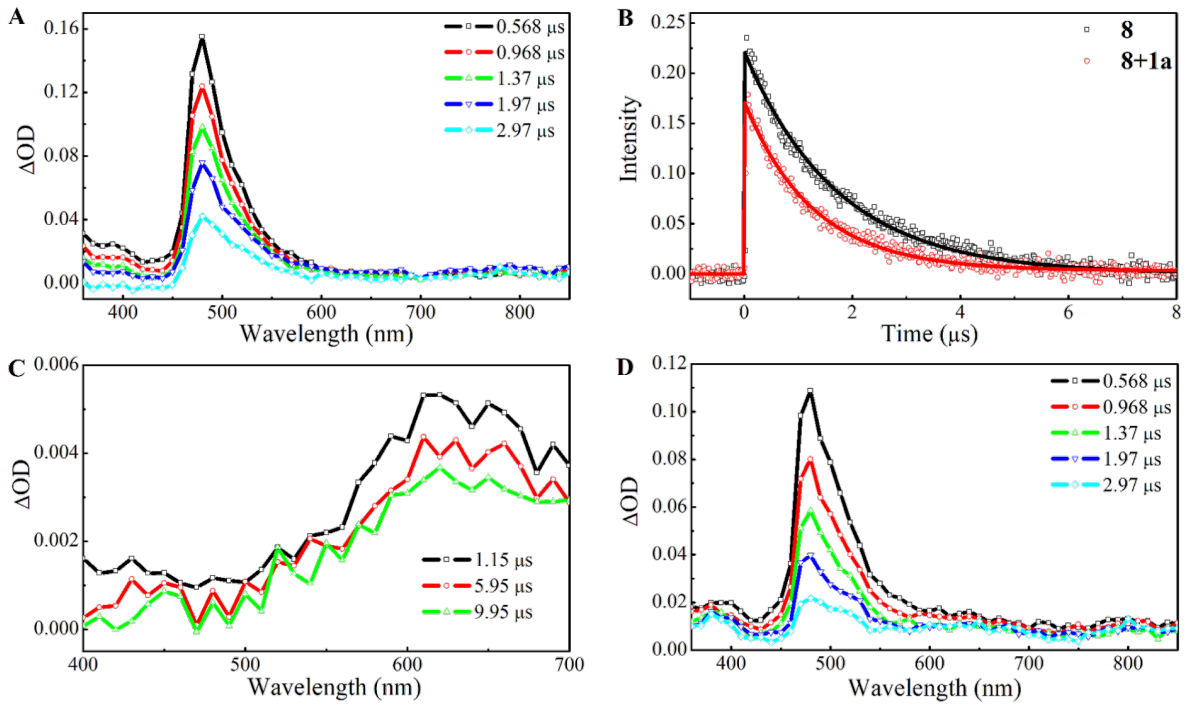

Figure 2: (A) ns-Transient absorption spectra of photocatalyst **8** in degassed DMSO recorded at different delay times (excitation wavelength = 355 nm). (B) ns-TA kinetic profile probed at 480 nm for photocatalyst **8** in the absence and presence of xanthate **1a**. (C) and (D) ns-Transient absorption spectra of xanthate **1a** and **8** in the presence of **1a** in degassed DMSO recorded at different delay times, respectively (excitation wavelength = 355 nm).

either an energy-transfer or an electron-transfer mechanism. For the same delay times and in the presence of **1a**, the ΔOD values in Figure 2D are smaller than those of photocatalyst **8** in the absence of the xanthate (Figure 2A). This is due to the quenching of the ^{3}MLCT state of the photocatalyst. If an electron-transfer process occurs from photocatalyst **8** to xanthate **1a**, the ΔOD values in the UV region should be noticeably higher due to the TA band contribution from bpy^- connected to an Ir metal center of the +4 oxidation state (i.e., absorption due to $[Ir^{IV}\{dF(CF_3)ppy\}_2](dtbpy^-)]$ species) [55]. However, this was not observed in Figure 2D; suggesting that quenching is due to energy transfer rather than electron transfer, and in agreement with the thermodynamic consideration where single-electron reduction of xanthate **1a** likely does not proceed with the excited photocatalyst **8**. We therefore propose that the observed PL quenching is due to energy transfer from the excited ^{3}MLCT state of photocatalyst **8** to the triplet state of xanthate **1a**. When comparing the normalized TA spectra of photocatalyst **8** in the absence and presence of xanthate **1a** (see Supporting Information File 1, Figure S4), an additional contribution from a broad ΔOD band that stretches from 500 nm to 800 nm is seen for the latter which is attributed to the absorption of the xanthic acid radical. In this case, the xanthic acid radical is formed from the homolytic bond cleavage of the excited triplet state of **1a** formed by direct 355 nm laser light excitation and triplet–triplet energy transfer involving the excited photocatalyst **8**.

To confirm the possibility of a direct photoexcitation of xanthate **1** using blue LED light irradiation as an alternative mechanism, a steady-state UV–vis absorption spectroscopy study of xanthate **1a** was conducted (Figure 3). The UV–vis absorption spectrum of **1a** (1 mM in DMSO) showed absorption bands at 340–390 nm assigned to the n→π* electronic transition of the C=S bond as a characteristic peak of thiocarbonyl containing compounds [56]. In fact, the reaction of **1a** and **2a** under 365 nm UV lamp irradiation without a photocatalyst delivered product **3aa** in 75% yield (Table 1, entry 9). This indicates the excitation of xanthate **1a** through an n→π* electronic transition of the C=S bond is in operation in the UV irradiation process.

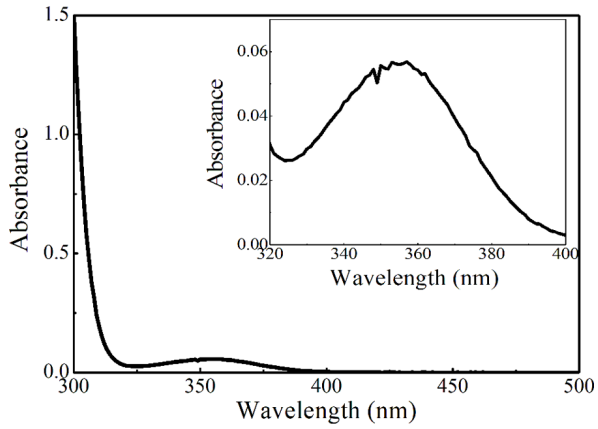

Figure 3: UV–vis absorption spectrum of **1a** (1 mM solution in DMSO).

The involvement of a radical chain mechanism was further confirmed by calculating the quantum yield (Φ) because a chain process provides multiple equivalents of product per photon absorbed by the photocatalyst (Φ > 1). The photon flux of blue LED (λ_{max} = 469 nm) was determined using the potassium ferrioxalate actinometer [57,58]. After irradiation of the mixture of xanthate **1a** and olefin **2b** under optimal reaction conditions with blue LED light irradiation for 4 h (Scheme 3), product **3ab** was obtained in 58% yield. This is consistent with 12 equivalents of xanthate adduct **3ab** produced per photon absorbed by the photocatalyst **8** (Φ = 12).

On the basis of these observations, a proposed triplet sensitization mechanism is illustrated in Scheme 4. In this reaction, photocatalyst **8** serves as a catalyst of an initiation step through energy transfer from photoexcited **8*** to xanthate **1** to form excited xanthate **1*** and regeneration of **8** in the ground state [59-61]. The resulting excited xanthate **1*** induces homolytic scission of the C–S bond to generate the stabilized S-radical and C-radical **A**, which then enters the innate radical chain-propagation mechanism to provide xanthate adduct **3**. It is worth noting that at the wavelength of the light source used (469 nm), xanthate **1a** absorbs a negligible amount of light (Figure 3) and the majority of triplet **1a** formed is due to energy transfer from excited catalyst **8***.

Scheme 3: Determination of quantum yield.

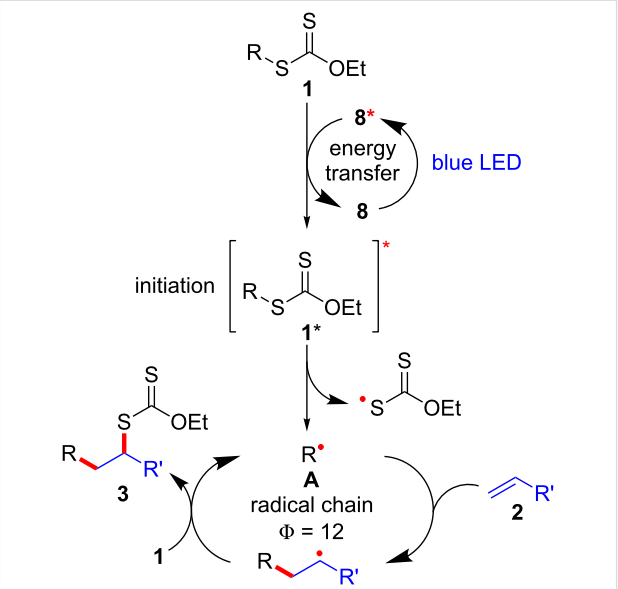

Scheme 4: Proposed reaction mechanism.

Having optimized the reaction conditions on the photocatalytic degenerative transfer of xanthates, we next explored the scope of olefins **2** using xanthate **1a** (Table 2). The present method tolerated a variety of functionalities such as acetyl, cyano, silyl, ethoxy, *N*-Boc amino, boryl, hydroxy, and halogen groups, affording xanthate adducts **3ab**–**ai** in good yields (Table 2, entries 1–8). We found strained 1,1-disubstituted olefins such as methylenecyclopropane **2j** and methylenecyclobutane (**2k**) are amenable to the current protocol (Table 2, entries 9 and 10), whereas the reaction of methylenecyclopentane (**2l**) afforded not only the desired xanthate adduct **3al** in 60% yield but also the substituted cyclopentene **3al'** in 18% yield (Table 2, entry 11), implicating that the redox process is partially operating along with the main radical chain process. Norbornene (**2m**) was found reactive for degenerative transfer of xanthate **1a** (Table 2, entry 12). The reaction was also applied to dienes **2n** and **2o**, which led the formation of functionalized cyclopentane **3an** and pyrrolidine **3ao**, respectively, via 5-*exo*-trig radical cyclization (Table 2, entries 13 and 14). The present method was capable in functionalizing olefins **2p** and **2q** installed on steroid scaffolds with high efficiency (Table 2, entries 15 and 16).

We next examined the reactions of various xanthates **1** with allyl acetate (**2b**, Table 3). The reactions of ketonyl xanthates having phenyl, *para*-bromophenyl, methyl, cyclopropyl, *N*,*O*-dimethyl acetylhydroxamate, and chloromethyl moieties proceeded smoothly, producing xanthate adducts **3bb**–**gb** in good yields (Table 3, entries 1–6). Notably, the photocatalyti-

Table 2: Scope of olefins.[a]

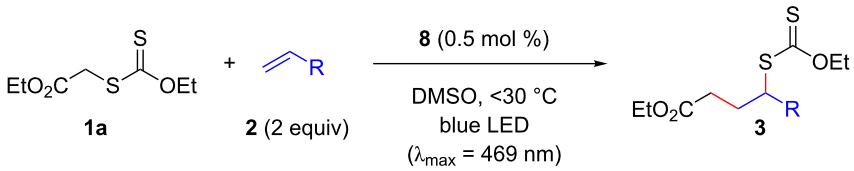

Entry	Olefins **2**		Products **3**	Yield[b] (time)
	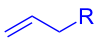 **2**	R	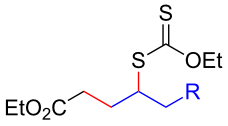	
1	**2b**	OAc	**3ab**	88% (18 h)
2	**2c**	CN	**3ac**	73% (45 h)
3	**2d**	$SiMe_3$	**3ad**	85% (46 h)
4[c]	**2e**	OEt	**3ae**	70% (41 h)
5[c]	**2f**	NHBoc	**3af**	80% (61 h)
6[d]	**2g**	Bpin	**3ag**	72% (30 h)
7	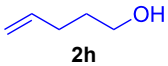 **2h**		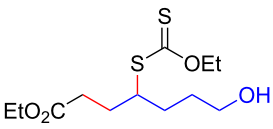 **3ah**	84% (37 h)

Table 2: Scope of olefins.[a] (continued)

8	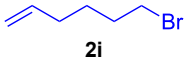 **2i**	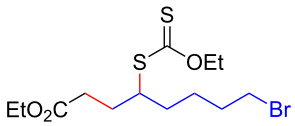 **3ai**	73% (48 h)
9	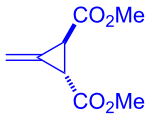 **2j**	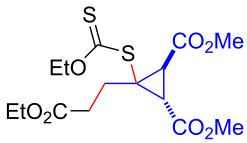 **3aj**	64% (48 h)
10	 **2k**	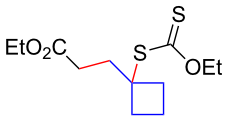 **3ak**	90% (26 h)
11[d]	 **2l**	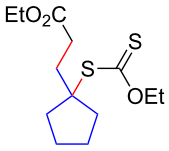 **3al**	60% (20 h)
		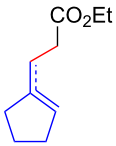 **3al'**	18%[e] (20 h) *endo*/*exo* = 80:20
12	 **2m**	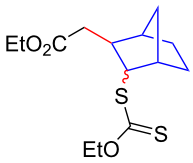 **3am**	73% (10 h) (dr = 78:22)
13	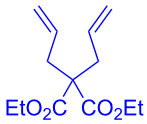 **2n**	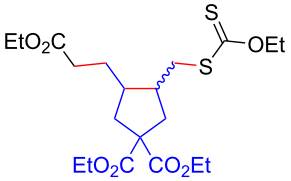 **3an**	68% (24 h) (dr = 88:12)
14	 **2o**	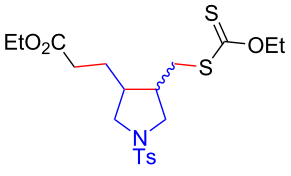 **3ao**	74% (13 h) (dr = 71:29)

Table 2: Scope of olefins.[a] (continued)

15[f]	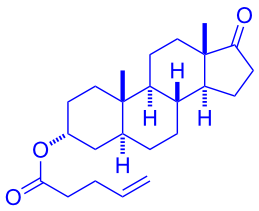 **2p**	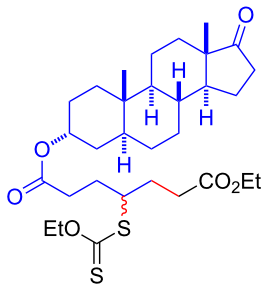 **3ap**	94% (26 h) (dr = 50:50)
16[g]	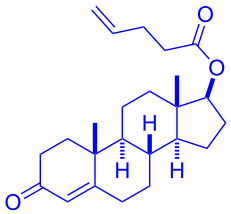 **2q**	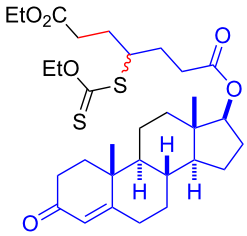 **3aq**	80% (50 h) (dr = 50:50)

[a]The reactions were conducted using xanthate **1a** (0.3–0.5 mmol), olefin **2** (2 equiv) and **8** (0.5 mol %) in DMSO (1 M) at <30 °C with irradiation of a blue LED strip (λ_{max} = 469 nm) under an argon atmosphere. [b]Isolated yields are stated. [c]1 mol % of **8** was used. [d]4 equiv of olefin **2** were used. [e]NMR yield using 1,1,2,2-tetrachloroethane as an internal standard. [f]The reaction was conducted in DMSO/DCE 1:1 (0.5 M). [g]The reaction was conducted in DMSO/DCE 3:5 (0.4 M).

Table 3: Scope of xanthates.[a]

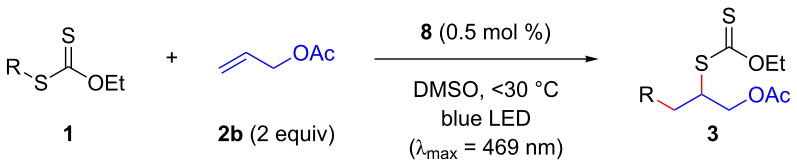

Entry	Xanthates **1**	Products **3**	Yield[b] (time)
1	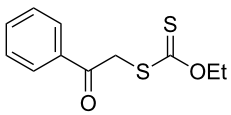 **1b**	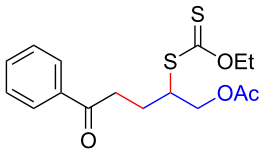 **3bb**	78% (44 h)
2	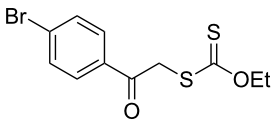 **1c**	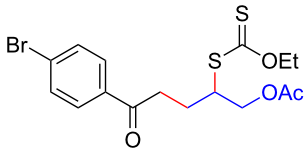 **3cb**	69% (47 h)
3	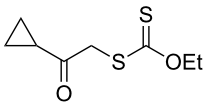 **1d**	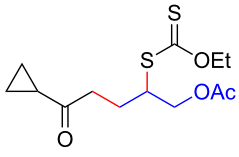 **3db**	59% (51 h)

Table 3: Scope of xanthates.[a] (continued)

4[c]	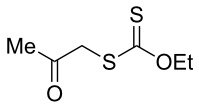 **1e**	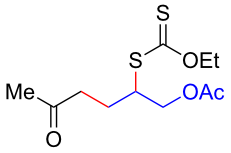 **3eb**	82% (71 h)
5	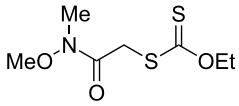 **1f**	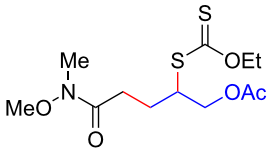 **3fb**	81% (27 h)
6	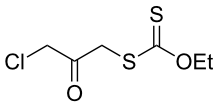 **1g**	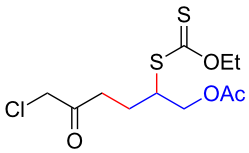 **3gb**	75% (17 h)
7[d]	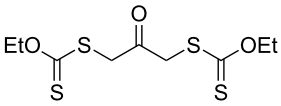 **1h**	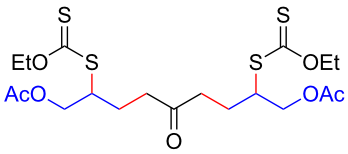 **3hb**	69% (52 h) (dr = 52:48)
8	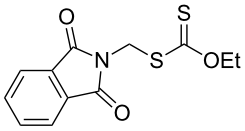 **1i**	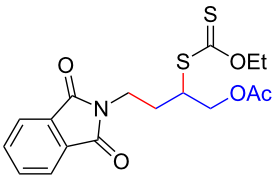 **3ib**	80% (41 h)
9	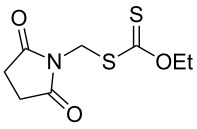 **1j**	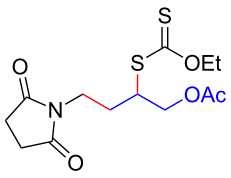 **3jb**	56% (24 h)
10	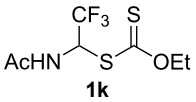 **1k**	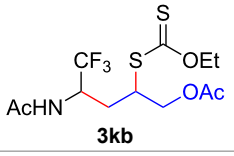 **3kb**	74% (24 h) (dr = 63:37)

[a]The reactions were conducted using xanthate **1** (0.3 mmol), olefin **2b** (2 equiv) and **8** (0.5 mol %) in DMSO (1 M) at <30 °C with irradiation of a blue LED strip (λ_{max} = 469 nm) under an argon atmosphere. [b]Isolated yields are stated. [c]1 mol % of **8** was used. [d]Five equivalents of olefin **2b** were used.

cally cleavable aryl bromide (Table 3, entry 2) and the α-chlorocarbonyl moiety (Table 3, entry 6) were also stable under the current reaction conditions [62,63]. Furthermore, double addition of bisxanthate **1h** was successfully achieved in the presence of 5 equiv of olefin **2b**, giving **3hb** in 69% yield (Table 3, entry 7). This method is also suitable for generating α-aminoalkyl radicals from phthalimidomethyl and succinimidomethyl xanthates [64], as well as α-trifluoromethylamino xanthate **1k** [65] to afford desired products **3ib**–**kb** in good to moderate yields (Table 3, entries 8–10).

Conclusion

We have established a protocol for a photoinduced radical addition of xanthates to olefins using an iridium-based photocata-

lyst under blue LED irradiation, leading to diverse xanthate adducts. This reaction proceeds through a radical-chain propagation mechanism via an initiation involving a triplet-sensitization process of xanthates by an excited iridium-based photocatalyst.

Supporting Information

Supporting Information File 1

Full experimental details and analytical data.
[https://www.beilstein-journals.org/bjoc/content/supplementary/1860-5397-14-283-S1.pdf]

Acknowledgements

This work was supported by funding from Nanyang Technological University and the Singapore Ministry of Education (Academic Research Fund Tier 1: RG2/15 and RG2/18 for S.C. and Academic Research Fund Tier 1: RG115/16 for E.K.L.Y.).

ORCID® iDs

Atsushi Kaga - https://orcid.org/0000-0001-5439-6627
Joel Yi Jie Lim - https://orcid.org/0000-0001-7179-2613
Yunpeng Lu - https://orcid.org/0000-0003-2493-7853
Shunsuke Chiba - https://orcid.org/0000-0003-2039-023X

References

1. Zard, S. Z. *Acc. Chem. Res.* **2018,** *51,* 1722–1733. doi:10.1021/acs.accounts.8b00201
2. Quiclet-Sire, B.; Zard, S. Z. *Synlett* **2017,** *28,* 2685–2696. doi:10.1055/s-0036-1590809
3. Quiclet-Sire, B.; Zard, S. Z. *Isr. J. Chem.* **2017,** *57,* 202–217. doi:10.1002/ijch.201600094
4. Zard, S. Z. *Org. Biomol. Chem.* **2016,** *14,* 6891–6912. doi:10.1039/c6ob01087c
5. Quiclet-Sire, B.; Zard, S. Z. *Synlett* **2016,** *27,* 680–701. doi:10.1055/s-0035-1561300
6. Debien, L.; Quiclet-Sire, B.; Zard, S. Z. *Acc. Chem. Res.* **2015,** *48,* 1237–1253. doi:10.1021/acs.accounts.5b00019
7. Zard, S. Z. *J. Phys. Org. Chem.* **2012,** *25,* 953–964. doi:10.1002/poc.2976
8. Quiclet-Sire, B.; Zard, S. Z. *Chimia* **2012,** *66,* 404–412. doi:10.2533/chimia.2012.404
9. Quiclet-Sire, B.; Zard, S. Z. *Pure Appl. Chem.* **2011,** *83,* 519–551. doi:10.1351/pac-con-10-08-07
10. Quiclet-Sire, B.; Zard, S. Z. *Top. Curr. Chem.* **2006,** *264,* 201–236. doi:10.1007/128_029
11. Quiclet-Sire, B.; Zard, S. Z. *Chem. – Eur. J.* **2006,** *12,* 6002–6016. doi:10.1002/chem.200600510
12. Zard, S. Z. *Aust. J. Chem.* **2006,** *59,* 663–668. doi:10.1071/ch06263
13. Zard, S. Z. *Angew. Chem., Int. Ed. Engl.* **1997,** *36,* 672–685. doi:10.1002/anie.199706721
14. Czaplyski, W. L.; Na, C. G.; Alexanian, E. J. *J. Am. Chem. Soc.* **2016,** *138,* 13854–13857. doi:10.1021/jacs.6b09414
15. Perrier, S. *Macromolecules* **2017,** *50,* 7433–7447. doi:10.1021/acs.macromol.7b00767
16. Chiefari, J.; Chong, Y. K.; Ercole, F.; Krstina, J.; Jeffery, J.; Le, T. P. T.; Mayadunne, R. T. A.; Meijs, G. F.; Moad, C. L.; Moad, G.; Rizzardo, E.; Thang, S. H. *Macromolecules* **1998,** *31,* 5559–5562. doi:10.1021/ma9804951
17. García-Merinos, J. P.; Hernández-Pérez, J. P.; Martínez-García, L.; Rojas-Lima, S.; López-Ruiz, H. *J. Mex. Chem. Soc.* **2007,** *51,* 209–212.
18. Boivin, J.; Nguyen, V. T. *Beilstein J. Org. Chem.* **2007,** *3,* No. 45. doi:10.1186/1860-5397-3-45
19. Charrier, N.; Gravestock, D.; Zard, S. Z. *Angew. Chem., Int. Ed.* **2006,** *45,* 6520–6523. doi:10.1002/anie.200601567
20. Jean-Baptiste, L.; Yemets, S.; Legay, R.; Lequeux, T. *J. Org. Chem.* **2006,** *71,* 2352–2359. doi:10.1021/jo052528y
21. Briggs, M. E.; Zard, S. Z. *Synlett* **2005,** 334–336. doi:10.1055/s-2004-837191
22. Tazhe Veetil, A.; Šolomek, T.; Ngoy, B. P.; Pavlíková, N.; Heger, D.; Klán, P. *J. Org. Chem.* **2011,** *76,* 8232–8242. doi:10.1021/jo201385b
23. Ferjančić, Z.; Čeković, Ž.; Saičić, R. N. *Tetrahedron Lett.* **2000,** *41,* 2979–2982. doi:10.1016/s0040-4039(00)00286-0
24. Maslak, V.; Čeković, Ž.; Saičić, R. N. *Synlett* **1998,** 1435–1437. doi:10.1055/s-1998-1946
25. Mestre, F.; Tailham, C.; Zard, S. Z. *Heterocycles* **1989,** *28,* 171–174. doi:10.3987/com-88-s77
26. Delduc, P.; Tailhan, C.; Zard, S. Z. *J. Chem. Soc., Chem. Commun.* **1988,** 308–310. doi:10.1039/c39880000308
27. López-Mendoza, P.; Díaz, J. E.; Loaiza, A. E.; Miranda, L. D. *Tetrahedron* **2018,** *74,* 5494–5502. doi:10.1016/j.tet.2018.04.079
28. Twilton, J.; Le, C.; Zhang, P.; Shaw, M. H.; Evans, R. W.; MacMillan, D. W. C. *Nat. Rev. Chem.* **2017,** *1,* No. 0052. doi:10.1038/s41570-017-0052
29. Cambié, D.; Bottecchia, C.; Straathof, N. J. W.; Hessel, V.; Noël, T. *Chem. Rev.* **2016,** *116,* 10276–10341. doi:10.1021/acs.chemrev.5b00707
30. Romero, N. A.; Nicewicz, D. A. *Chem. Rev.* **2016,** *116,* 10075–10166. doi:10.1021/acs.chemrev.6b00057
31. Skubi, K. L.; Blum, T. R.; Yoon, T. P. *Chem. Rev.* **2016,** *116,* 10035–10074. doi:10.1021/acs.chemrev.6b00018
32. Ravelli, D.; Protti, S.; Fagnoni, M. *Chem. Rev.* **2016,** *116,* 9850–9913. doi:10.1021/acs.chemrev.5b00662
33. Kärkäs, M. D.; Porco, J. A., Jr.; Stephenson, C. R. J. *Chem. Rev.* **2016,** *116,* 9683–9747. doi:10.1021/acs.chemrev.5b00760
34. Shaw, M. H.; Twilton, J.; MacMillan, D. W. C. *J. Org. Chem.* **2016,** *81,* 6898–6926. doi:10.1021/acs.joc.6b01449
35. Corrigan, N.; Shanmugam, S.; Xu, J.; Boyer, C. *Chem. Soc. Rev.* **2016,** *45,* 6165–6212. doi:10.1039/c6cs00185h
36. Prier, C. K.; Rankic, D. A.; MacMillan, D. W. C. *Chem. Rev.* **2013,** *113,* 5322–5363. doi:10.1021/cr300503r
37. Narayanam, J. M. R.; Stephenson, C. R. J. *Chem. Soc. Rev.* **2011,** *40,* 102–113. doi:10.1039/b913880n
38. Ding, C.; Fan, C.; Jiang, G.; Pan, X.; Zhang, Z.; Zhu, J.; Zhu, X. *Macromol. Rapid Commun.* **2015,** *36,* 2181–2185. doi:10.1002/marc.201500427
39. Shanmugam, S.; Xu, J.; Boyer, C. *Macromolecules* **2014,** *47,* 4930–4942. doi:10.1021/ma500842u
40. Xu, J.; Jung, K.; Atme, A.; Shanmugam, S.; Boyer, C. *J. Am. Chem. Soc.* **2014,** *136,* 5508–5519. doi:10.1021/ja501745g
41. Phommalysack-Lovan, J.; Chu, Y.; Boyer, C.; Xu, J. *Chem. Commun.* **2018,** *54,* 6591–6606. doi:10.1039/c8cc02783h

42. Huang, Z.; Noble, B. B.; Corrigan, N.; Chu, Y.; Satoh, K.; Thomas, D. S.; Hawker, C. J.; Moad, G.; Kamigaito, M.; Coote, M. L.; Boyer, C.; Xu, J. *J. Am. Chem. Soc.* **2018,** *140,* 13392–13406. doi:10.1021/jacs.8b08386
43. Aerts, A.; Lewis, R. W.; Zhou, Y.; Malic, N.; Moad, G.; Postma, A. *Macromol. Rapid Commun.* **2018,** *39,* 1800240. doi:10.1002/marc.201800240
44. Fu, C.; Huang, Z.; Hawker, C. J.; Moad, G.; Xu, J.; Boyer, C. *Polym. Chem.* **2017,** *8,* 4637–4643. doi:10.1039/c7py00713b
45. Xu, J.; Fu, C.; Shanmugam, S.; Hawker, C. J.; Moad, G.; Boyer, C. *Angew. Chem., Int. Ed.* **2017,** *56,* 8376–8383. doi:10.1002/anie.201610223
46. Teegardin, K.; Day, J. I.; Chan, J.; Weaver, J. *Org. Process Res. Dev.* **2016,** *20,* 1156–1163. doi:10.1021/acs.oprd.6b00101
47. Lowry, M. S.; Goldsmith, J. I.; Slinker, J. D.; Rohl, R.; Pascal, R. A.; Malliaras, G. G.; Bernhard, S. *Chem. Mater.* **2005,** *17,* 5712–5719. doi:10.1021/cm051312+
48. Shen, T.; Zhao, Z.-G.; Yu, Q.; Xu, H.-J. *J. Photochem. Photobiol., A* **1989,** *47,* 203–212. doi:10.1016/1010-6030(89)87066-2
49. Du, Y.; Pearson, R. M.; Lim, C.-H.; Sartor, S. M.; Ryan, M. D.; Yang, H.; Damrauer, N. H.; Miyake, G. M. *Chem. – Eur. J.* **2017,** *23,* 10962–10968. doi:10.1002/chem.201702926
50. Singh, A.; Teegardin, K.; Kelly, M.; Prasad, K. S.; Krishnan, S.; Weaver, J. D. *J. Organomet. Chem.* **2015,** *776,* 51–59. doi:10.1016/j.jorganchem.2014.10.037
51. Strieth-Kalthoff, F.; James, M. J.; Teders, M.; Pitzer, L.; Glorius, F. *Chem. Soc. Rev.* **2018,** *47,* 7190–7202. doi:10.1039/c8cs00054a
52. Xiao, W.-J.; Zhou, Q.-Q.; Zou, Y.-Q.; Lu, L.-Q. *Angew. Chem., Int. Ed.* **2018**. doi:10.1002/anie.201803102
53. Teders, M.; Henkel, C.; Anhäuser, L.; Strieth-Kalthoff, F.; Gómez-Suárez, A.; Kleinmans, R.; Kahnt, A.; Rentmeister, A.; Guldi, D.; Glorius, F. *Nat. Chem.* **2018,** *10,* 981–988. doi:10.1038/s41557-018-0102-z
54. van As, D. J.; Connell, T. U.; Brzozowski, M.; Scully, A. D.; Polyzos, A. *Org. Lett.* **2018,** *20,* 905–908. doi:10.1021/acs.orglett.7b03565
55. Ichimura, K.; Kobayashi, T.; King, K. A.; Watts, R. J. *J. Phys. Chem.* **1987,** *91,* 6104–6106. doi:10.1021/j100308a012
56. Coyle, J. D. *Tetrahedron* **1985,** *41,* 5393–5425. doi:10.1016/s0040-4020(01)91341-9
57. Cismesia, M. A.; Yoon, T. P. *Chem. Sci.* **2015,** *6,* 5426–5434. doi:10.1039/c5sc02185e
58. Hatchard, C. G.; Parker, C. A. *Proc. R. Soc. London, Ser. A* **1956,** *235,* 518–536. doi:10.1098/rspa.1956.0102
59. Studer, A.; Curran, D. P. *Angew. Chem., Int. Ed.* **2016,** *55,* 58–102. doi:10.1002/anie.201505090
60. Christmann, J.; Ibrahim, A.; Charlot, V.; Croutxé-Barghorn, C.; Ley, C.; Allonas, X. *ChemPhysChem* **2016,** *17,* 2309–2314. doi:10.1002/cphc.201600034
61. Arceo, E.; Montroni, E.; Melchiorre, P. *Angew. Chem., Int. Ed.* **2014,** *53,* 12064–12068. doi:10.1002/anie.201406450
62. Devery, J. J., III; Nguyen, J. D.; Dai, C.; Stephenson, C. R. J. *ACS Catal.* **2016,** *6,* 5962–5967. doi:10.1021/acscatal.6b01914
63. Kim, H.; Lee, C. *Angew. Chem., Int. Ed.* **2012,** *51,* 12303–12306. doi:10.1002/anie.201203599
64. Quiclet-Sire, B.; Zard, S. Z. *Org. Lett.* **2008,** *10,* 3279–3282. doi:10.1021/ol801162m
65. Gagosz, F.; Zard, S. Z. *Org. Lett.* **2003,** *5,* 2655–2657. doi:10.1021/ol034812m

License and Terms

The definitive version of this article is the electronic one which can be found at:
doi:10.3762/bjoc.14.283

BEILSTEIN JOURNAL OF ORGANIC CHEMISTRY

Tandem copper and photoredox catalysis in photocatalytic alkene difunctionalization reactions

Nicholas L. Reed, Madeline I. Herman, Vladimir P. Miltchev and Tehshik P. Yoon*

Letter

Open Access

Address:
Department of Chemistry, University of Wisconsin–Madison, 1101 University Avenue, Madison, Wisconsin 53706, United States

Email:
Tehshik P. Yoon* - tyoon@chem.wisc.edu

* Corresponding author

Keywords:
copper; diamination; oxidative functionalization; oxyamination; photoredox catalysis; radical

Beilstein J. Org. Chem. **2019,** *15,* 351–356.
doi:10.3762/bjoc.15.30

Received: 13 November 2018
Accepted: 22 January 2019
Published: 05 February 2019

This article is part of the thematic issue "Reactive intermediates part I: radicals".

Associate Editor: C. Stephenson

Abstract

Oxidative alkene difunctionalization reactions are important in synthetic organic chemistry because they can install polar functional groups onto simple non-polar alkene moieties. Many of the most common methods for these reactions rely upon the reactivity of pre-oxidized electrophilic heteroatom donors that can often be unstable, explosive, or difficult to handle. Herein, we describe a method for alkene oxyamination and diamination that utilizes simple carbamate and urea groups as nucleophilic heteroatom donors. This method uses a tandem copper–photoredox catalyst system that is operationally convenient. The identity of the terminal oxidant is critical in these studies. Ag(I) salts proved to be unique in their ability to turn over the copper cocatalyst without deleteriously impacting the reactivity of the organoradical intermediates.

Introduction

Over the past decade, a renewed interest in synthetic photochemistry has resulted in the discovery of a broad range of powerful new bond-forming transformations [1-4]. Much of this work has been premised on the ability of visible light-activated photocatalysts to generate highly reactive odd-electron intermediates via photoinduced electron transfer processes. A major theme of research that has emerged from these studies is the application of various cocatalysts to intercept the organoradical intermediates of photoredox reactions and modulate their subsequent reactivity [5,6]. The combination of photoredox catalysis with transition metals, Lewis acids, and organocatalysts has been productively utilized in asymmetric transformations [7-9], cross-couplings [10-12], and oxidative decarboxylation reactions [13,14], among others. The use of a cocatalyst to control these photochemical transformations enables reactions that are not accessible from the native reactivity of the organoradical intermediates by themselves.

Our laboratory is interested in the design of photochemical strategies for oxidative functionalization reactions [15,16]. We recently described [17] a new approach to alkene difunctionalization that combines the photoredox activation of electron-rich

alkenes with copper(II)-mediated oxidation of electron-rich radicals as described by Kochi [18-20]. These studies resulted in the development of a general new protocol for oxyamination (Figure 1a) and diamination (Figure 1b) of alkenes. The mechanism we have proposed for photocatalytic oxyamination is outlined in Figure 1c. Photoinduced one-electron oxidation of an appropriately electron-rich styrene **1** results in the formation of a radical cation $\mathbf{1}^{\bullet+}$ that is susceptible to attack by various heteroatomic nucleophiles, including carbamates [21,22]. Subsequent oxidation of radical **7** by Cu(II) affords a formally cationic intermediate that is trapped by the carbamoyl oxygen to afford oxonium **8**. The loss of the *tert*-butyl cation provides the oxyamination product **2**, which can be isolated in good yields with excellent diastereoselectivity. Turnover of the photocatalyst can be coupled to the reduction of Cu(I) to Cu(0), which can be observed precipitating from solution over the course of the reaction.

Copper(II) salts have been demonstrated to be convenient terminal oxidants in a variety of synthetically useful catalytic reactions [23-26]. They are easily handled, are available from commodity chemicals for nominal cost, and present minimal environmental and health concerns in large-scale applications. The use of stoichiometric copper(II) reagents, however, could become prohibitive in certain applications where specific, synthetically laborious ligand sets might be required, as in enantioselective catalytic oxidation reactions or certain cross-coupling applications. We wondered, therefore, if catalytic loadings of copper(II) salts might be used in these reactions by adding a secondary terminal oxidant to turn over the intermediate

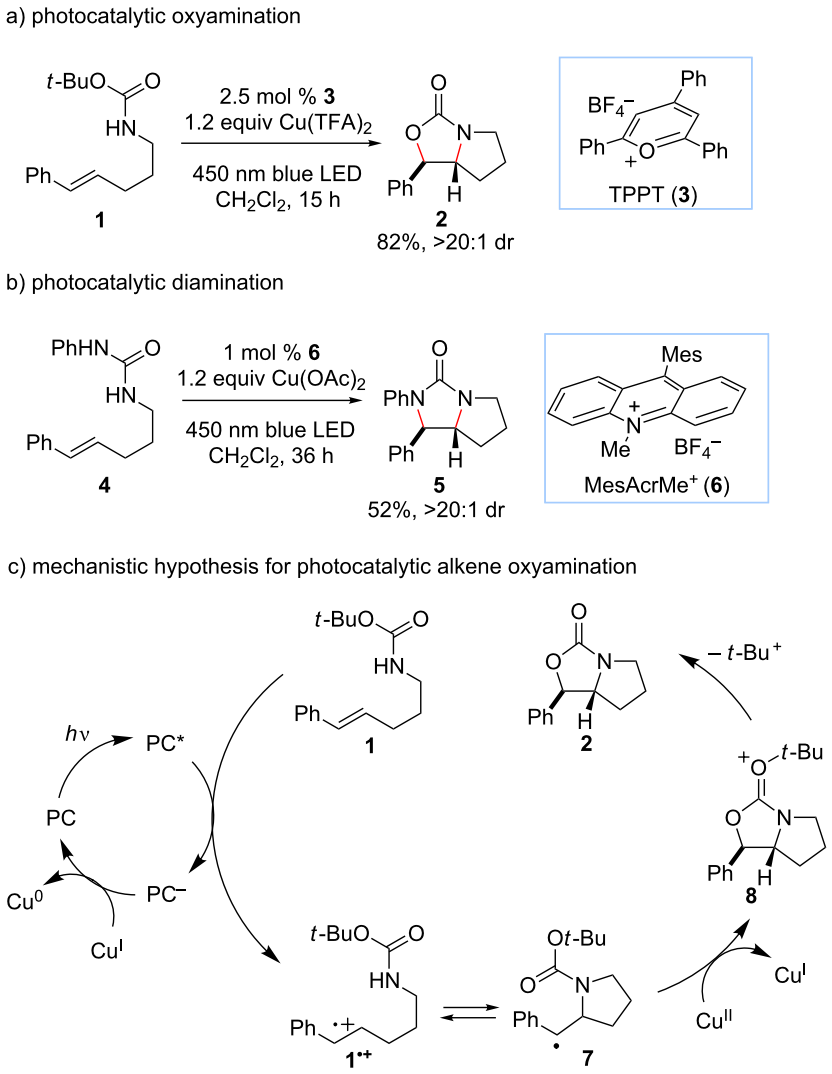

Figure 1: a) Photocatalytic oxyamination, b) photocatalytic diamination, and c) proposed mechanism for photocatalytic oxyamination using copper(II) as a terminal oxidant.

copper(I) complex. We describe herein the results of this investigation, which has led to the identification of a tandem photoredox copper(II) catalytic system for the net-oxidative difunctionalization of alkenes.

Results and Discussion

A range of mild oxidants can oxidize copper(I) to copper(II), and the use of dioxygen for this purpose is frequently exploited to effect synthetically useful copper-catalyzed aerobic oxidation reactions [27,28]. However, the use of molecular oxygen as a terminal oxidant presents unique challenges in photoredox chemistry. Triplet dioxygen rapidly quenches the excited state of most common photoredox catalysts [29-31], decreasing their effective lifetimes and producing singlet dioxygen or superoxide, which can react destructively with many common organic functional groups. Moreover, the organoradical intermediates that characterize much of photoredox chemistry can react rapidly with ground-state dioxygen to afford unstable hydroperoxy radicals that can also decompose unproductively [32,33]. Indeed, in our previous study of photocatalytic alkene difunctionalization, we found that dioxygen and similar commonly used terminal oxidants resulted in unproductive decomposition of the substrates [17], and that Cu(II) oxidants were uniquely suitable in this application. At the outset of this investigation, therefore, we imagined that the identification of a co-oxidant for use with catalytic Cu(II) might face similar practical constraints. Ideally, we hoped to identify a terminal oxidant that would be compatible with the chemistry of the radical intermediates, would not generate any highly reactive oxygen species, and would not produce toxic or chromatographically problematic byproducts.

As a starting point for our optimization studies, we examined the intramolecular oxyamination of carbamate **1** (Table 1), a reaction we had previously studied under stoichiometric Cu(II) conditions and found to proceed in good yield using 2.5 mol % 2,4,6-triphenylpyrylium tetrafluoroborate (TPPT, **3**) as a photocatalyst and 1.2 equiv of $Cu(TFA)_2$ as a stoichiometric oxidant. We lowered the loading of $Cu(TFA)_2$ to 10 mol % and assessed the effect of a series of alternate oxidants that have been used in other copper-catalyzed oxidation reactions. Most failed to produce significant quantities of the desired product (Table 1, entries 1–3). As expected, the use of oxygen as a terminal oxidant resulted in rapid conversion of **1** to an intractable mixture of decomposition products, with only trace formation of the desired oxyamination product (Table 1, entry 1). Other oxidants afforded less decomposition but were not effective in turning over the Cu(II) cocatalyst (Table 1, entries 2 and 3). Of all of the oxidants screened, silver(I) salts were found to be uniquely effective at mediating turnover of the copper(II) catalyst [34-36]. After screening commercially available silver(I) salts, Ag_2CO_3 was found to be the optimal terminal oxidant (Table 1, entry 5). There is a competitive silver-mediated photodecomposition process that consumes the starting alkene unproductively, and thus the copper(II)/silver(I) ratio was tuned to optimize the efficiency of the desired oxyamination process (Table 1, entries

Table 1: Optimization of dual-catalytic reaction conditions[a].

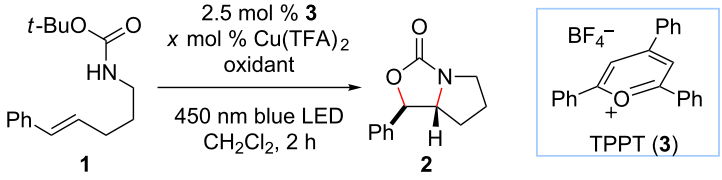

entry	$Cu(TFA)_2$ (mol %)	oxidant	yield[b]
1	10	air	8%
2	10	$K_2S_2O_8$ (3 equiv)	trace
3	10	MnO_2 (3 equiv)	9%
4	10	Ag_2O (3 equiv)	25%
5	10	Ag_2CO_3 (3 equiv)	43%
6	30	Ag_2CO_3 (3 equiv)	54%
7	**30**	**Ag_2CO_3 (1 equiv)**	**70%**
8	0	Ag_2CO_3 (1 equiv)	7%
9	30	none	10%
10[c]	30	Ag_2CO_3 (1 equiv)	3%
11[d]	30	Ag_2CO_3 (1 equiv)	trace

[a]All reactions were conducted in degassed CH_2Cl_2 and irradiated with a 15 W blue LED flood lamp for 2 h. [b]Yields were determined by ^1H NMR analysis of the unpurified reaction mixtures using phenanthrene as an internal standard. [c]No TPPT. [d]No light.

5–7). Optimal conditions were found to be 2.5 mol % TPPT, 30 mol % $Cu(TFA)_2$, and 1 equiv Ag_2CO_3 in CH_2Cl_2 (Table 1, entry 7). Finally, control experiments validated the necessity of each reaction component. Minimal product formation was observed when $Cu(TFA)_2$, Ag_2CO_3, TPPT, or light were omitted from the reaction (Table 1, entries 8–11), confirming that the combination of photoredox and copper(II) catalysis is critical to achieve good reactivity.

We found that these optimized reaction conditions are applicable to both oxyamination and diamination reactions. Experiments probing the scope of these transformations are summarized in Figure 2. A range of styrenes bearing varying electron-donating and electron-withdrawing substituents smoothly undergo oxyamination (**9**–**12**), as do *ortho*-substituted styrenes (**13**). The presence of an electron-rich heterocycle is also tolerated (**14**), without any evidence of oxidative decomposition of this sensitive functional group. Modifications to the alkyl tether (**15**) did not adversely affect the reaction. Intermolecular oxyamination of styrenes is also feasible using these conditions. While simple styrenes polymerize rapidly under these conditions, a range of β-substituted styrenes undergo smooth oxyamination using *tert*-butyl carbamate as the nucleophilic nitrogen atom source (**16**–**18**). Finally, alkene diamination is also readily achieved using *N*-phenylureas as nucleophiles, although acridinium photocatalyst **6** afforded modestly higher yields in these reactions (**19**–**21**).

A complete mechanistic picture of this reaction will require additional experimentation; however, control experiments demonstrate that Ag_2CO_3 is not a competent terminal oxidant on its own (Table 1, entry 9) and that the presence of Cu(II) is critical for the oxyamination to occur (Table 1, entry 8). Moreover, our previous studies demonstrated that Cu(II) can serve as a competent terminal oxidant in a stoichiometric fashion. Thus, it seems clear that the role of the Ag(I) additive in this reaction is to re-oxidize Cu(I) to Cu(II), and that the Cu(II) salt in this transformation is indeed a cocatalyst for the oxidative difunctionalization of styrenes. Efforts to render this transformation enantioselective by utilizing chiral Cu(II) complexes have thus far not been successful. A screen of several classes of privileged ligands for asymmetric copper catalysis produced only racemic oxyamination products. We interpret this observation as an indication that Cu(II) is unable to control the stereochemistry of the C–N bond-forming step, as one might expect from its proposed role in radical oxidation (Figure 1C).

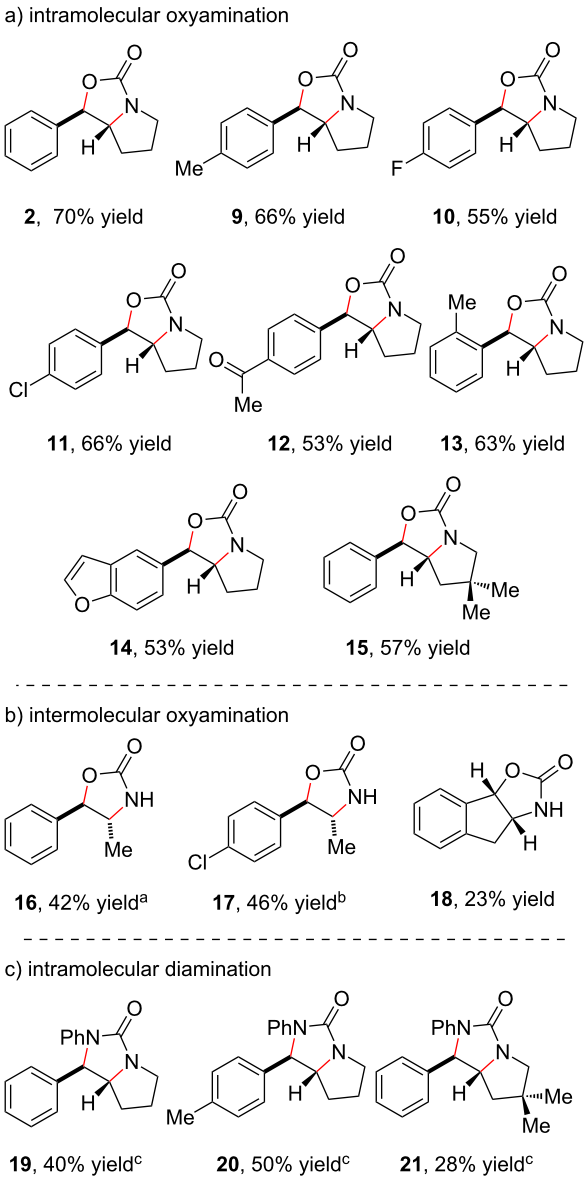

Figure 2: Scope studies for dual-catalytic alkene difunctionalization using 2.5 mol % **3**, 30 mol % $Cu(TFA)_2$, and a 15 W blue flood lamp. Diastereomer ratios >20:1 unless otherwise noted. [a]3:1 dr. [b]10:1 dr. [c]Reaction conducted using $MesAcrMe^+$ (**6**) as photocatalyst.

Conclusion

These studies have demonstrated that the copper-mediated alkene difunctionalization reactions recently reported by our laboratory can be rendered catalytic in Cu(II) by adding a secondary terminal oxidant, and that Ag(I) salts appear to be uniquely effective in this capacity. This work thus provides a platform for the development of enantioselective photocatalytic alkene difunctionalization reactions that can use a chiral Cu(II) complex as a substoichiometric catalyst rather than as a terminal oxidant. Moreover, much of the utility of photoredox catalysis has been predicated on its ability to generate radical intermediates under mild and operationally convenient conditions. The ability to intercept transient photogenerated organoradical intermediates and divert them towards carbocation reactivity is an intriguing paradigm for the expansion of photoredox chemistry

towards net oxidative transformations. Current studies in our laboratory are investigating the further application of copper cocatalysts to a wide range of alternate photoredox-mediated oxidative transformations.

Supporting Information

Supporting Information File 1

Full experimental details for all reactions.
[https://www.beilstein-journals.org/bjoc/content/supplementary/1860-5397-15-30-S1.pdf]

Acknowledgements

This work was funded by the NIH (GM095666). The mass spectroscopy facilities at UW–Madison are funded in part by the NIH (S10 OD020022), as are the NMR facilities (S10 OD012245).

ORCID® iDs

Nicholas L. Reed - https://orcid.org/0000-0003-4234-5464
Madeline I. Herman - https://orcid.org/0000-0003-1156-2968
Tehshik P. Yoon - https://orcid.org/0000-0002-3934-4973

References

1. Narayanam, J. M. R.; Stephenson, C. R. J. *Chem. Soc. Rev.* **2011,** *40,* 102–113. doi:10.1039/b913880n
2. Prier, C. K.; Rankic, D. A.; MacMillan, D. W. C. *Chem. Rev.* **2013,** *113,* 5322–5363. doi:10.1021/cr300503r
3. Romero, N. A.; Nicewicz, D. A. *Chem. Rev.* **2016,** *116,* 10075–10166. doi:10.1021/acs.chemrev.6b00057
4. Zou, Y.-Q.; Hörmann, F. M.; Bach, T. *Chem. Soc. Rev.* **2018,** *47,* 278–290. doi:10.1039/c7cs00509a
5. Skubi, K. L.; Blum, T. R.; Yoon, T. P. *Chem. Rev.* **2016,** *116,* 10035–10074. doi:10.1021/acs.chemrev.6b00018
6. Twilton, J.; Le, C.; Zhang, P.; Shaw, M. H.; Evans, R. W.; MacMillan, D. W. C. *Nat. Rev. Chem.* **2017,** *1,* No. 0052. doi:10.1038/s41570-017-0052
7. Nicewicz, D. A.; MacMillan, D. W. C. *Science* **2008,** *322,* 77–80. doi:10.1126/science.1161976
8. Rono, L. J.; Yayla, H. G.; Wang, D. Y.; Armstrong, M. F.; Knowles, R. R. *J. Am. Chem. Soc.* **2013,** *135,* 17735–17738. doi:10.1021/ja4100595
9. Du, J.; Skubi, K. L.; Schultz, D. M.; Yoon, T. P. *Science* **2014,** *344,* 392–396. doi:10.1126/science.1251511
10. Ye, Y.; Sanford, M. S. *J. Am. Chem. Soc.* **2012,** *134,* 9034–9037. doi:10.1021/ja301553c
11. Tellis, J. C.; Primer, D. N.; Molander, G. A. *Science* **2014,** *345,* 433–436. doi:10.1126/science.1253647
12. Zuo, Z.; Ahneman, D. T.; Chu, L.; Terrett, J. A.; Doyle, A. G.; MacMillan, D. W. C. *Science* **2014,** *345,* 437–440. doi:10.1126/science.1255525
13. Tlahuext-Aca, A.; Candish, L.; Garza-Sanchez, R. A.; Glorius, F. *ACS Catal.* **2018,** *8,* 1715–1719. doi:10.1021/acscatal.7b04281
14. Sun, X.; Chen, J.; Ritter, T. *Nat. Chem.* **2018,** *10,* 1229–1233. doi:10.1038/s41557-018-0142-4
15. Parrish, J. D.; Ischay, M. A.; Lu, Z.; Guo, S.; Peters, N. R.; Yoon, T. P. *Org. Lett.* **2012,** *14,* 1640–1643. doi:10.1021/ol300428q
16. Blum, T. R.; Zhu, Y.; Nordeen, S. A.; Yoon, T. P. *Angew. Chem., Int. Ed.* **2014,** *53,* 11056–11059. doi:10.1002/anie.201406393
17. Reed, N. L.; Herman, M. I.; Miltchev, V. P.; Yoon, T. P. *Org. Lett.* **2018,** *20,* 7345–7350. doi:10.1021/acs.orglett.8b03345
18. Kochi, J. K.; Bemis, A. *J. Am. Chem. Soc.* **1968,** *90,* 4038–4051. doi:10.1021/ja01017a022
19. Kochi, J. K.; Bemis, A.; Jenkins, C. L. *J. Am. Chem. Soc.* **1968,** *90,* 4616–4625. doi:10.1021/ja01019a018
20. Jenkins, C. L.; Kochi, J. K. *J. Am. Chem. Soc.* **1972,** *94,* 856–865. doi:10.1021/ja00758a025
21. Nguyen, T. M.; Manohar, N.; Nicewicz, D. A. *Angew. Chem., Int. Ed.* **2014,** *53,* 6198–6201. doi:10.1002/anie.201402443
22. Margrey, K. A.; Nicewicz, D. A. *Acc. Chem. Res.* **2016,** *49,* 1997–2006. doi:10.1021/acs.accounts.6b00304
23. Zabawa, T. P.; Kasi, D.; Chemler, S. R. *J. Am. Chem. Soc.* **2005,** *127,* 11250–11251. doi:10.1021/ja053335v
24. Baran, P. S.; DeMartino, M. P. *Angew. Chem., Int. Ed.* **2006,** *45,* 7083–7086. doi:10.1002/anie.200603024
25. Stuart, D. R.; Fagnou, K. *Science* **2007,** *316,* 1172–1175. doi:10.1126/science.1141956
26. Hyster, T. K.; Rovis, T. *J. Am. Chem. Soc.* **2010,** *132,* 10565–10569. doi:10.1021/ja103776u
27. Wendlandt, A. E.; Suess, A. M.; Stahl, S. S. *Angew. Chem., Int. Ed.* **2011,** *50,* 11062–11087. doi:10.1002/anie.201103945
28. McCann, S. D.; Stahl, S. S. *Acc. Chem. Res.* **2015,** *48,* 1756–1766. doi:10.1021/acs.accounts.5b00060
29. Winterle, J. S.; Kliger, D. S.; Hammond, G. S. *J. Am. Chem. Soc.* **1976,** *98,* 3719–3721. doi:10.1021/ja00428a062
30. Srinivasan, V. S.; Podolski, D.; Westrick, N. J.; Neckers, D. C. *J. Am. Chem. Soc.* **1978,** *100,* 6513–6515. doi:10.1021/ja00488a048
31. Takizawa, S.-y.; Aboshi, R.; Murata, S. *Photochem. Photobiol. Sci.* **2011,** *10,* 895–903. doi:10.1039/c0pp00265h
32. Maillard, B.; Ingold, K. U.; Scaiano, J. C. *J. Am. Chem. Soc.* **1983,** *105,* 5095–5099. doi:10.1021/ja00353a039
33. Ohkubo, K.; Nanjo, T.; Fukuzumi, S. *Org. Lett.* **2005,** *7,* 4265–4268. doi:10.1021/ol051696+
34. Wang, Z.; Ni, J.; Kuninobu, Y.; Kanai, M. *Angew. Chem., Int. Ed.* **2014,** *53,* 3496–3499. doi:10.1002/anie.201311105
35. Rao, W.-H.; Shi, B.-F. *Org. Lett.* **2015,** *17,* 2784–2787. doi:10.1021/acs.orglett.5b01198
36. Wang, F.; Hu, Q.; Shu, C.; Lin, Z.; Min, D.; Shi, T.; Zhang, W. *Org. Lett.* **2017,** *19,* 3636–3639. doi:10.1021/acs.orglett.7b01559

BEILSTEIN JOURNAL OF ORGANIC CHEMISTRY

A diastereoselective approach to axially chiral biaryls via electrochemically enabled cyclization cascade

Hong Yan[1], Zhong-Yi Mao[1], Zhong-Wei Hou[1], Jinshuai Song[2] and Hai-Chao Xu[*1]

Letter

Open Access

Address:
[1]State Key Laboratory of Physical Chemistry of Solid Surfaces, Key Laboratory of Chemical Biology of Fujian Province, iChEM and College of Chemistry and Chemical Engineering, Xiamen University, People's Republic of China and [2]College of Chemistry and Molecular Engineering, Zhengzhou University, Zhengzhou 450001, People's Republic of China

Email:
Hai-Chao Xu[*] - haichao.xu@xmu.edu.cn

* Corresponding author

Keywords:
axial chirality; biaryl; electrochemistry; oxidation; radical

Beilstein J. Org. Chem. **2019,** *15,* 795–800.
doi:10.3762/bjoc.15.76

Received: 03 January 2019
Accepted: 16 March 2019
Published: 28 March 2019

This article is part of the thematic issue "Reactive intermediates part I: radicals".

Guest Editor: T. P. Yoon

Abstract

A diastereoselective approach to axially chiral imidazopyridine-containing biaryls has been developed. The reactions proceed through a radical cyclization cascade to construct the biaryls with good to excellent central-to-axial chirality transfer.

Introduction

Axially chiral biaryls are prevalent in natural products, bioactive molecules and organocatalysts [1,2]. Among the many methods that have been developed for the synthesis of chiral biaryls [3-10], reactions that take avantage of the central-to-axial chirality transfer have been less explored [11-14]. In addition, an antroposelective synthesis of imidazopyridine-based biaryls has not been reported.

Nitrogen-centered radicals (NCRs) are attractive reactive intermediates for organic synthesis as they provide opportunities for the efficient construction of C–N bonds [15-19]. Recently, the generation of NCRs through electron transfer-based methods has been attracting attention. Organic electrochemistry is a powerful tool for adding or taking electrons from organic molecules to promote redox reactions because of its reagent-free feature and the tunability of electric current and potential [20-30]. We [31-34] and others [35-41] have studied the reactions of electrochemically generated NCRs. Particularly, we have recently reported an electrochemical synthesis of imidazo-fused N-heteroaromatic compounds via a radical cyclization cascade [31]. Building on this work, we report herein an atroposelective synthesis of imidazopyridine-containing biaryls via central-to-axial chirality transfer (Scheme 1).

Results and Discussion

The substituents on the phenyl ring (R^1) and at the propargylic position (R^2) of carbamate **2** were varied to study their effects on the diastereoselectivity (Table 1). The electrolysis was con-

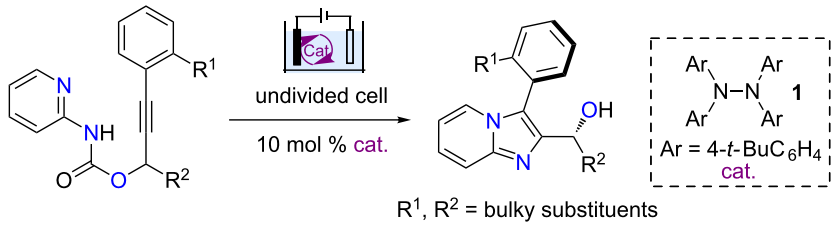

Scheme 1: Reaction design.

Table 1: Investigation on the effects of substituents on the diastereoselectivity.[a]

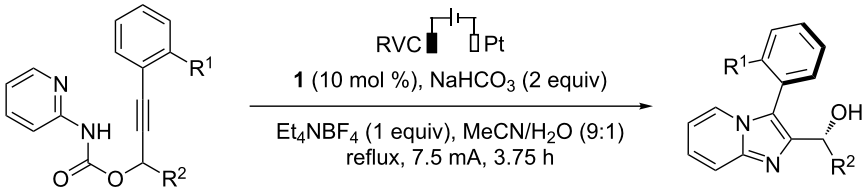

2a–d **3a–d**

Entry	Substrate	Product, yield,[b] dr[c]
1	**2a** (R^1 = *t*-Bu, R^2 = *t*-Bu)	(±)-**3a**, 68%, 14:1 dr
2	**2b** (R^1 = *t*-Bu, R^2 = iPr)	(±)-**3b**, 64%, 3:1 dr
3	**2c** (R^1 = Ph, R^2 = *t*-Bu)	(±)-**3c**, 73%, 2:1 dr
4	**2d** (R^1 = OiPr, R^2 = *t*-Bu)	(±)-**3d**, 78%, 3:1 dr

[a]Reaction conditions: undivided cell, **1** (0.03 mmol), **2** (0.3 mmol), H_2O (1 mL), MeCN (9 mL), 3.5 F mol^{-1}. [b]Isolated yield. [c]Determined by ^1H NMR analysis of the crude reaction mixture.

ducted under previously established conditions employing a three-necked round-bottomed flask as the cell, a reticulated vitreous carbon (RVC) anode and a platinum plate cathode [31]. The reaction was carried in refluxing MeCN/H_2O (9:1) with tetraarylhydrazine **1** as the redox catalyst, $NaHCO_3$ (2 equiv) as an additive, and Et_4NBF_4 (1 equiv) as the supporting electrolyte. These investigations indicated that bulky tertiary groups at both R^1 and R^2 positions were needed to ensure efficient chirality transfer. Hence, carbamate **2a** (Table 1, entry 1) bearing a *t*-Bu group at R^1 and R^2 positions, respectively, reacted to give imidazopyridine-based biaryl **3a** in 68% yield with good diastereoselectivity (14:1 dr). Replacing the *t*-Bu group at the propargylic position with iPr (Table 1, entry 2) or on the phenyl ring with Ph (Table 1, entry 3) or OiPr (Table 1, entry 4) all resulted in low diastereoselectivity (2:1 to 3:1).

The scope of the electrosynthesis was investigated by varying the peripheral substituents of the carbamate substrate **2** (Scheme 2). The pyridyl ring could be substituted at positions 4, 5 and 6 with a range of substituents with diverse electronic properties such as OMe (**3e**), Br (**3f**), CF_3 (**3g**), CN (**3h**), Cl (**3i**), and Me (**3j**). Pyridyl rings bearing multiple substituents were also tolerated (**3k** and **3l**). The stereochemistry of the biaryl product was determined by obtaining an X-ray crystal structure of **3k**. The *t*-Bu-substituted phenyl ring on the alkyne moiety containing an extra OMe (**3m**) or Me (**3n** and **3o**) group was tolerated albeit with reduced diastereoselectivity. The *t*-Bu group on the phenyl ring and at the propargylic position could be replaced with other bulky tertiary substituents to afford a range of functionalized biaryl products (**3p**–**w**). The electrochemical conditions were compatible with several functional groups including aryltrimethylsilane (**3p**), silyl ether (**3q**–**s**), ester (**3t**) and cylic ketal (**3u**). Note that all the diastereomers were separable by flash column chromatography.

Heating a solution of the major isomer of **3n** in MeCN at 80 °C for 4 h did not lead to isomerization, suggesting that the stereoselectivity of the reaction was not controlled by relative thermodynamic stability of the diastereomers. The major isomer of **3c**, which contained a sterically less demanding Ph group at the R^1 position (cf. Table 1), did not isomerize at room temperature for 1 year. However, heating a solution of this compound in MeCN

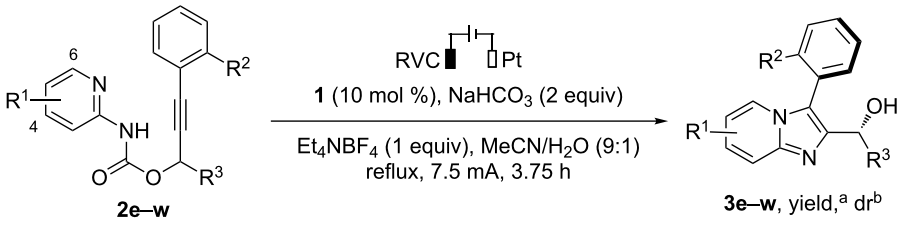

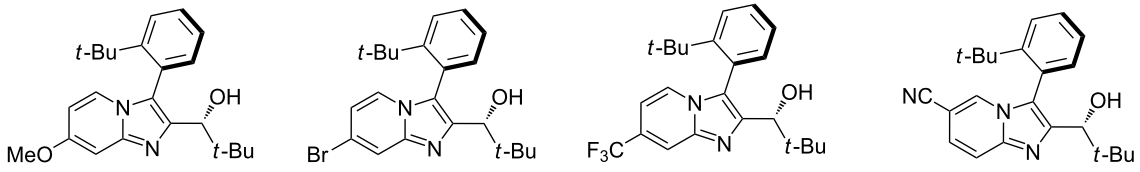
(±)-**3e**, 76%, 8:1 dr

(±)-**3f**, 66%, 11:1 dr

(±)-**3g**, 80%, 11:1 dr

(±)-**3h**, 62%, 12:1 dr

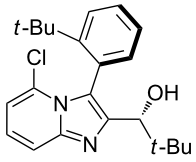
(±)-**3i**, 82%, 14:1 dr

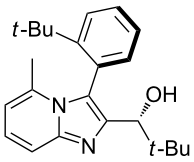
(±)-**3j**, 78%, 8:1 dr

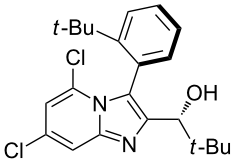
(±)-**3k**, 48%, >20:1 dr

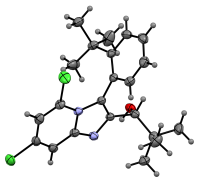
X-ray (**3k**)
[CCDC 1888229]

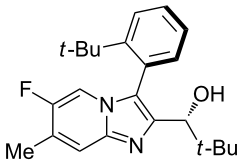
(±)-**3l**, 65%, 10:1 dr

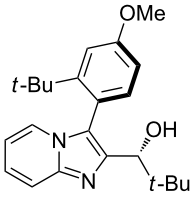
(±)-**3m**, 91%,c 5:1 dr

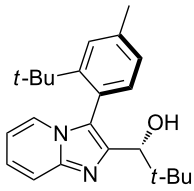
(±)-**3n**, 82%,c 7:1 dr

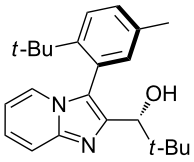
(±)-**3o**, 75%, 10:1 dr

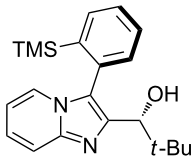
(±)-**3p**, 83%, 6:1 dr

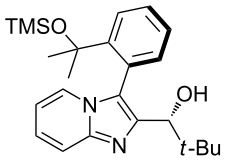
(±)-**3q**, 88%, 9:1 dr

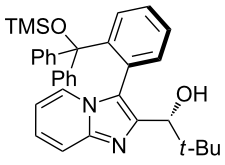
(±)-**3r**, 43%, >20:1 dr

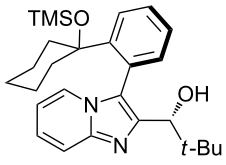
(±)-**3s**, 55%, 10:1 dr

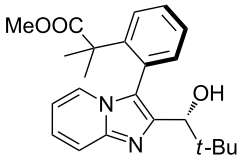
(±)-**3t**, 96%, >20:1 dr

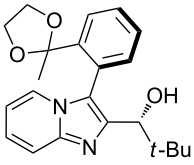
(±)-**3u**, 72%, 10:1 dr

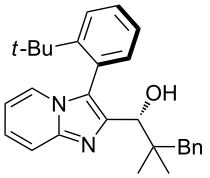
(±)-**3v**, 70%, 9:1 dr

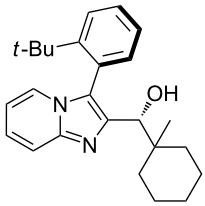
(±)-**3w**, 64%, 8:1 dr

Scheme 2: Scope of electrochemical synthesis of axially chiral biaryls. Reaction conditions: undivided cell, **2** (0.3 mmol), H_2O (1 mL), MeCN (9 mL), 3.5 F mol^{-1}. [a]Isolated yield of the major diastereomer. [b]Determined by ^1H NMR analysis of crude reaction mixture. [c]Combined yield of the two diastereomers.

at 80 °C for 4 h resulted in a mixture of diastereomers in a ratio of 3:1. These results suggest that the sterically demanding substituents at R^1 and R^2 positions (cf. Table 1) are critical to ensure good stereoselectivity during the product formation and to prevent isomerization after the reaction.

A mechanism for the electrochemical synthesis was proposed based on the results from our previous work [31] and of this work (Scheme 3). The redox catalyst **1** is oxidized at the anode to give radical cation **I**. In the meanwhile, H_2O is reduced at the cathode to afford HO^- and H_2. The base generated at the cathode deprotonates **2a** to give its conjugate base **II**. The anionic **II** is oxidized by radical cation **I** through single electron transfer (SET) to give radical intermediate **III**, which undergoes a biscyclization to give **V**. Further oxidation of **V** followed by hydrolysis of the cyclic carbamate moiety leads to the formation of **3a**.

Based on the proposed reaction mechanism and the results mentioned above, the cyclization of vinyl radical **IV** to give **V** is the atroposelective step. Density functional theory (DFT)-based calculations suggested that the cyclization of **IV** could be explained by a Curtin–Hammett scenario (Scheme 4) [42]. Specifically, the equilibrium of the conformations **IV** and **IV′** is

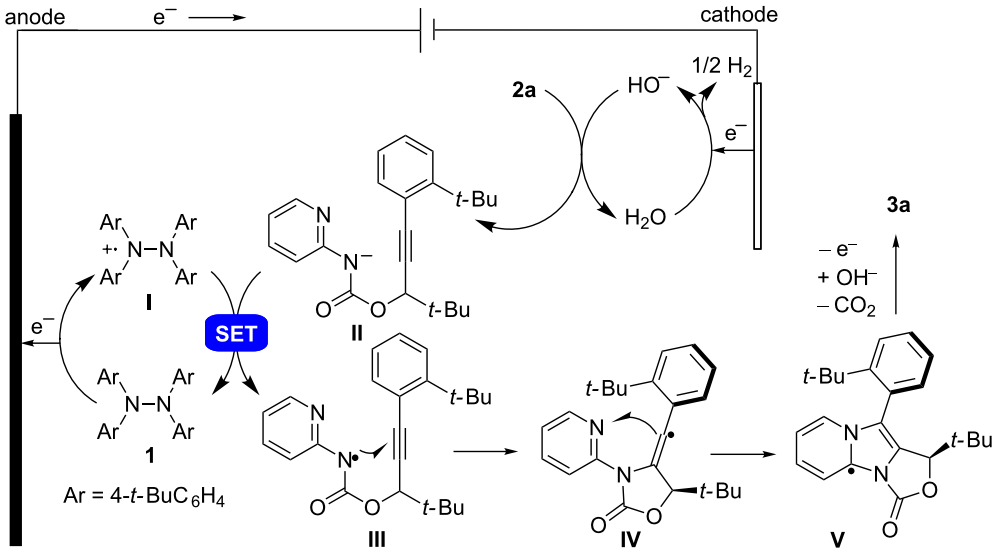

Scheme 3: Proposed reaction mechanism for the electrochemical synthesis of **3a**.

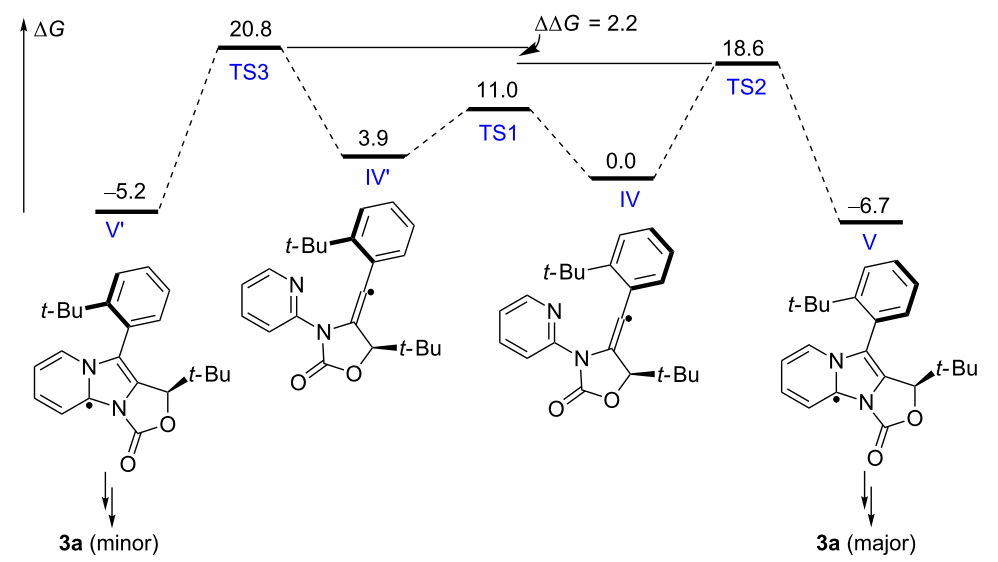

Scheme 4: Computation investigation on the vinyl radical cyclization. DFT (M06-2X/6-31G*) calculated energetics (kcal mol^{-1}) are Gibbs free energies in MeCN.

much faster than their respectively cyclizations to give **V** and **V′**. Since **TS2** is relatively lower in energy than **TS3**, **V** is formed as the major product.

Conclusion

In summary, we have developed a diastereoselective approach for the synthesis of axially chiral biaryls through an electricity-powered cyclization cascade. The reactions employ easily assembled starting materials and afford functionalized imidazo-pyridine-based biaryls in good to high yields and diastereoselectivity.

Supporting Information

Supporting Information File 1

Experimental part.
[https://www.beilstein-journals.org/bjoc/content/supplementary/1860-5397-15-76-S1.pdf]

Acknowledgements

Financial support of this research from MOST (2016YFA0204100), NSFC (21672178), and the Fundamental Research Funds for the Central Universities, is acknowledged.

ORCID® iDs

Jinshuai Song - https://orcid.org/0000-0002-1909-9253
Hai-Chao Xu - https://orcid.org/0000-0002-3008-5143

References

1. Bringmann, G.; Gulder, T.; Gulder, T. A. M.; Breuning, M. *Chem. Rev.* **2011,** *111,* 563–639. doi:10.1021/cr100155e
2. Pu, L. *Chem. Rev.* **1998,** *98,* 2405–2494. doi:10.1021/cr970463w
3. Tanaka, K. *Chem. – Asian J.* **2009,** *4,* 508–518. doi:10.1002/asia.200800378
4. Wallace, T. W. *Org. Biomol. Chem.* **2006,** *4,* 3197–3210. doi:10.1039/b608470m
5. Bringmann, G.; Price Mortimer, A. J.; Keller, P. A.; Gresser, M. J.; Garner, J.; Breuning, M. *Angew. Chem., Int. Ed.* **2005,** *44,* 5384–5427. doi:10.1002/anie.200462661
6. Ma, G.; Sibi, M. P. *Chem. – Eur. J.* **2015,** *21,* 11644–11657. doi:10.1002/chem.201500869
7. Link, A.; Sparr, C. *Chem. Soc. Rev.* **2018,** *47,* 3804–3815. doi:10.1039/c7cs00875a
8. Wang, Y.-B.; Tan, B. *Acc. Chem. Res.* **2018,** *51,* 534–547. doi:10.1021/acs.accounts.7b00602
9. Yang, H.; Yang, X.; Tang, W. *Tetrahedron* **2016,** *72,* 6143–6174. doi:10.1016/j.tet.2016.08.042
10. Wencel-Delord, J.; Panossian, A.; Leroux, F. R.; Colobert, F. *Chem. Soc. Rev.* **2015,** *44,* 3418–3430. doi:10.1039/c5cs00012b
11. Raut, V. S.; Jean, M.; Vanthuyne, N.; Roussel, C.; Constantieux, T.; Bressy, C.; Bugaut, X.; Bonne, D.; Rodriguez, J. *J. Am. Chem. Soc.* **2017,** *139,* 2140–2143. doi:10.1021/jacs.6b11079
12. Vorogushin, A. V.; Wulff, W. D.; Hansen, H.-J. *J. Am. Chem. Soc.* **2002,** *124,* 6512–6513. doi:10.1021/ja0201505
13. Guo, F.; Konkol, L. C.; Thomson, R. J. *J. Am. Chem. Soc.* **2011,** *133,* 18–20. doi:10.1021/ja108717r
14. Qiu, L.; Kwong, F. Y.; Wu, J.; Lam, W. H.; Chan, S.; Yu, W.-Y.; Li, Y.-M.; Guo, R.; Zhou, Z.; Chan, A. S. C. *J. Am. Chem. Soc.* **2006,** *128,* 5955–5965. doi:10.1021/ja0602694
15. Kärkäs, M. D. *Chem. Soc. Rev.* **2018,** *47,* 5786–5865. doi:10.1039/c7cs00619e
16. Zhao, Y.; Xia, W. *Chem. Soc. Rev.* **2018,** *47,* 2591–2608. doi:10.1039/c7cs00572e
17. Chen, J.-R.; Hu, X.-Q.; Lu, L.-Q.; Xiao, W.-J. *Chem. Soc. Rev.* **2016,** *45,* 2044–2056. doi:10.1039/c5cs00655d
18. Zard, S. Z. *Chem. Soc. Rev.* **2008,** *37,* 1603–1618. doi:10.1039/b613443m
19. Xiong, T.; Zhang, Q. *Chem. Soc. Rev.* **2016,** *45,* 3069–3087. doi:10.1039/c5cs00852b
20. Yan, M.; Kawamata, Y.; Baran, P. S. *Chem. Rev.* **2017,** *117,* 13230–13319. doi:10.1021/acs.chemrev.7b00397
21. Wiebe, A.; Gieshoff, T.; Möhle, S.; Rodrigo, E.; Zirbes, M.; Waldvogel, S. R. *Angew. Chem., Int. Ed.* **2018,** *57,* 5594–5619. doi:10.1002/anie.201711060
22. Möhle, S.; Zirbes, M.; Rodrigo, E.; Gieshoff, T.; Wiebe, A.; Waldvogel, S. R. *Angew. Chem., Int. Ed.* **2018,** *57,* 6018–6041. doi:10.1002/anie.201712732
23. Feng, R.; Smith, J. A.; Moeller, K. D. *Acc. Chem. Res.* **2017,** *50,* 2346–2352. doi:10.1021/acs.accounts.7b00287
24. Moeller, K. D. *Chem. Rev.* **2018,** *118,* 4817–4833. doi:10.1021/acs.chemrev.7b00656
25. Yan, M.; Kawamata, Y.; Baran, P. S. *Angew. Chem., Int. Ed.* **2018,** *57,* 4149–4155. doi:10.1002/anie.201707584
26. Yang, Q.-L.; Fang, P.; Mei, T.-S. *Chin. J. Chem.* **2018,** *36,* 338–352. doi:10.1002/cjoc.201700740
27. Tang, S.; Liu, Y.; Lei, A. *Chem* **2018,** *4,* 27–45. doi:10.1016/j.chempr.2017.10.001
28. Yoshida, J.-i.; Kataoka, K.; Horcajada, R.; Nagaki, A. *Chem. Rev.* **2008,** *108,* 2265–2299. doi:10.1021/cr0680843
29. Jiang, Y.; Xu, K.; Zeng, C. *Chem. Rev.* **2018,** *118,* 4485–4540. doi:10.1021/acs.chemrev.7b00271
30. Francke, R.; Little, R. D. *Chem. Soc. Rev.* **2014,** *43,* 2492–2521. doi:10.1039/c3cs60464k
31. Hou, Z.-W.; Mao, Z.-Y.; Melcamu, Y. Y.; Lu, X.; Xu, H.-C. *Angew. Chem., Int. Ed.* **2018,** *57,* 1636–1639. doi:10.1002/anie.201711876
32. Hou, Z.-W.; Yan, H.; Song, J.-S.; Xu, H.-C. *Chin. J. Chem.* **2018,** *36,* 909–915. doi:10.1002/cjoc.201800301
33. Hou, Z.-W.; Mao, Z.-Y.; Song, J.; Xu, H.-C. *ACS Catal.* **2017,** *7,* 5810–5813. doi:10.1021/acscatal.7b02105
34. Hou, Z.-W.; Mao, Z.-Y.; Zhao, H.-B.; Melcamu, Y. Y.; Lu, X.; Song, J.; Xu, H.-C. *Angew. Chem., Int. Ed.* **2016,** *55,* 9168–9172. doi:10.1002/anie.201602616
35. Gieshoff, T.; Kehl, A.; Schollmeyer, D.; Moeller, K. D.; Waldvogel, S. R. *J. Am. Chem. Soc.* **2017,** *139,* 12317–12324. doi:10.1021/jacs.7b07488
36. Xu, H.-C.; Moeller, K. D. *J. Am. Chem. Soc.* **2008,** *130,* 13542–13543. doi:10.1021/ja806259z
37. Gieshoff, T.; Schollmeyer, D.; Waldvogel, S. R. *Angew. Chem., Int. Ed.* **2016,** *55,* 9437–9440. doi:10.1002/anie.201603899
38. Kehl, A.; Breising, V. M.; Schollmeyer, D.; Waldvogel, S. R. *Chem. – Eur. J.* **2018,** *24,* 17230–17233. doi:10.1002/chem.201804638

39. Lin, M.-Y.; Xu, K.; Jiang, Y.-Y.; Liu, Y.-G.; Sun, B.-G.; Zeng, C.-C. *Adv. Synth. Catal.* **2018,** *360,* 1665–1672. doi:10.1002/adsc.201701536
40. Zhang, S.; Li, L.; Xue, M.; Zhang, R.; Xu, K.; Zeng, C. *Org. Lett.* **2018,** *20,* 3443–3446. doi:10.1021/acs.orglett.8b00981
41. Hu, X.; Zhang, G.; Bu, F.; Nie, L.; Lei, A. *ACS Catal.* **2018,** *8,* 9370–9375. doi:10.1021/acscatal.8b02847
42. Seeman, J. I. *J. Chem. Educ.* **1986,** *63,* 42–48. doi:10.1021/ed063p42

License and Terms

BEILSTEIN JOURNAL OF ORGANIC CHEMISTRY

Photochemical generation of the 2,2,6,6-tetramethylpiperidine-1-oxyl (TEMPO) radical from caged nitroxides by near-infrared two-photon irradiation and its cytocidal effect on lung cancer cells

Ayato Yamada[1], Manabu Abe[*1,2,3], Yoshinobu Nishimura[*4], Shoji Ishizaka[1,2], Masashi Namba[2,5], Taku Nakashima[2,5], Kiyofumi Shimoji[5] and Noboru Hattori[*2,5]

Full Research Paper

Open Access

Address:
[1]Department of Chemistry, Graduate School of Science, Hiroshima University, 1-3-1 Kagamiyama, Higashi-Hiroshima, Hiroshima 739-8526, Japan, [2]Hiroshima Research Centre for Photo-Drug-Delivery Systems (HiU-P-DDS), Hiroshima University, 1-3-1 Kagamiyama, Higashi-Hiroshima, Hiroshima 739-8526, Japan, [3]JST-CREST, K's Gobancho 6F, 7, Gobancho, Chiyoda-ku, Tokyo 102-0075, Japan, [4]Graduate School of Pure and Applied Sciences, University of Tsukuba, 1-1-1 Tennoudai, Tsukuba, Ibaraki 305-8571, Japan and [5]Department of Molecular and Internal Medicine, Graduate School of Biomedical & Health Sciences, Hiroshima University, 1-2-3 Kasumi, Minami-ku, Hiroshima, Hiroshima 734-8551, Japan

Email:
Manabu Abe[*] - mabe@hiroshima-u.ac.jp; Yoshinobu Nishimura[*] - nishimura@chem.tsukuba.ac.jp; Noboru Hattori[*] - nhattori@hiroshima-u.ac.jp

* Corresponding author

Keywords:
caged compound; nitroxide; photolysis; radical; theranostics; two-photon

Beilstein J. Org. Chem. **2019,** *15,* 863–873.
doi:10.3762/bjoc.15.84

Received: 01 February 2019
Accepted: 16 March 2019
Published: 10 April 2019

This article is part of the thematic issue "Reactive intermediates part I: radicals".

Guest Editor: T. P. Yoon

Abstract

Novel caged nitroxides (nitroxide donors) with near-infrared two-photon (TP) responsive character, 2,2,6,6-tetramethyl-1-(1-(2-(4-nitrophenyl)benzofuran-6-yl)ethoxy)piperidine (**2a**) and its regioisomer **2b**, were designed and synthesized. The one-photon (OP) (365 ± 10 nm) and TP (710–760 nm) triggered release (i.e., uncaging) of the 2,2,6,6-tetramethylpiperidine-1-oxyl (TEMPO) radical under air atmosphere were discovered. The quantum yields for the release of the TEMPO radical were 2.5% (**2a**) and 0.8% (**2b**) in benzene at ≈1% conversion of **2**, and 13.1% (**2a**) and 12.8% (**2b**) in DMSO at ≈1% conversion of **2**. The TP uncaging efficiencies were determined to be 1.1 GM at 740 nm for **2a** and 0.22 GM at 730 nm for **2b** in benzene. The cytocidal effect of compound **2a** on lung cancer cells under photolysis conditions was also assessed to test the efficacy as anticancer agents. In a medium containing 100 μg mL^{-1} of **2a** exposed to light, the number of living cells decreased significantly compared to the unexposed counterparts (65.8% vs 85.5%).

Introduction

Nitroxides (aminoxyl radicals) possess a delocalized unpaired electron and exhibit negligible dimerization reactivity, making them persistent open-shell species [1-4]. In addition to their ease of handling, nitroxides are highly sensitive to electron paramagnetic resonance (EPR) spectroscopy and redox reactions. Therefore, nitroxides have been developed and utilized in diverse and crucial applications, not only in chemistry, but also in biology, physiology, and energy sciences. These applications include spin-labels [5-7], fluorophore-nitroxide probes [8], contrast agents in magnetic resonance imaging (MRI) [9], polarization transfer agents for nuclear magnetic resonance (NMR) [10-13], and radical batteries [14,15]. Furthermore, the efficient synthesis of polymers with narrow molecular mass distributions has been accomplished using nitroxides as a mediator, i.e., so-called nitroxide-mediated polymerization (NMP) [16-20], and the nitroxide-mediated synthesis of ketones from alcohols is also well utilized in organic synthesis [21-25]. The huge number of studies concerning nitroxides clearly indicates the importance of new methods of generating nitroxides for the future development of science and technology. Notably, in physiological studies [26-32], spatiotemporal control of nitroxide generation is a key approach for investigating the role of redox-active nitroxides in mediating oxidative stress in organisms [27-32].

In 1997, Scaiano and co-workers reported the triplet-xanthone sensitized generation of the 2,2,6,6-tetramethylpiperidine-1-oxyl (TEMPO) radical from alkoxyamine **1** under ultraviolet (355 nm) irradiation (Scheme 1) [33]. De-aerated conditions are necessary for the triplet-sensitized generation of TEMPO due to the triplet quenching ability of O_2. The polymerization reactions were initiated via photochemical reaction [34-36]. For physiological studies, however, the photochemical release of nitroxides should be achieved in the presence of O_2. Thus, the triplet sensitized method may not be useful for physiological studies. The application of alkoxyamines as theranostic agents [37-40] has been proposed and reported by Brémond and co-workers [41,42].

Near-infrared (NIR) photons are excellent light sources in physiological studies as this wavelength of light is less harmful to living tissue than ultraviolet irradiation. Deeper penetration of NIR photons into biological samples is possible using NIR radiation with wavelengths of 650–1050 nm (= 27–44 kcal mol^{-1}). However, in general, chromophores do not absorb at such long wavelengths and the photon energy is too low for bond-cleavage reactions to generate (i.e., uncage) functional molecules. For example, the bond-dissociation energy of the weak $PhCH_2$–OPh, linkage is reported to be 52.1 kcal mol^{-1} [43]. These issues can be solved by using the NIR-two-photon (TP)

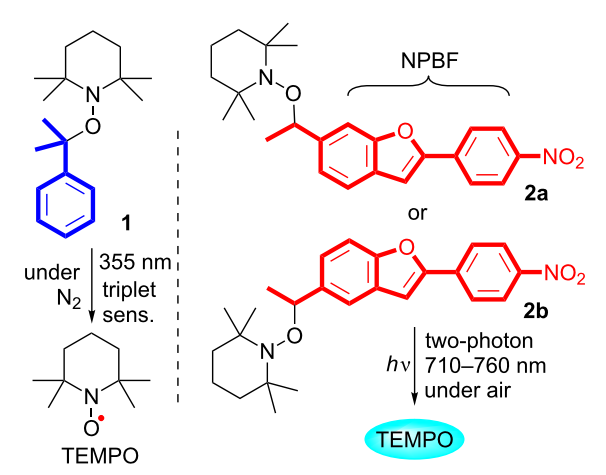

Scheme 1: Photochemical generation of TEMPO radical.

excitation technique [44], in which a molecule is electronically excited to the same state generated by one-photon (OP) excitation in the UV–vis region [45]. In addition to the advantages of TP excitation, three-dimensional control of the electronic excitation is possible because the probability of TP excitation is proportional to the square of the light intensity [46]. The light-induced generation of nitroxides using the TP excitation technique, i.e., the concentration jump of nitroxides, is one promising method of exploring the role of these species in life phenomena [47-54] and of promoting site-selective chemical reactions such as polymerization. Very recently, Guillaneuf and co-workers reported the two-photon-induced release of nitroxides in a materials science study [55].

In the last decade, we developed a TP-responsive photo-labile protecting group [56-58] with simple cyclic stilbene structures such as 2-(4-nitrophenyl)benzofuran (NPBF) that absorb in the NIR region of 710–760 nm for the uncaging of bioactive substances such as glutamate and Ca^{2+} [59-64]. Herein, we report the synthesis of new caged nitroxides (nitroxide donors) **2a** and **2b** having the TP-responsive NPBF chromophore and the NIR TP-triggered generation of the 2,2,6,6-tetramethylpiperidine-1-oxyl (TEMPO) radical under atmospheric conditions using these species (Scheme 1). Because free radicals are cytotoxic due to their strong DNA-damaging activity [65], they play important roles as anticancer therapeutic agents [66]. Among the free radicals, nitroxides including the TEMPO radical have unique properties, where they can act not only as radical scavengers, but also as anticancer agents [67]. Due to the unique properties described above, nitroxides are not toxic to normal host cells and exhibit toxicity only to tumor cells. Thus, nitroxides are ideal candidates as anticancer therapeutic agents. Based on this knowledge, the cytocidal effect of the

radical released from compound **2a** on lung cancer cells was tested in vitro, in addition to the fundamental study.

Results and Discussion

The caged-TEMPOs **2a** and **2b** were synthesized as shown in Scheme 2. The new compounds, 5-ethyl- and 6-ethyl-2-(4-nitrophenyl)benzofuran (**5a** and **5b**), were synthesized from 1-ethynyl-4-nitrobenzene (**4**) that was prepared from the commercially available 1-iodo-4-nitrobenzene (**3**) [68]. The TEMPO moiety was introduced at the benzylic position of **5a** and **5b** using the copper-catalyzed radical reaction in the presence of *tert*-butyl hydroperoxide (TBHP) to afford **2a** and **2b** in 38% and 52% yield, respectively [69]. The caged TEMPOs **2a** and **2b** were thermally stable in benzene below 320 K (47 °C), as confirmed by electron paramagnetic resonance (EPR) spectroscopic analysis. Significant thermal decomposition of **2a** and **2b** was observed at ≈340 K (67 °C), as indicated by the typical EPR signals (see Supporting Information File 1, Figure S1).

The photophysical data for the new compounds **2a**,**b** and **5a**,**b** are summarized in Table 1. The absorption maxima of compounds **2** and **5** were observed at ≈370 nm with a molar extinction coefficient ε ≈20000 M^{-1} cm^{-1} in both benzene and DMSO. The emission profile showed a significant solvent effect. The fluorescence quantum yields in DMSO of **5a** and **5b** were determined to be 16.1 and 8.6%, respectively, although no emission was observed from these compounds in non-polar benzene, indicating that the excited state has zwitterionic character. The charge transfer transition was supported by time-dependent density functional theory (TD-DFT) calculations for **5a** at the CAM-B3LYP/6-31G(d) level of theory (Supporting Information File 1, Figure S2). The fluorescence quantum yields of caged-TEMPO **2a** and **2b** were found to be 2.9 and 2.2% in DMSO, which are much smaller than those of **5a** and **5b**, respectively, suggesting the chemical reactivity of the singlet excited states of **2a** and **2b**.

Time-correlated single photon counting (TCSPC) measurement was performed at 298 K in DMSO to estimate the fluorescence lifetime (τ) of **2** and **5** (Table 1). Single-exponential decay curves were observed for **5a** and **5b**, respectively (Supporting Information File 1, Figure S3). The lifetimes determined by

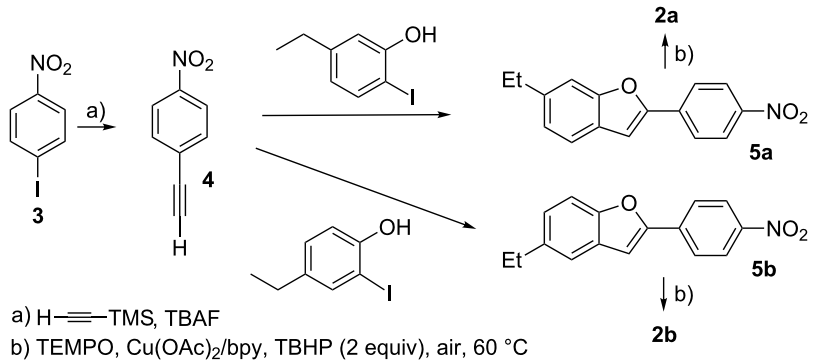

Scheme 2: Synthesis of caged nitroxides **2a** and **2b**.

Table 1: Photophysical data for **2a**, **2b**, **5a**, and **5b** in benzene (DMSO).

Entry		λ_{abs} [nm][a]	ε [M^{-1} cm^{-1}]	λ_{em} [nm][b]	$\Phi_f \times 10^2$ [c]	τ [ps][d]
1	**2a**	371 (375)	24800 (23100)	– (576)	≈0.0 (2.9)	– (220, 1370)[e]
2	**2b**	366 (370)	23000 (23400)	– (564)	≈0.0 (2.2)	– (390, 890)[f]
3	**5a**	372 (378)	23800 (20000)	– (577)	≈0.0 (16.1)	– (1430)
4	**5b**	367 (372)	22300 (19000)	– (563)	≈0.0 (8.6)	– (870)

[a]Absorption maximum of **2a**, **2b**, **5a**, **5b**. [b]Emission maximum of **2a** (1.18 × 10^{-6} M), **2b** (1.18 × 10^{-6} M), **5a** (1.16 × 10^{-6} M), **5b** (1.12 × 10^{-6} M). [c]Fluorescence quantum yields. The standard sample 9,10-diphenylanthracene (Φ_f = 0.91) was used for determining the quantum yields. [d]Fluorescence lifetime monitored at 560 nm. The concentrations were the same as those used for the fluorescence measurements. [e]Each contribution is 57% and 43%, respectively. [f]Each contribution is 70% and 30%, respectively.

single-exponential fitting were 1430 (**5a**) and 870 ps (**5b**), respectively (Table 1, entries 3 and 4). Double-exponential decay was, however, observed for the TEMPO-substituted NPBF derivatives **2a** and **2b**, where the lifetimes were 220 (57%) and 1370 ps (43%) for **2a**, and 390 (70%) and 890 ps (30%) for **2b** (Table 1, entries 1 and 2). For **2a** and **2b**, intermolecular charge transfer processes induced by the TEMPO moiety may account for the double-exponential decay curves to some extent.

OP photolysis of **2a** (5 mM) was first conducted in benzene at ≈298 K using 365 nm light (6.02×10^{15} photons s^{-1}) under atmospheric conditions (Figure 1). Clean release of the TEMPO radical was confirmed by measuring the electron paramagnetic resonance (EPR) signals of the typical nitroxide, A_N = 15.5 G (g = 2.00232, Figure 1 and Figure 2c). The first-order rate constant for generation of TEMPO in the bulk photoreaction was found to be $k = 1.6 \times 10^{-5}$ s^{-1}. The amount of photochemically released TEMPO radical was determined by comparing the EPR intensity with the calibration curve of the standard TEMPO sample (Supporting Information File 1, Figure S4). The chemical yield of TEMPO was 80% after 10 min irradiation in benzene under air atmosphere (Figure 2g). Secondary photoreaction of TEMPO gradually decreased the chemical yield of TEMPO. The quantum yield (Φ) for photochemical release of the TEMPO radical was 2.5% at ≈1% conversion in the photolysis of **2a** in benzene under atmospheric conditions. Similar photochemical generation of the TEMPO radical was conducted with **2b** (5 mM, Supporting Information File 1, Figure S5 and Figure 2d,h). The clean generation of the TEMPO radical was also observed during photolysis under 365 nm irradiation in benzene at ≈298 K under atmospheric conditions, although the reaction was slower than that of **2a**, $k = 5.5 \times 10^{-6}$ s^{-1}; Φ = 0.8% at ≈1% conversion of **2b**. However, the chemical yield of TEMPO was also high (81% after 20 min irradiation under the same conditions), although slow photochemical decomposition of TEMPO was observed with prolonged irradiation (Figure 2h). In DMSO, the quantum yield

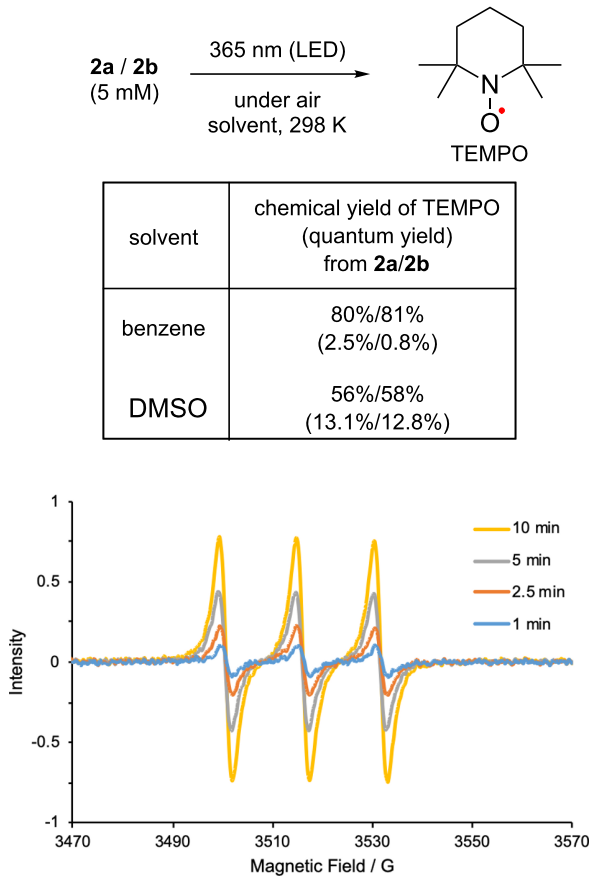

Figure 1: Photochemical generation of TEMPO from **2a** and **2b**. EPR spectra acquired during the photolysis of **2a** (5 mM) in benzene using 365 nm LED light under air atmosphere.

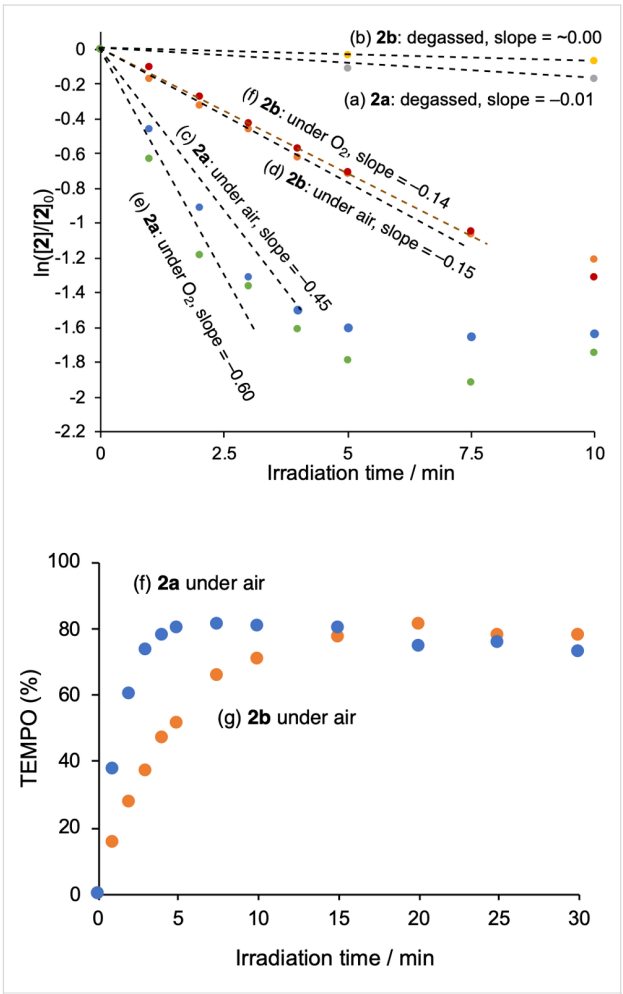

Figure 2: Time profile for photochemical generation of TEMPO radical from **2** (5 mM) at ≈298 K in benzene: (a) from **2a** under degassed conditions, (b) from **2b** under degassed conditions, (c,g) from **2a** under air conditions, (d,h) from **2b** under air conditions, (e) from **2a** under O_2, (f) from **2b** under O_2.

for the formation of TEMPO increased significantly to 13.1% (from **2a**) and 12.8% (from **2b**) at ≈1% conversion of **2** under atmospheric conditions (Figure 1). The notable effect of the solvent on the TEMPO generation may be due to the increase in the lifetime of the excited states. Photochemical decomposition of TEMPO in DMSO was found to be faster than that in benzene, but the chemical yield of TEMPO (56% from **2a** and 58% from **2b** after 40 s irradiation) was found to be lower than that obtained in benzene (Figure 1).

To obtain insight into the mechanism of generation of the TEMPO radical, the photolysis of **2** was conducted under degassed conditions using the freeze-pump-thaw (FPT) method (Figure 2a,b). Interestingly, the generation of the TEMPO radical was highly suppressed under the photolysis conditions (Figure 2a,b). Under air conditions, however, the photochemical release of TEMPO was detected in benzene, as shown in Figure 2c,d. Faster formation of TEMPO was observed when O_2 atmosphere was used instead of an air atmosphere (Figure 2e,f). Therefore, the O_2 molecule may play an important role in clean generation of the TEMPO radical during photolysis. Indeed, the compounds oxidized at the benzylic carbon, **6** and **7**, were isolated in 15% (15%) and 56% (42%) yield in the photolysis of **2a** and **2b** under atmospheric conditions, respectively (Scheme 3), indicating that under degassed conditions, the photochemically generated radical pair returns to the starting compound **2** with rapid radical recombination. Over 70% of the caged TEMPO **2a** and ≈85% of **2b** were recovered after 2 h of irradiation under degassed conditions. The retarded formation of TEMPO after 5 min of irradiation is due to the decrease in the relative absorbance of **2a** to those of primary photoproducts (Figure 2c,e).

The TP photolysis of **2a** (10 mM) and **2b** (10 mM) was carried out in benzene under atmospheric conditions using 710, 720, 730, 740, 750, and 760 nm near infrared light from a Ti:sapphire laser (pulse width 100 fs, 80 MHz) emitting at an average of 700 mW (Figure 3 for **2a** and Supporting Information File 1, Figure S6 for **2b**). The typical EPR signals of TEMPO were also observed after TP excitation of **2a** and **2b** (Supporting Information File 1, Figure S7). The formation of TEMPO at 740 nm, $k_{740} = 4.9 \times 10^{-6}$ s^{-1} in the bulk photoreaction, was the fastest in the TP-uncaging reaction of **2a** (Figure 3). For the uncaging reaction of **2b**, the rate of consumption under 730 nm irradiation, $k_{730} = 1.6 \times 10^{-6}$ s^{-1}, was larger than those at other wavelengths (Supporting Information File 1, Figure S6).

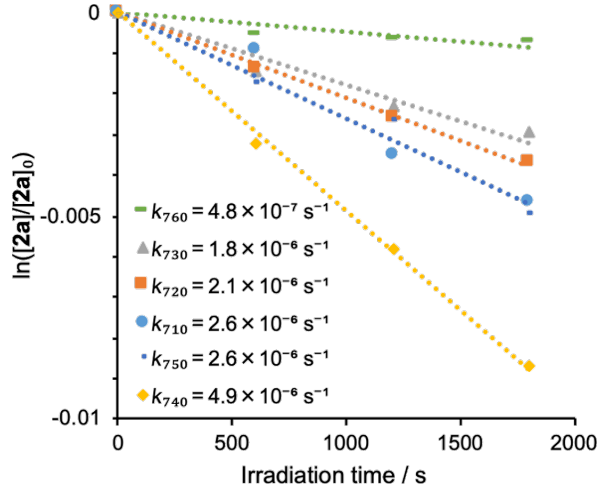

Figure 3: Time profile, ln([**2a**]/[**2a**]$_0$) versus irradiation time, of two-photon uncaging reaction of TEMPO in the photolysis of **2a** in benzene, at wavelengths of 710–760 nm and power of 700 mW.

The TP action spectra of **2a** and **2b** in benzene are shown in Figure 4, where the spectra were obtained by extrapolation from the absolute TP cross-section of the parent NPBF (18 GM) at

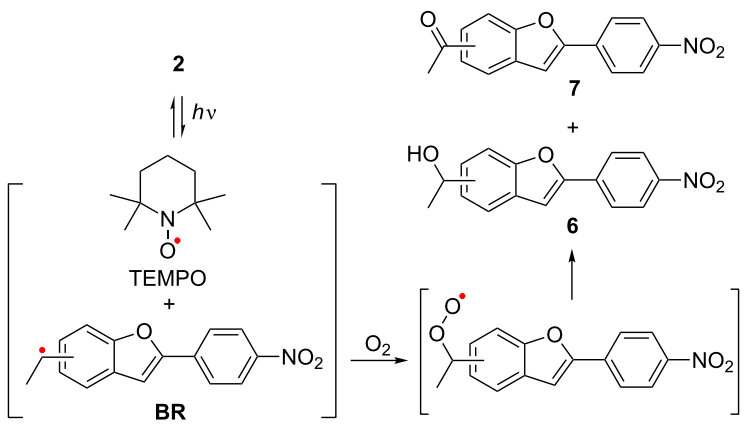

Scheme 3: Photochemical generation of TEMPO radical and photoproducts **6** and **7** under air atmosphere.

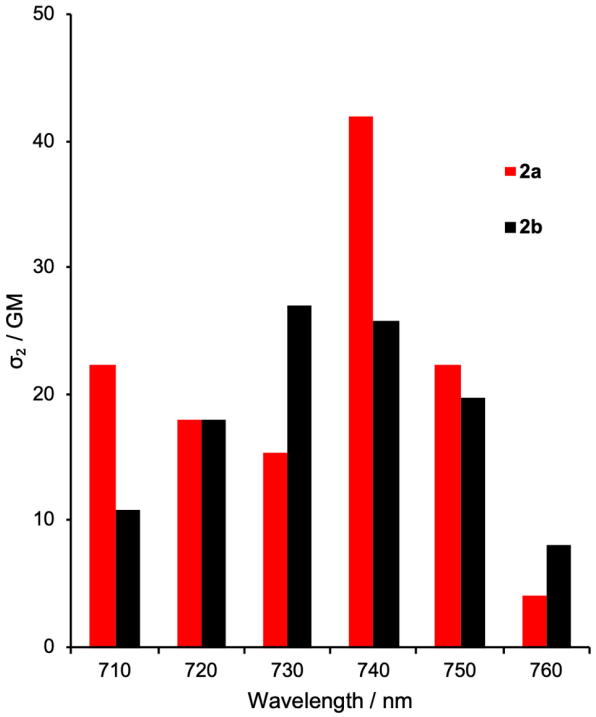

Figure 4: ESR spectra acquired during the photolysis of **2a** (5 mM) in benzene using 365 nm light.

720 nm [58]. The TP cross-section of **2a** was higher than that of **2b** by ≈15 GM. This higher GM value may be due to the stronger donor–acceptor character of **2a** relative to that of **2b**, because the electron-donating alkyl group is located at the *para*-position of the *p*-nitrophenyl group in **2a**.

As observed in the OP uncaging reaction at 365 nm, the efficiency of the TP-induced TEMPO uncaging reaction of **2a** was almost three times higher than that of **2b** in benzene. This is attributed to the substituent effect of the *meta*-alkoxy group on the reactivity in the electronically excited states [70]. Moreover, the relative stability of radicals **BRa** and **BRb** generated by the photolysis of **2a** and **2b** had an important impact on the uncaging efficiency. The isodesmic reaction shown in Scheme 4 suggests the radical **BRa** derived from **2a** was 2.04 kcal mol^{-1} more stable than **BRb** generated from **2b** based on DFT calculations at the B3LYP/6-31G(d) level of theory. In DMSO, no significant difference between **2a** and **2b** was observed for the photochemical release of the TEMPO species, although the solvent effect is not clearly explained.

As mentioned above, the spatiotemporally controlled generation of the radical pair of TEMPO and **BR** was confirmed in the photolysis of compounds **2a** and **2b**. Because free radicals play important roles as anticancer therapeutic agents, the cytocidal effect of the radical released from compound **2a** was also tested in vitro using lung cancer cells. One hundred thousand Lewis lung carcinoma (LLC) cells were seeded into 24-well plates (medium: DMEM) and incubated overnight at 37 °C under an atmosphere of 95% air and 5% CO_2. The medium was replaced with fresh phenol-red free DMEM containing various concentrations of **2a** (0, 10, 100 μg mL^{-1}) and further incubated for 4 h under the same conditions. Without exposure to light, **2a** itself exhibited slight cytotoxicity based on trypan blue exclusion, and ≈80–90% living cells remained in the medium containing of 100 μg mL^{-1} of **2a** (Supporting Information File 1, Figure S8).

The cytocidal effect of the radicals released from compound **2a** on LLC cells was also tested. Four hours after 1 min exposure to 360 nm light in various concentrations of **2a**-containing medium, the number of living cells decreased in a **2a** concentration-dependent manner (Supporting Information File 1, Figure S9). After exposure of the cells in the medium containing 100 μg mL^{-1} of **2a**, the number of living cells decreased significantly compared to that without exposure (66.5% vs 87.8%, Supporting Information File 1, Figure S10). An irradiation-time-dependent decline in the viability of the LLC cells was also observed (Figure 5). To evaluate whether the cytocidal effect was due to photochemical radical generation, cells exposed to 360 nm light for 1 min and the unexposed congeners were stained by using a ROS-ID oxidative stress detection kit (Enzo Life Sciences, Farmingdale, NY, U.S.A.). Reactive oxygen species (ROS) were detected in the cells irradiated in the **2a**-containing medium, but not in the non-irradiated cells in

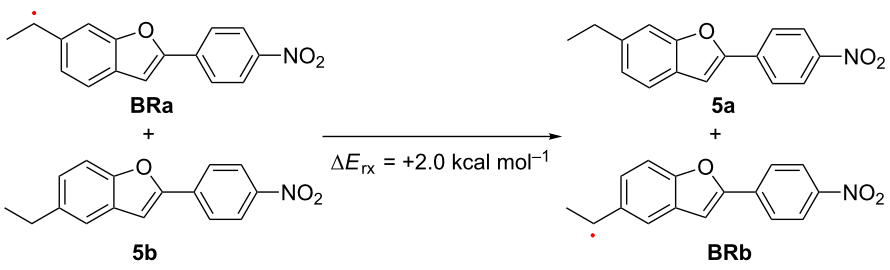

Scheme 4: Isodesmic reaction from **BRa** and **5b** to **5a** and **BRb**.

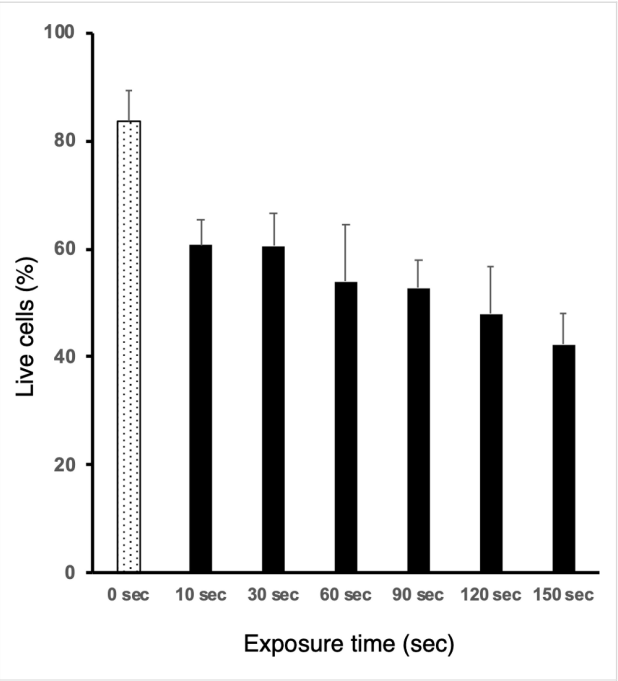

Figure 5: Irradiation time-dependent decline in viability of LLC cells with compound **2a**.

2a-containing medium or the irradiated cells without **2a**-containing medium (Figure 6). Thus, the preliminary analyses indicated that the photochemical generation of radicals from **2a** induced cancer cell death in vitro, although no in vivo study was performed because of the low water solubility of **2a**. At this point, we cannot rule out generate of ROS by photosensitization of the chromophore in the presence of O_2 for the cytotoxicity.

Conclusion

In the present study, novel caged nitroxides **2a** and **2b** having a TP-responsive chromophore were synthesized, and OP- and TP-induced generation of the TEMPO radical with these species was examined. The quantum yields for generation of the TEMPO radical from **2a** and **2b** were determined to be 2.5% and 0.8% in benzene, respectively. The quantum yields in DMSO were found to be higher than those in benzene, 13.1% and 12.8%, respectively. The OP-uncaging efficiency ($\varepsilon \times \Phi$) was found to be 480 and 175 for **2a** and **2b**, respectively, at 360 ± 10 nm, in benzene, and 3026 and 2995 in DMSO, respectively. The TP efficiency of the TEMPO uncaging reaction was found to be 1.1 GM at 740 nm for **2a** and 0.22 GM at 730 nm for **2b** in benzene. The TP-induced clean release of the TEMPO radical is expected to be applicable to further physiological studies and site-selective polymerization reactions.

Experimental

All reagents were purchased from commercial sources and were used without additional purification, unless otherwise mentioned. Caged nitroxides **2a** and **2b** were prepared according to the methods described previously (Scheme 2) and were isolated by silica gel column chromatography and GPC. ^{1}H and ^{13}C NMR spectra were reported in parts per million (δ) by using $CDCl_3$. IR spectra were recorded with a FTIR spectrometer. UV–vis spectra were taken by a SHIMADZU UV-3600 Plus spectrophotometer. Mass spectra were measured by a Mass Spectrometric Thermo Fisher Scientific LTQ Orbitrap XL, performed by the Natural Science Center for Basic Research and Development (N-BARD), Hiroshima University.

Preparation of caged compounds **2a** and **2b**

6-Ethyl-2-(4-nitrophenyl)benzofuran (5a). 4-Nitro-1-iodobenzene (16.3 g, 65.5 mmol), $Pd(dppf)Cl_2$ (0.97 g, 1.3 mmol), PPh_3 (recrystallized, 0.51 g, 1.9 mmol) and CuI (0.25 g, 1.3 mmol) were added under N_2 atmosphere followed by toluene (97 mL) and iPr_2NH (49 mL, 359 mmol). The mixture was stirred for 10 min, and TMSA (11.5 mL, 81.6 mmol) in toluene (64 mL) was added at room temperature. It was stirred until all iodobenzene was consumed (20 min). TBAF 1 M in THF (100 mL, 100 mmol) was added followed by 5-ethyl-2-iodophenol (21.6 g, 86.9 mmol). The temperature was increased to 80 °C, and the mixture was stirred for 21.5 h. The reaction was quenched with 10% aqueous citric acid (400 mL)

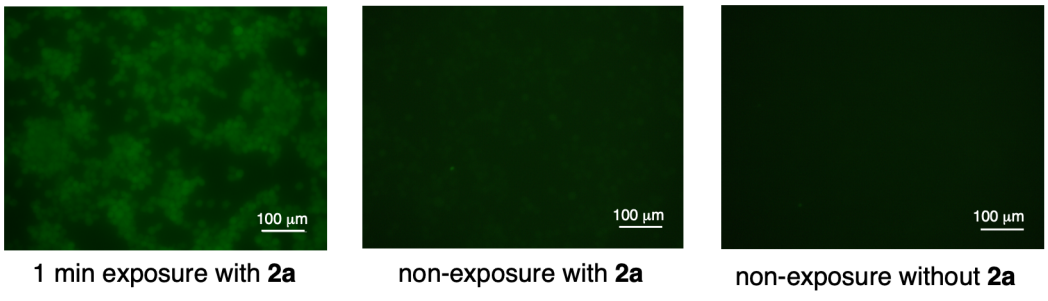

Figure 6: Detection of intracellular ROS only in irradiated LLC cells with **2a**-containing medium.

and extracted with DCM. The combined extracts were washed with 10% aqueous NaOH (400 mL), water and dried with anhydrous $MgSO_4$. The solvent was removed by rotary evaporation and the crude product was purified by silica gel column chromatography (hexane/EtOAc 10:1, v/v) to give 6-ethyl-2-(4-nitrophenyl)benzofuran (**5a**, 10.0 g, 57.3%). mp 114 °C; IR (KBr, cm^{-1}): 3429, 2968, 1601, 1520, 1344, 1108, 828, 825, 754, 692; ^{1}H NMR (400 MHz, $CDCl_3$) δ (ppm) 8.30 (d, *J* = 9.0 Hz, 2H), 7.98(d, *J* = 9.0 Hz, 2H), 7.54 (d, *J* = 8.0 Hz, 1H), 7.39 (s, 1H), 7.20 (d, *J* = 0.9 Hz, 1H), 7.14 (dd, *J* = 8.0, 1.4 Hz, 1H), 2.80 (q, *J* = 7.6 Hz, 2H), 1.32 (t, *J* = 7.6 Hz, 3H); ^{13}C NMR (100 MHz, $CDCl_3$) δ (ppm) 156.05 (C), 152.86 (C), 147.12 (C), 143.06 (C), 136.56 (C), 126.43 (C), 125.01 (CH), 124.33 (CH), 124.07 (CH), 121.22 (CH), 110.42 (CH), 105.12 (CH), 29.25 (CH_2), 15.84 (CH_3); HRMS–ESI (*m*/*z*): [M^-] calcd. for $C_{16}H_{13}NO_3$, 267.09009; found, 267.09064.

2,2,6,6-Tetramethyl-1-(1-(2-(4-nitrophenyl)benzofuran-6-yl)ethoxy)piperidine (2a). Under air, TEMPO (0.23 g, 1.5 mmol), 6-ethyl-2-(4-nitrophenyl)benzofuran (**5a**, 1.26 g, 4.72 mmol), $Cu(OAc)_2$ (16.5 mg, 0.092 mmol), bpy (13.8 mg, 0.094 mmol), TBHP (aqueous 70%, 0.41 mL, 2.9 mmol) were added into a two-necked flask in the dark. The reaction was stirred at 60 °C for 15 h. Upon completion, the mixture was purified silica gel column chromatography (hexane/ether 15:1, v/v) to give **2a** (236 mg, 37.8%). mp 109 °C; IR (KBr, cm^{-1}): 3429, 2934, 1600, 1521, 1345, 1062, 825; ^{1}H NMR (400 MHz, $CDCl_3$) δ (ppm) 8.31 (d, *J* = 9.0 Hz, 2H), 7.99 (d, *J* = 9.0 Hz, 2H), 7.57 (d, *J* = 8.1 Hz, 1H), 7.54 (s, 1H), 7.25 (dd, *J* = 8.1, 1.2 Hz, 1H), 7.21 (d, *J* = 0.7 Hz, 1H), 4.91 (q, *J* = 6.7 Hz, 1H), 1.54 (d, *J* = 6.6 Hz, 3H), 1.51 (s, 3H), 1.32 (s, 6H), 1.20 (s, 3H), 1.05 (s, 3H), 0.66 (s, 3H); ^{13}C NMR (100 MHz, $CDCl_3$) δ (ppm) 155.69 (C), 153.25 (C), 147.18 (C), 144.70 (C), 136.50 (C), 127.39 (C), 125.08 (CH), 124.33 (CH), 122.65 (CH), 121.04 (CH), 109.47 (CH), 105.13 (CH), 83.28 (CH), 59.79 (C), 40.43 (CH_2), 34.23 (CH_3) , 23.82 (CH_2), 20.40 (CH_3), 17.24 (CH3); HRMS–ESI (*m*/*z*): [M + H]$^+$ calcd. for $C_{25}H_{30}N_2O_4$, 423.22783; found, 423.22754.

5-Ethyl-2-(4-nitrophenyl)benzofuran (5b). 4-Nitro-1-iodobenzene (16.8 g, 67.5 mmol), $Pd(dppf)Cl_2$ (1.0 g, 1.3 mmol), PPh_3 (recrystallized, 0.53 g, 2.0 mmol) and CuI (0.26 g, 1.3 mmol) were added under N_2 atmosphere followed by toluene (100 mL) and iPr_2NH (50.5 mL, 370 mmol). The mixture was stirred for 10 min, and TMSA (1.75 mL, 12.5 mmol) in toluene (10 mL) was added at room temperature. It was stirred until all iodobenzene was consumed (20 min). TBAF 1 M in THF (100 mL, 100 mmol) was added followed by 4-ethyl-2-iodophenol (22.22 g, 89.6 mmol). The temperature was increased to 80 °C, and the mixture was stirred for 20 h. The reaction was quenched with 10% aqueous citric acid (666 mL) and extracted with DCM. Combined extracts were washed with 10% aqueous NaOH (666 mL), water and dried with anhydrous $MgSO_4$. The solvent was removed by rotary evaporation and the crude product was purified silica gel column chromatography (hexane/EtOAc 10:1, v/v) to give 5-ethyl-2-(4-nitrophenyl)benzofuran (**5b**, 12.2 g, 67.6%). mp 129 °C; IR (KBr, cm^{-1}): 2922, 1601, 1514, 1340, 1194, 853, 811, 754, 690; ^{1}H NMR (400 MHz, $CDCl_3$) δ (ppm) 8.30 (d, *J* = 9.0 Hz, 2H), 7.99 (d, *J* = 9.0 Hz, 2H), 7.46 (d, *J* = 9.2 Hz, 1H), 7.44 (s, 1H), 7.21 (dd, *J* = 8.4, 1.8 Hz, 1H), 7.19 (d, *J* = 0.8 Hz, 1H), 2.76 (q, *J* = 7.6 Hz, 2H) 1.30 (t, *J* = 7.6 Hz, 3H); ^{13}C NMR (100 MHz, $CDCl_3$) δ (ppm) 154.12 (C), 153.38 (C), 147.21 (C), 139.74 (C), 136.47 (C), 128.79 (C), 126.24 (CH), 125.12 (CH), 124.29 (CH), 120.14 (CH), 111.12 (CH), 105.04 (CH), 28.83 (CH_2), 16.15 (CH_3); HRMS–ESI (*m*/*z*): [M^-] calcd. for $C_{16}H_{13}NO_3$, 267.09009; found, 267.09030.

2,2,6,6-Tetramethyl-1-(1-(2-(4-nitrophenyl)benzofuran-5-yl)ethoxy)piperidine (2b). Under air, TEMPO (46.8 mg, 0.3 mmol), 5-ethyl-2-(4-nitrophenyl)benzofuran (**5b**, 267 mg, 1 mmol), $Cu(OAc)_2$ (3.6 mg, 0.02 mmol), bpy (3.1 mg, 0.02 mmol), TBHP (aqueous 70%, 0.086 mL, 0.6 mmol) were added into a Schlenk tube in the dark. The reaction was stirred at 60 °C for 16.5 h. Upon completion, the mixture was purified by silica gel column chromatography (hexane/ether 15:1, v/v) to give **2b** (66 mg, 52%). mp 144 °C; IR (KBr, cm^{-1}): 2922, 1602, 1520, 1342, 1108, 852, 746; ^{1}H NMR (400 MHz, $CDCl_3$) δ (ppm) 8.31 (d, *J* = 9.0 Hz, 2H), 7.99 (d, *J* = 9.0 Hz, 2H), 7.57 (d, *J* = 1.6 Hz, 1H), 7.50 (d, *J* = 8.6 Hz, 1H), 7.36 (dd, *J* = 8.6, 1.7 Hz, 1H), 7.23 (s, 1H), 4.88 (q, *J* = 6.6 Hz, 1H), 1.53 (d, *J* = 6.7 Hz, 3H), 1.51 (s, 3H), 1.33 (s, 6H), 1.19 (s, 3H), 1.02 (s, 3H), 0.60 (s, 3H); ^{13}C NMR (100 MHz, $CDCl_3$) δ (ppm) 154.75 (C), 153.43 (C), 147.24 (C), 141.55 (C), 136.47 (C), 128.34 (C), 125.15 (CH), 125.04 (CH), 124.32 (CH), 119.50 (CH), 110.98 (CH), 105.39 (CH), 83.13 (CH), 59.76 (C), 40.42 (CH_2), 34.37 (CH_3), 23.78 (CH_2), 20.38 (CH_3), 17.24 (CH_3); HRMS–ESI (*m*/*z*): [M + H]$^+$ calcd. for $C_{25}H_{30}N_2O_4$; 423.22783; found 423.22757.

1-(2-(4-Nitrophenyl)benzofuran-6-yl)ethan-1-ol (6a). mp 133 °C; ^{1}H NMR (400 MHz, $CDCl_3$) δ (ppm) 8.31 (d, *J* = 9.0 Hz, 2H), 7.99 (d, *J* = 9.0 Hz, 2H), 7.61 (d, *J* = 7.7 Hz, 1H), 7.61 (s, 1H), 7.30 (dd, *J* = 8.1, 1.3 Hz, 1H), 7.22 (s, 1H), 5.06 (m, 1H), 1.90 (d, *J* = 3.6 Hz, 1H), 1.57 (d, *J* = 6.5 Hz, 3H); ^{13}C NMR (100 MHz, $CDCl_3$) δ (ppm) 155.72 (C), 153.61 (C), 147.24 (C), 144.47 (C), 136.26 (C), 127.96 (C), 125.16 (CH), 124.34 (CH), 121.56 (CH), 121.34 (CH), 108.33 (CH), 104.97 (CH), 70.50 (CH), 25.58 (CH_3).

1-(2-(4-Nitrophenyl)benzofuran-5-yl)ethan-1-ol (6b). mp 149 °C; ^{1}H NMR (400 MHz, $CDCl_3$) δ (ppm) 8.30 (d, *J* =

9.0 Hz, 2H), 7.99 (d, J = 9.0 Hz, 2H), 7.66 (s, 1H), 7.53 (d, J = 8.5 Hz, 1H), 7.39 (dd, J = 8.5, 1.7 Hz, 1H), 7.22 (s, 1H), 5.04 (q, J = 6.4 Hz, 1H), 1.88 (s, 1H), 1.57 (d, J = 6.4 Hz, 3H); ^{13}C NMR (100 MHz, $CDCl_3$) δ (ppm) 154.93 (C), 153.81 (C), 147.29 (C), 141.48 (C), 136.22 (C), 128.74 (C), 125.24 (CH), 124.32 (CH), 123.67 (CH), 118.28 (CH), 111.45 (CH), 105.14 (CH), 70.47 (CH), 25.64 (CH_3); HRMS–ESI (m/z): [M^-] calcd. for $C_{16}H_{13}NO_4$, 283.08501; found, 283.08548.

1-(2-(4-Nitrophenyl)benzofuran-6-yl)ethan-1-one (7a). mp 214 °C; ^{1}H NMR (400 MHz, $CDCl_3$) δ (ppm) 8.35 (d, J = 8.9 Hz, 2H), 8.18 (s, 1H), 8.05 (d, J = 8.9 Hz, 1H), 7.93 (dd, J = 8.2, 1.3 Hz, 1H), 7.71 (d, J = 8.2 Hz, 1H), 7.29 (s, 1H), 2.70 (s, 3H); ^{13}C NMR (100 MHz, $CDCl_3$) δ (ppm) 197.22 (C), 156.45 (C), 155.12 (C), 147.82 (C), 135.52 (C), 134.84 (C), 132.93 (C), 125.76 (CH), 124.41 (CH), 123.88 (CH), 121.41 (CH), 111.79 (CH), 104.85 (CH), 26.86 (CH_3).

1-(2-(4-Nitrophenyl)benzofuran-5-yl)ethan-1-one (7b). mp 229 °C; ^{1}H NMR (400 MHz, $CDCl_3$) δ (ppm) 8.34 (d, J = 9.0 Hz, 2H), 8.30 (s, 1H), 8.04 (d, J = 8.6 Hz, 1H), 8.03 (d, J = 9.0 Hz, 2H), 7.62 (d, J = 8.7, 1H), 7.32 (s, 1H), 2.69 (s, 3H); ^{13}C NMR (100 MHz, $CDCl_3$) δ (ppm) 197.35 (C), 157.84 (C), 154.86 (C), 147.63 (C), 135.59 (C), 133.41 (C), 128.79 (C), 126.38 (CH), 125.51 (CH), 124.40 (CH), 122.86 (CH), 111.57 (CH), 105.38 (CH), 26.82 (CH_3); HRMS–ESI (m/z): [M^-] calcd. for $C_{16}H_{11}NO_4$, 281.06936; found, 281.06970.

Photoirradiation of LLC cells with compound **2a**

One hundred thousand Lewis lung carcinoma (LLC) cells were seeded into a 24-well plate (medium: DMEM) and incubated overnight at 37 °C in an atmosphere of 95% air and 5% CO_2. The medium was replaced with fresh phenol-red free DMEM containing 100 μg/mL of compound **2a**. Four hours after various irradiation time of 360 nm light (0, 10, 30, 60, 90, 120, and 150 s) using a fluorescence microscope (BIOREVO BZ-9000, Keyence, Osaka, Japan), cell viability was determined by trypan blue exclusion. Bars represent the mean ± standard deviation (n = 4).

Detection of intracellular ROS in irradiated LLC cells with **2a**-containing medium

Fifty thousand Lewis lung carcinoma (LLC) cells were seeded into 24-well plate (medium: DMEM) and incubated overnight at 37 °C in an atmosphere of 95% air and 5% CO_2. The medium was replaced with fresh phenol-red free DMEM containing 0 or 100 μg/mL of compound **2a**. Thirty minutes after 1 min or no exposure of 360 nm light using a fluorescence microscope (BIOREVO BZ-9000, Keyence, Osaka, Japan), intracellular ROS were detected using the ROS-ID Oxidative Stress Detection Kit (Enzo Life Sciences, Farmingdale, NY, USA) in conjunction with fluorescence microscopy. Intracellular ROS was detected in the form of green fluorescence signals. Bars, 100 μm.

Supporting Information

Supporting Information File 1

^{1}H and ^{13}C NMR charts for new compounds and Figures S1–S8.
[https://www.beilstein-journals.org/bjoc/content/supplementary/1860-5397-15-84-S1.pdf]

Acknowledgements

The NMR and MS measurements were performed at N-BARD, Hiroshima University. This work was supported by a Grant-in-Aid for Scientific Research JP17H0302200 from the Ministry of Education, Culture, Sports, Science and Technology, Japan. This work was partly supported by a research grant from Takahashi Industrial and Economic Research Foundation.

ORCID® iDs

Ayato Yamada - https://orcid.org/0000-0002-0631-0806
Manabu Abe - https://orcid.org/0000-0002-2013-4394
Yoshinobu Nishimura - https://orcid.org/0000-0002-9982-141X
Shoji Ishizaka - https://orcid.org/0000-0001-9866-5809
Taku Nakashima - https://orcid.org/0000-0002-0035-674X
Kiyofumi Shimoji - https://orcid.org/0000-0001-5382-4730

References

1. Keana, J. F. W. *Chem. Rev.* **1978,** *78,* 37–64. doi:10.1021/cr60311a004
2. Janzen, E. G. *Acc. Chem. Res.* **1971,** *4,* 31–40. doi:10.1021/ar50037a005
3. Eckert, H. *Chem. – Eur. J.* **2017,** *23,* 5893–5914. doi:10.1002/chem.201604685
4. Krumkacheva, O.; Bagryanskaya, E. *J. Magn. Reson.* **2017,** *280,* 117–126. doi:10.1016/j.jmr.2017.02.015
5. Kim, N.-K.; Murali, A.; DeRose, V. J. *Chem. Biol.* **2004,** *11,* 939–948. doi:10.1016/j.chembiol.2004.04.013
6. Sicoli, G.; Wachowius, F.; Bennati, M.; Höbartner, C. *Angew. Chem., Int. Ed.* **2010,** *49,* 6443–6447. doi:10.1002/anie.201000713
7. Weinrich, T.; Jaumann, E. A.; Scheffer, U. M.; Prisner, T. F.; Göbel, M. W. *Beilstein J. Org. Chem.* **2018,** *14,* 1563–1569. doi:10.3762/bjoc.14.133
8. Kakavandi, R.; Ravat, P.; Savu, S.-A.; Borozdina, Y. B.; Baumgarten, M.; Casu, M. B. *ACS Appl. Mater. Interfaces* **2015,** *7,* 1685–1692. doi:10.1021/am508854u
9. Krishna, M. C.; English, S.; Yamada, K.; Yoo, J.; Murugesan, R.; Devasahayam, N.; Cook, J. A.; Golman, K.; Ardenkjaer-Larsen, J. H.; Subramanian, S.; Mitchell, J. B. *Proc. Natl. Acad. Sci. U. S. A.* **2002,** *99,* 2216–2221. doi:10.1073/pnas.042671399

10. Hall, D. A.; Maus, D. C.; Gerfen, G. J.; Inati, S. J.; Becerra, L. R.; Dahlquist, F. W.; Griffin, R. G. *Science* **1997,** *276,* 930–932. doi:10.1126/science.276.5314.930
11. Matsuki, Y.; Maly, T.; Ouari, O.; Karoui, H.; Le Moigne, F.; Rizzato, E.; Lyubenova, S.; Herzfeld, J.; Prisner, T.; Tordo, P.; Griffin, R. G. *Angew. Chem., Int. Ed.* **2009,** *48,* 4996–5000. doi:10.1002/anie.200805940
12. Bagryanskaya, E. G.; Marque, S. R. A. *Chem. Rev.* **2014,** *114,* 5011–5056. doi:10.1021/cr4000946
13. Abe, M. *Chem. Rev.* **2013,** *113,* 7011–7088. doi:10.1021/cr400056a
14. Nishide, H.; Oyaizu, K. *Science* **2008,** *319,* 737–738. doi:10.1126/science.1151831
15. Oltean, V.-A.; Renault, S.; Valvo, M.; Brandell, D. *Materials* **2016,** *9,* No. 142. doi:10.3390/ma9030142
16. Kermagoret, A.; Gigmes, D. *Tetrahedron* **2016,** *72,* 7672–7685. doi:10.1016/j.tet.2016.07.002
17. Guégain, E.; Guillaneuf, Y.; Nicolas, J. *Macromol. Rapid Commun.* **2015,** *36,* 1227–1247. doi:10.1002/marc.201500042
18. Nicolas, J.; Guillaneuf, Y.; Lefay, C.; Bertin, D.; Gigmes, D.; Charleux, B. *Prog. Polym. Sci.* **2013,** *38,* 63–235. doi:10.1016/j.progpolymsci.2012.06.002
19. Bertin, D.; Gigmes, D.; Marque, S. R. A.; Tordo, P. *Chem. Soc. Rev.* **2011,** *40,* 2189–2198. doi:10.1039/c0cs00110d
20. Hawker, C. J.; Bosman, A. W.; Harth, E. *Chem. Rev.* **2001,** *101,* 3661–3688. doi:10.1021/cr990119u
21. Huple, D. B.; Ghorpade, S.; Liu, R.-S. *Adv. Synth. Catal.* **2016,** *358,* 1348–1367. doi:10.1002/adsc.201600018
22. Ciriminna, R.; Palmisano, G.; Pagliaro, M. *ChemCatChem* **2015,** *7,* 552–558. doi:10.1002/cctc.201402896
23. Cao, Q.; Dornan, L. M.; Rogan, L.; Hughes, N. L.; Muldoon, M. J. *Chem. Commun.* **2014,** *50,* 4524–4543. doi:10.1039/c3cc47081d
24. Wertz, S.; Studer, A. *Green Chem.* **2013,** *15,* 3116–3134. doi:10.1039/c3gc41459k
25. Tebben, L.; Studer, A. *Angew. Chem., Int. Ed.* **2011,** *50,* 5034–5068. doi:10.1002/anie.201002547
26. Goeldner, M.; Givens, R., Eds. *Dynamic Studies in Biology;* Wiley-VCH: Weinheim, 2005.
27. Soule, B. P.; Hyodo, F.; Matsumoto, K.; Simone, N. L.; Cook, J. A.; Krishna, M. C.; Mitchell, J. B. *Free Radical Biol. Med.* **2007,** *42,* 1632–1650. doi:10.1016/j.freeradbiomed.2007.02.030
28. Hoye, A. T.; Davoren, J. E.; Wipf, P.; Fink, M. P.; Kagan, V. E. *Acc. Chem. Res.* **2008,** *41,* 87–97. doi:10.1021/ar700135m
29. Oliveira, C.; Benfeito, S.; Fernandes, C.; Cagide, F.; Silva, T.; Borges, F. *Med. Res. Rev.* **2018,** *38,* 1159–1187. doi:10.1002/med.21461
30. Matsuoka, Y.; Yamato, M.; Yamada, K.-i. *J. Clin. Biochem. Nutr.* **2016,** *58,* 16–22. doi:10.3164/jcbn.15-105
31. Wilcox, C. S. *Pharmacol. Ther.* **2010,** *126,* 119–145. doi:10.1016/j.pharmthera.2010.01.003
32. Prescott, C.; Bottle, S. E. *Cell Biochem. Biophys.* **2017,** *75,* 227–240. doi:10.1007/s12013-016-0759-0
33. Scaiano, J. C.; Connolly, T. J.; Mohtat, N.; Pliva, C. N. *Can. J. Chem.* **1997,** *75,* 92–97. doi:10.1139/v97-014
34. Guillaneuf, Y.; Bertin, D.; Gigmes, D.; Versace, D.-L.; Lalevée, J.; Fouassier, J.-P. *Macromolecules* **2010,** *43,* 2204–2212. doi:10.1021/ma902774s
35. Versace, D.-L.; Lalevée, J.; Fouassier, J.-P.; Gigmes, D.; Guillaneuf, Y.; Bertin, D. *J. Polym. Sci., Part A: Polym. Chem.* **2010,** *48,* 2910–2915. doi:10.1002/pola.24071
36. Yoshida, E. *Colloid Polym. Sci.* **2010,** *288,* 1639–1643. doi:10.1007/s00396-010-2287-6
37. Kelkar, S. S.; Reineke, T. M. *Bioconjugate Chem.* **2011,** *22,* 1879–1903. doi:10.1021/bc200151q
38. Melancon, M. P.; Zhou, M.; Li, C. *Acc. Chem. Res.* **2011,** *44,* 947–956. doi:10.1021/ar200022e
39. Chen, G.; Qiu, H.; Prasad, P. N.; Chen, X. *Chem. Rev.* **2014,** *114,* 5161–5214. doi:10.1021/cr400425h
40. Lim, E.-K.; Kim, T.; Paik, S.; Haam, S.; Huh, Y.-M.; Lee, K. *Chem. Rev.* **2015,** *115,* 327–394. doi:10.1021/cr300213b
41. Audran, G.; Brémond, P.; Franconi, J.-M.; Marque, S. R. A.; Massot, P.; Mellet, P.; Parzy, E.; Thiaudière, E. *Org. Biomol. Chem.* **2014,** *12,* 719–723. doi:10.1039/c3ob42076k
42. Audran, G.; Brémond, P.; Marque, S. R. A. *Chem. Commun.* **2014,** *50,* 7921–7928. doi:10.1039/c4cc01364f
43. Luo, Y.-R. *Handbook of Bond Dissociation Energies in Organic Compounds;* CRC Press: Boca Raton, FL, U.S.A., 2002; p 215.
44. Göppert-Mayer, M. *Ann. Phys. (Berlin, Ger.)* **1931,** *401,* 273–294. doi:10.1002/andp.19314010303
45. Boyd, M. *Non-Linear Optics,* 2nd ed.; Elsevier: London, 2003.
46. Kawata, S.; Sun, H.-B.; Tanaka, T.; Takada, K. *Nature* **2001,** *412,* 697–698. doi:10.1038/35089130
47. Momotake, A.; Lindegger, N.; Niggli, E.; Barsotti, R. J.; Ellis-Davies, G. C. R. *Nat. Methods* **2006,** *3,* 35–40. doi:10.1038/nmeth821
48. Matsuzaki, M.; Ellis-Davies, G. C. R.; Nemoto, T.; Miyashita, Y.; Iino, M.; Kasai, H. *Nat. Neurosci.* **2001,** *4,* 1086–1092. doi:10.1038/nn736
49. Mayer, G.; Heckel, A. *Angew. Chem., Int. Ed.* **2006,** *45,* 4900–4921. doi:10.1002/anie.200600387
50. Ellis-Davies, G. C. R. *ACS Chem. Neurosci.* **2011,** *2,* 185–197. doi:10.1021/cn100111a
51. Bort, G.; Gallavardin, T.; Ogden, D.; Dalko, P. I. *Angew. Chem., Int. Ed.* **2013,** *52,* 4526–4537. doi:10.1002/anie.201204203
52. Terenziani, F.; Katan, C.; Badaeva, E.; Tretiak, S.; Blanchard-Desce, M. *Adv. Mater. (Weinheim, Ger.)* **2008,** *20,* 4641–4678. doi:10.1002/adma.200800402
53. Papageorgiou, G.; Ogden, D. C.; Barth, A.; Corrie, J. E. T. *J. Am. Chem. Soc.* **1999,** *121,* 6503–6504. doi:10.1021/ja990931e
54. Matsuzaki, M.; Hayama, T.; Kasai, H.; Ellis-Davies, G. C. R. *Nat. Chem. Biol.* **2010,** *6,* 255–257. doi:10.1038/nchembio.321
55. Baron, M.; Morris, J. C.; Telitel, S.; Clément, J.-L.; Lalevée, J.; Morlet-Savary, F.; Spangenberg, A.; Malval, J.-P.; Soppera, O.; Gigmes, D.; Guillaneuf, Y. *J. Am. Chem. Soc.* **2018,** *140,* 3339–3344. doi:10.1021/jacs.7b12807
56. Klán, P.; Šolomek, T.; Bochet, C. G.; Blanc, A.; Givens, R.; Rubina, M.; Popik, V.; Kostikov, A.; Wirz, J. *Chem. Rev.* **2013,** *113,* 119–191. doi:10.1021/cr300177k
57. Jakkampudi, S.; Abe, M. In *Elsevier Reference Module in Chemistry, Molecular Sciences and Chemical Engineering*, 2018, Chapter 13667.
58. Chitose, Y.; Abe, M. Design and synthesis of two-photon responsive chromophores for application to uncaging reactions. *Photochemistry;* The Royal Society of Chemistry, 2018; Vol. 46, pp 219–241. doi:10.1039/9781788013598-00219
59. Abe, M.; Chitose, Y.; Jakkampudi, S.; Thuy, P. T. T.; Lin, Q.; Van, B. T.; Yamada, A.; Oyama, R.; Sasaki, M.; Katan, C. *Synthesis* **2017,** *49,* 3337–3346. doi:10.1055/s-0036-1590813
60. Boinapally, S.; Huang, B.; Abe, M.; Katan, C.; Noguchi, J.; Watanabe, S.; Kasai, H.; Xue, B.; Kobayashi, T. *J. Org. Chem.* **2014,** *79,* 7822–7830. doi:10.1021/jo501425p

61. Komori, N.; Jakkampudi, S.; Motoishi, R.; Abe, M.; Kamada, K.; Furukawa, K.; Katan, C.; Sawada, W.; Takahashi, N.; Kasai, H.; Xue, B.; Kobayashi, T. *Chem. Commun.* **2016,** *52,* 331–334. doi:10.1039/c5cc07664a
62. Jakkampudi, S.; Abe, M.; Komori, N.; Takagi, R.; Furukawa, K.; Katan, C.; Sawada, W.; Takahashi, N.; Kasai, H. *ACS Omega* **2016,** *1,* 193–201. doi:10.1021/acsomega.6b00119
63. Chitose, Y.; Abe, M.; Furukawa, K.; Katan, C. *Chem. Lett.* **2016,** *45,* 1186–1188. doi:10.1246/cl.160586
64. Chitose, Y.; Abe, M.; Furukawa, K.; Lin, J.-Y.; Lin, T.-C.; Katan, C. *Org. Lett.* **2017,** *19,* 2622–2625. doi:10.1021/acs.orglett.7b00957
65. Fukuhara, K.; Nakashima, T.; Abe, M.; Masuda, T.; Hamada, H.; Iwamoto, H.; Fujitaka, K.; Kohno, N.; Hattori, N. *Free Radical Biol. Med.* **2017,** *106,* 1–9. doi:10.1016/j.freeradbiomed.2017.02.014
66. Noh, J.; Kwon, B.; Han, E.; Park, M.; Yang, W.; Cho, W.; Yoo, W.; Khang, G.; Lee, D. *Nat. Commun.* **2015,** *6,* No. 6907. doi:10.1038/ncomms7907
67. Lewandowski, M.; Gwozdzinski, K. *Int. J. Mol. Sci.* **2017,** *18,* No. 2490. doi:10.3390/ijms18112490
68. Bosiak, M. J. *ACS Catal.* **2016,** *6,* 2429–2434. doi:10.1021/acscatal.6b00190
69. Li, L.; Yu, Z.; Shen, Z. *Adv. Synth. Catal.* **2015,** *357,* 3495–3500. doi:10.1002/adsc.201500544
70. Zimmerman, H. E. *J. Am. Chem. Soc.* **1995,** *117,* 8988–8991. doi:10.1021/ja00140a014

License and Terms

BEILSTEIN JOURNAL OF ORGANIC CHEMISTRY

Vicinal difunctionalization of alkenes by four-component radical cascade reaction of xanthogenates, alkenes, CO, and sulfonyl oxime ethers

Shuhei Sumino[1], Takahide Fukuyama[1], Mika Sasano[1], Ilhyong Ryu[*1,2], Antoine Jacquet[3], Frédéric Robert[3] and Yannick Landais[*3]

Letter

Open Access

Address:
[1]Department of Chemistry, Osaka Prefecture University, Sakai, Osaka 599-8531, Japan, [2]Department of Applied Chemistry, National Chiao Tung University, Hsinchu, Taiwan and [3]University of Bordeaux, Institute of Molecular Sciences, UMR-CNRS 5255, 351 cours de la libération, Talence, 33405 Cedex, France

Email:
Ilhyong Ryu[*] - ryu@c.s.osakafu-u.ac.jp; Yannick Landais[*] - yannick.landais@u-bordeaux.fr

* Corresponding author

Keywords:
CO; multicomponent reaction; radicals; sulfonyl oxime ethers; xanthogenates

Beilstein J. Org. Chem. **2019,** *15,* 1822–1828.
doi:10.3762/bjoc.15.176

Received: 04 October 2018
Accepted: 16 July 2019
Published: 31 July 2019

This article is part of the thematic issue "Reactive intermediates part I: radicals".

Guest Editor: T. P. Yoon

Abstract

Four-component coupling reactions between xanthogenates, alkenes, CO, and sulfonyl oxime ethers were studied. In the presence of hexabutylditin, working as a propagating radical reagent, the chain reaction proceeds, as expected, taking into account reagents polarities, affording the corresponding functionalized α-keto oximes. Although yields are modest, this rare one-pot four-component process is easy to carry out and the resulting compounds, bearing multiple functionalities, have the potential for further elaboration.

Introduction

Multicomponent reactions constitute a powerful and highly efficient tool in organic synthesis to build up intricate compounds from simple molecules in a single operation [1-5]. Needless to say, the contribution by radical chemistry is not trivial [5-7]. While alkenes and alkynes have served as efficient radical donor/acceptor type C2 synthons in multicomponent radical reactions, CO and isonitriles were shown to react as donor/acceptor type C1 synthons [6-15]. In this context, sulfonyl oxime ethers are powerful acceptors of type C1 synthon [8,16,17], which terminates the multicomponent reaction by a β-scission of RSO_2 radicals [18-20]. Recently, one of us reported on a three-component radical reaction using xanthogenates, alkenes, and sulfonyl oxime ethers (Scheme 1, reaction 1) [21,22]. The reaction proceeds efficiently to provide good yields of α-alkoxyimino esters, potential precursors of lactams, lactones and β-keto esters. Since the three-component

radical reaction involving alkyl halides and two radical C1 synthons, CO and sulfonyl oxime ethers, is known to be feasible [23-25], we were tempted to explore a novel class of four-component radical reaction [26-28] incorporating a xanthogenate, an alkene, CO, and a sulfonyl oxime ether (Scheme 1, reaction 2). This paper reports on the synthesis of functionalized α-keto oximes through such a one-pot, four-component procedure.

Results and Discussion

We first investigated the reaction of xanthate **1a** [29], 1-octene (**2a**), CO, and sulfonyl oxime ether **3a** as a model reaction. When the mixture of **1a**, **2a** (5 equiv), and **3a** (1.2 equiv) in C_6H_6 (16 mL) in the presence of hexabutylditin as a radical mediator, and DTBHN (di-*tert*-butyl hyponitrite) as a radical initiator was heated under CO (130 atm) at 45 °C for 16 h, the envisaged four-component coupling product, keto oxime **5a**, was obtained in 43% yield, along with the three-component product **4a** (**4a**/**5a** = 9:91) (Table 1, entry 1). In this reaction, several unidentified byproducts were also formed. Since the conversion of **1a** (ca. 70%) was incomplete, a higher concentration ([**1a**] = 0.05 M) using 8 mL of C_6H_6 was employed, resulting in a higher conversion (ca. 80%), affording **5a** in 47% yield (Table 1, entry 2). The use of DCE (1,2-dichloroethane) as a solvent gave a 50% yield of **5a** (Table 1, entry 3). The present four-component product also proceeded under

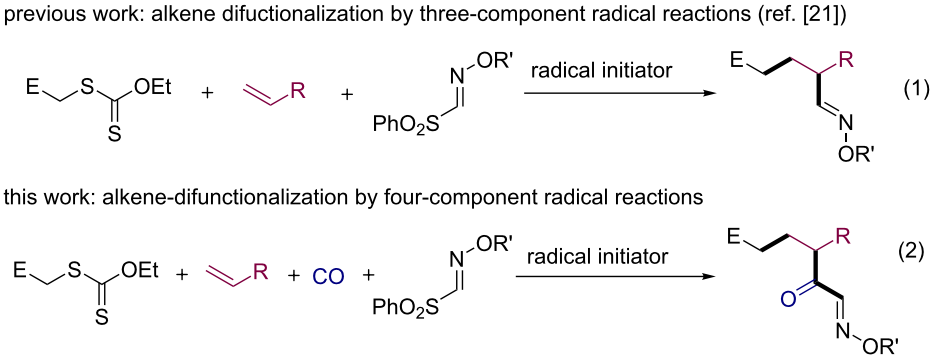

Scheme 1: Concept: Alkene difuctionalization by four-component radical reaction using xanthates, alkenes, CO and sulfonyl oxime ethers.

Table 1: Four-component coupling reaction of ethyl 2-((ethoxycarbonothioyl)thio)acetate (**1a**), 1-octene (**2a**), CO, and sulfonyl oxime ether **3a** under radical conditions[a].

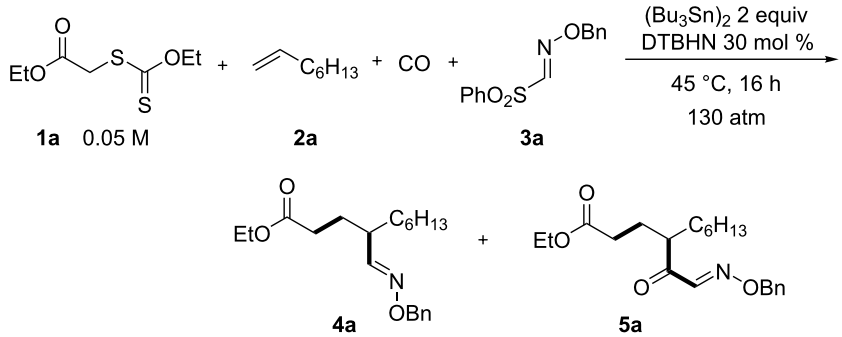

entry	solvent	**2a** (equiv)	**3a** (equiv)	ratio[b] (**4a**/**5a**)	**5a**[c] (%)
1[d]	C_6H_6	5.0	1.2	9:91	43
2	C_6H_6	5.0	1.2	13:87	47 (39)
3	DCE	5.0	1.2	9:91	50 (43)
4[e]	DCE	5.0	1.2	8:92	41 (38)
5	DCE	10.0	1.5	13:87	56 (52)

[a]Reaction conditions: **1a** (0.4 mmol), **2a** (2 or 4 mmol), CO (130 atm), **3a** (0.48 or 0.6 mmol), DTBHN (0.12 mmol), $(Bu_3Sn)_2$ (0.8 mmol), C_6H_6 or DCE (8 mL), 45 °C, 16 h. [b]Determined by GC. [c]GC yields determined by using nonane as an internal standard. Isolated yields by silica gel chromatography are given in the parenthesis. [d]C_6H_6 (16 mL). Conversion of **1a** = ca. 70%. [e]Irradiation by Xe lamp was carried out in the absence of DTBHN.

photoirradiation conditions in the absence of costly DTBHN (Table 1, entry 4). The reaction with 10 equivalents of **2a** together with 1.5 equivalents of **3a** led to a higher conversion (ca. 90%), affording acceptable yield and selectivity (Table 1, entry 5).

With optimized reaction conditions in hand (Table 1, entry 5), we then examined the generality of this four-component radical cascade reaction using xanthates **1**, olefins **2**, CO, and oxime esters **3**, leading to **5a–l** (Figure 1). The xanthate **1b**, bearing a phenyl ester, gave similarly to **1a**, α-keto oxime **5b** in moderate yield. The reaction of **1a** or **1b** with vinylcyclohexane (**2b**) in the presence of CO and **3a** afforded the corresponding α-keto oximes **5c** and **5d** in 54 or 32% yield, respectively. The conditions were shown to be compatible with the presence of nitriles, ethers and halogens. Alkenes having a *tert*-butyldimethylsilyl ether such as 6-siloxy-1-hexene **2c** thus participated to the reaction to give **5e** in 57% yield. Alkenes having a chlorine atom, as in **2d**, were also competent substrates in the present four-component coupling reaction, affording **5f**, albeit in modest yield.

The reaction of **1a** with 6-heptenenitrile (**2e**) and 5-hexen-2-one (**2f**) gave the corresponding four-component coupling products **5g** and **5h**, in 34 and 41% yield, respectively. The reaction with cyano-substituted sulfonyl oxime ester **3b** also worked well to provide cyano-functionalized α-keto oximes. **5i**, **5j**, and **5k** were thus accessible through the four-component coupling reaction between xanthogenates, alkenes, CO, and **3b** in acceptable isolated yields (39–50%). Finally, the reaction between acetophenone xanthate **1c**, **2b** and **3a** gave the corresponding keto oxime **5l** in 39% yield. The functionalized α-keto oximes obtained herein should be useful scaffolds for further functionalization. Indeed, the α-keto oximes were reported to be used for the synthesis of a variety of synthetic intermediates, including functionalized keto-aldehydes [22], aminoalcohols [30], triazoles [31], just to name a few.

A reaction mechanism is finally proposed for the four-component cascade reaction, which is depicted in Figure 2 [22-24,32-34]. Initially, α-carbonyl radical **A** [8] was generated by the reaction of the tributyltin radical with **1a**. The electrophilic

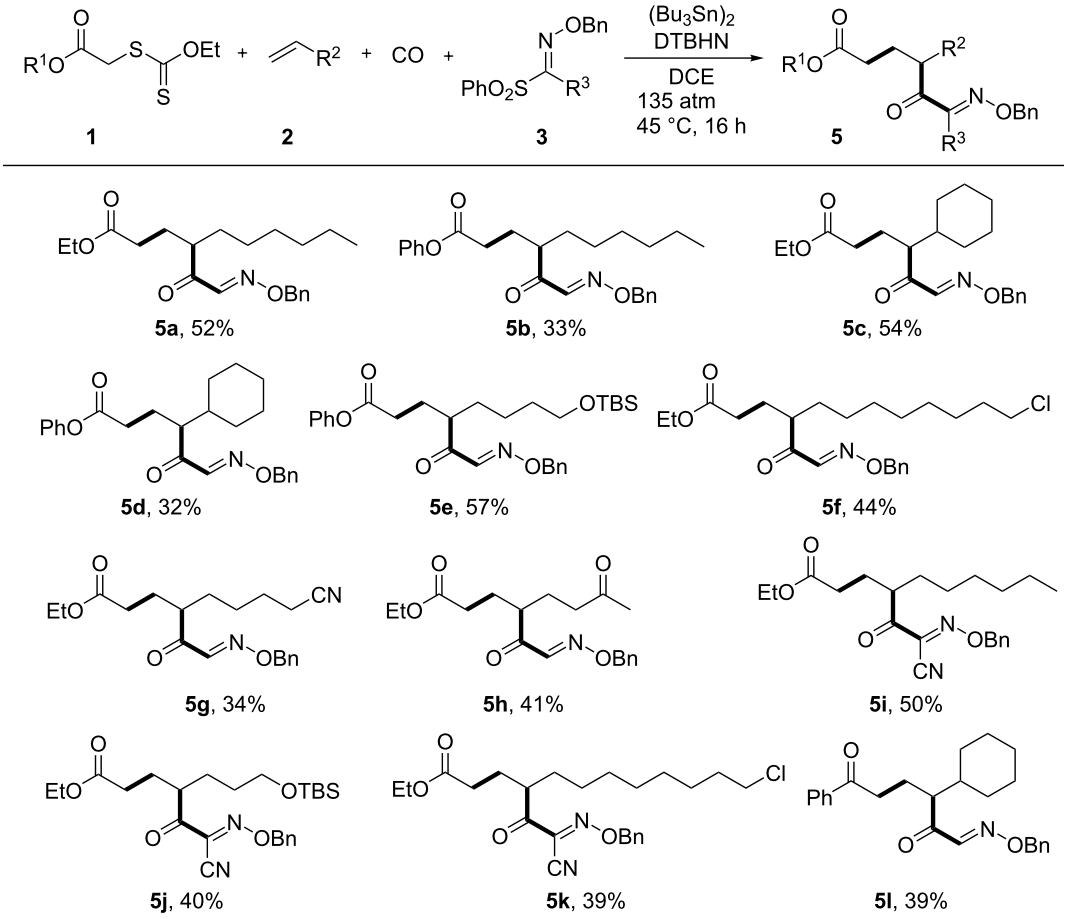

Figure 1: Vicinal difunctionalization of alkenes by four-component radical cascade reaction using xanthogenate **1**, alkenes **2**, CO, and sulfonyl oxime ethers **3** leading to **5a–l**. Reaction conditions: **1** (0.4 mmol), **2** (4 mmol), CO (130 atm), **3** (0.5 mmol), DTBHN (30 mol %), $(Bu_3Sn)_2$ (0.8 mmol), DCE (8 mL), 45 °C, 16 h.

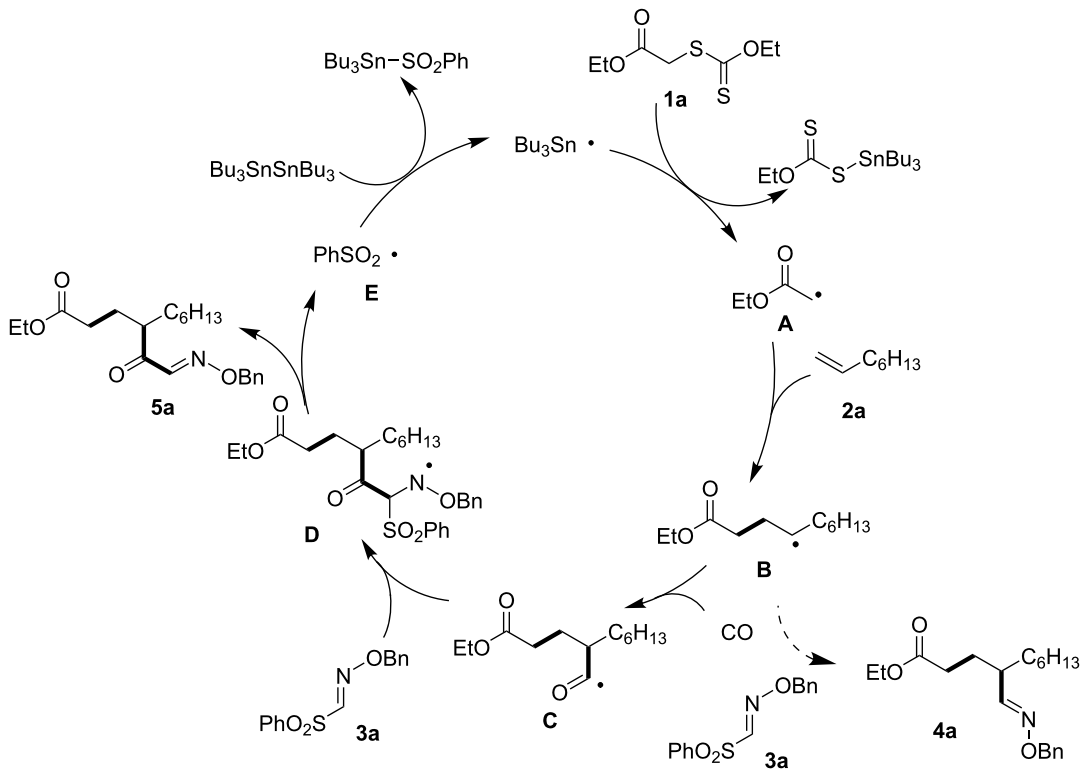

Figure 2: Proposed radical chain mechanism.

α-carbonyl radical **A** does not react with CO even at high CO pressure [6], and therefore selectively adds to electron-rich olefin **2a** to form a carbon-centered radical **B**. The radical **B**, regarded as a nucleophilic radical, then undergoes radical carbonylation with CO to give an acyl radical **C** [35], which then adds to electron-deficient sulfonyl oxime ether **3a** to afford **5a**. The resulting radical **D** then undergoes β-fragmentation providing **5a** along with the phenylsulfonyl radical **E**. S_H2 reaction between radical **E** and hexabutylditin regenerates the tributyltin radical which sustains the radical chain. Since radical **B** can also add to sulfonyl oxime ether **3a**, we used high CO pressure conditions to encourage the radical carbonylation to form acyl radical **C**.

Conclusion

In summary, we demonstrated that a four-component radical cascade reaction, between xanthogenates, alkenes, CO, and sulfonyl oxime ethers, can proceed under radical mediated conditions, using hexabutylditin as a radical chain carrier, to give the corresponding keto-oximes in moderate yields. A variety of functional groups are tolerated under the high CO pressure and temperature conditions. Among multicomponent reactions, specific four-component reactions are still rare [26-28]. The present procedure, which is easy to carry out using an autoclave in a single operation, shows that a fine tuning of the reaction conditions (pressure and temperature) and reagents polarities offer a straightforward access to polyfunctionalized substrates from readily available starting materials.

Experimental

General information

^{1}H NMR spectra were recorded on a JEOL ECP-500 (500 MHz) and JEOL ECS-400 (400 MHz) spectrometers in $CDCl_3$ and referenced at 0.00 ppm for TMS. ^{13}C NMR spectra were recorded on a JEOL ECP-500 (125 MHz) and JEOL ECS-400 (100 MHz) spectrometers in $CDCl_3$ and referenced at 77.00 ppm for $CHCl_3$. Chemical shifts are reported in parts per million (δ). Splitting patterns are indicated as follows: br, broad; s, singlet; d, doublet; t, triplet; q, quartet; m, multiplet. Infrared spectra were obtained on a JASCO FT/IR-4100 spectrometer; absorptions were reported in reciprocal centimeters. High-resolution mass spectra were recorded on a JEOL MS700 spectrometer or Exactive Plus EMR (Thermo Fisher Scientific). The products were purified by flash chromatography on silica gel (Kanto Chem. Co. Silica Gel 60N (spherical, neutral, 40–50 μm)) and, if necessary, were further purified by recycling preparative HPLC (Japan Analytical Industry Co. Ltd., LC-918) equipped with GPC columns (JAIGEL-1H + JAIGEL-2H columns) using $CHCl_3$ as eluent. Xanthogenate **1a**,**b** [20], **1c** [36], alkene **2c** [37], and oxime ester **3a**,**b** [20] were pre-

pared according to reported procedures. Photoirradiation was carried out using a 500 W Xenon short arc lamp (Ushio Co. Ltd., lamp house: SX-UI500XQ, Xenon short arc lamp: UXL-500SX, power supply: BA-X500).

Typical procedure for the synthesis of **5a** under thermal conditions

A magnetic stirring bar, **1a** (90.1 mg, 0.4 mmol), **2a** (455.3 mg, 4.0 mmol), **3a** (141.4 mg, 0.51 mmol), $(Bu_3Sn)_2$ (474.7 mg, 0.82 mmol), DTBHN (21.4 mg, 0.12 mmol), and 1,2-dichloroethane (8 mL) were placed in a stainless steel autoclave. The autoclave was closed, purged three times with carbon monoxide, pressurized with 130 atm of CO and then stirred at 45 °C for 16 h. Excess CO was discharged at room temperature after the reaction. The reaction mixture was then filtered and concentrated in vacuo to give a residue, which was subjected to silica gel column chromatography using hexane/EtOAc 10:1 as eluent, affording **5a** (83.7 mg, 0.22 mmol, 52%).

Procedure for the synthesis of **5a** under photoirradiation conditions

A magnetic stirring bar, **1a** (82.0 mg, 0.39 mmol), **2a** (225.8 mg, 2.0 mmol), **3a** (133.1 mg, 0.48 mmol), $(Bu_3Sn)_2$ (452.6 mg, 0.78 mmol), and 1,2-dichloroethane (8 mL) were placed in a stainless-steel autoclave equipped with two sapphire glass windows and an inserted Pyrex glass liner. The autoclave was closed, purged three times with carbon monoxide, pressurized with 130 atm of CO and then irradiated by Xenon lamp (500 W) with stirring for 16 h. Excess CO was discharged after the reaction. The reaction mixture was then filtered and concentrated in vacuo to give a residue, which was subjected to silica gel column chromatography using hexane/EtOAc 10:1 as eluent, affording **5a** (52.9 mg, 0.15 mmol, 38%).

Ethyl (*E*)-4-(2-((benzyloxy)imino)acetyl)decanoate (5a): IR (neat, ZnSe) ν_{max} (cm^{-1}): 3065, 2955, 1732, 1584, 1455, 1303, 1210; ^1H NMR ($CDCl_3$, 400 MHz) δ 7.49 (s, 1H), 7.38–7.33 (m, 5H), 5.25 (s, 2H), 4.10–4.08 (m, 2H), 3.35–3.33 (m, 1H), 2.21–2.17 (m, 2H), 1.25–1.21 (m, 11H), 0.87 (t, *J* = 6.8 Hz, 3H); ^{13}C NMR ($CDCl_3$, 100 MHz) δ 201.7, 173.0, 148.0, 136.1, 128.6, 128.6, 128.5, 77.9, 60.3, 45.3, 32.1, 32.0, 31.6, 29.2, 27.1, 26.4, 22.6, 14.2, 14.1; EIMS *m*/*z* (relative intensity): 316 (4), 227 (8), 199 (2), 91 (100); HRMS–EI (*m*/*z*): $[M - C_2H_5O]^+$ calcd for $C_{19}H_{26}NO_3$, 316.1913; found, 316.1916.

Phenyl (*E*)-4-(2-((benzyloxy)imino)acetyl)decanoate (5b): IR (neat, ZnSe) ν_{max} (cm^{-1}): 2954, 2928, 1760, 1685, 1196, 1188; ^1H NMR ($CDCl_3$, 500 MHz) δ 7.54 (s, 1H), 7.39–7.34 (m, 8H), 7.24–7.21 (t, *J* = 7.4 Hz, 1H), 7.07–7.06 (d, *J* = 9.5 Hz, 11H), 5.25 (s, 2H), 3.49–3.44 (m, 1H), 2.57–2.45 (m, 2H), 2.13–2.04 (m, 1H), 1.98–1.89 (m, 1H), 1.72–1.62 (m, 1H), 1.48–1.40 (m, 1H), 1.29–1.22 (m, 10H), 0.89–0.86 (t, *J* = 7.5 Hz, 3H); ^{13}C NMR ($CDCl_3$, 125 MHz) δ 201.7, 171.7, 150.8, 148.2, 136.3, 129.5, 128.7, 128.6, 125.9, 121.7, 78.1, 45.4, 32.3, 32.2, 31.7, 29.4, 27.3, 26.5, 22.7, 14.2; EIMS *m*/*z* (relative intensity): 316 (1), 91 (100); HRMS–EI (*m*/*z*): $[M - C_6H_5O]^+$ calcd for $C_{19}H_{26}NO_3$, 316.1913; found, 316.1910.

Ethyl (*E*)-6-((benzyloxy)imino)-4-cyclohexyl-5-oxohexanoate (5c): IR (neat, ZnSe) ν_{max} (cm^{-1}): 3065, 2978, 1681, 1497, 1370, 1251, 1210; ^1H NMR ($CDCl_3$, 500 MHz) δ 7,48 (s, 1H), 7.38–7.33 (m, 5H), 5.25 (s, 2H), 4.12–4.06 (m, 2H), 3.27–3.23 (m, 1H), 2.22–2.17 (m, 1H), 2,13–2.06 (m, 1H), 1.96–1.92 (m, 1H), 1.86–1.85 (m, 1H), 1.71–1.59 (m, 5H), 1.25–1.22 (t, *J* = 7 Hz, 3H), 1.17–0.90 (m, 5H); ^{13}C NMR ($CDCl_3$, 125 MHz) δ 201.1, 173.1, 148.7, 148.6, 136.2, 128.6, 128.5, 77.9, 60.3, 51.0, 50.9, 40.3, 32.2, 26.3, 23.4, 14.3, 14.1; EIMS *m*/*z* (relative intensity): 359 (1), 125 (2), 109 (6), 91 (100); HRMS–EI (*m*/*z*): $[M]^+$ calcd for $C_{21}H_{29}NO_4$, 359.2097; found, 359.2067.

Phenyl (*E*)-6-((benzyloxy)imino)-4-cyclohexyl-5-oxohexanoate (5d): IR (neat, ZnSe) ν_{max} (cm^{-1}): 2927, 2852, 1759, 1682, 1492, 1197, 1135; ^1H NMR ($CDCl_3$, 500 MHz) δ 7.52 (s, 1H), 7.39–7.34 (m, 7H), 7.26–7.21 (m, 2H), 7.07–7.05 (m, 2H), 5.24 (s, 2H), 3.36–3.33 (m, 1H), 2.51–2.30 (m, 2H), 2.12–1.95 (m, 2H), 1.82–1.50 (m, 7H), 1.23–0.89 (m, 6H); ^{13}C NMR ($CDCl_3$, 100 MHz) δ 202.0, 171.8, 148.9, 136.4, 129.6, 128.9, 128.8, 128.8, 128.7, 126.0, 121.7, 78.1, 51.1, 40.5, 32.5, 31.6, 30.2, 26.5, 26.5, 23.5; EIMS *m*/*z* (relative intensity): 314 (53), 232 (8), 91 (100); HRMS–EI (*m*/*z*): $[M - C_6H_5O]^+$ calcd for $C_{19}H_{26}NO_3$, 314.1756, found, 314.1760.

Phenyl (*E*)-4-(2-((benzyloxy)imino)acetyl)-8-((*tert*-butyldimethylsilyl)oxy)octanoate (5e): IR (neat, ZnSe) ν_{max} (cm^{-1}): 2952, 2854, 1760, 1686, 1595, 1493. ^1H NMR ($CDCl_3$, 500 MHz) δ 7.49 (s, 1H), 7.35–7.33 (m, 8H), 7.20–7.19 (m, 1H), 7.04–7.02 (m, 2H), 5.21 (s, 2H), 3.54–3.50 (m, 2H), 3.50–3.40 (m, 1H), 2.45–2.42 (m, 2H), 2.08–2.03 (m, 1H), 1.93–1.87 (m, 1H), 1.71–1.61 (m, 1H), 1.56–1.40 (m, 3H), 0.85 (s, 9H), 0.06 (s, 6H); ^{13}C NMR ($CDCl_3$, 125 MHz) δ 201.4, 171.5, 150.6, 148.0, 136.0, 129.4, 128.6, 125.8, 121.5, 78.6, 62.7, 44.9, 31.9, 30.3, 28.3, 26.7, 26.4, 25.9, 18.3, −5.1, −5.3; EIMS *m*/*z* (relative intensity): 440 (20), 404 (24), 263 (20), 91 (100); HRMS–EI (*m*/*z*): $[M - OCH_2Ph]^+$ calcd for $C_{22}H_{34}NO_4Si$, 404.2257; found, 404.2260.

Ethyl (*E*)-4-(2-((benzyloxy)imino)acetyl)-12-chlorododecanoate (5f): IR (neat, ZnSe) ν_{max} (cm^{-1}): 2930, 2856, 1731, 1682, 1455, 1371, 699; ^1H NMR ($CDCl_3$, 500 MHz) δ 7.49 (s, 1H), 7.38–7.34 (m, 5H), 5.25 (s, 2H), 4.12–4.07 (m, 2H), 3.54–3.51 (t, *J* = 6.5 Hz, 2H), 3.37–3.35 (m, 1H), 2.24–2.15 (m,

2H), 1.96–1.92 (m, 1H), 1.83–1.73 (m, 3H), 1.65–1.58 (m,1H), 1.42–1.37 (m, 3H), 1.25–1.22 (m, 11H); ^{13}C NMR ($CDCl_3$, 125 MHz) 201.6, 173.1, 148.1, 128.6, 128.5, 77.9, 60.3, 45.4, 45.1, 32.6, 32.1, 32.0, 29.5, 29.2, 28.8, 27.1, 26.8, 26.5, 14.2; EIMS *m*/*z* (relative intensity): 378 (1), 289 (3), 105 (1), 91 (100); HRMS–EI (*m*/*z*): $[M - C_2H_5O]^+$ calcd for $C_{21}H_{29}NO_3Cl$, 379.1419; found, 378.1842.

Ethyl (*E*)-4-(2-((benzyloxy)imino)acetyl)-8-cyanooctanoate (5g): IR (neat, ZnSe) ν_{max} (cm^{-1}): 2938, 2246, 1683, 1731; ^{1}H NMR ($CDCl_3$, 400 MHz) δ 7.50 (s, 1H), 7.35–7.41 (m, 5H), 5.26 (s, 2H), 4.08–4.14 (m, 2H), 3.34–3.40 (m, 1H), 2.14–2.27 (m, 5H), 1.90–1.97 (m, 1H), 1.77–1.82 (m, 1H), 1.54–1.68 (m, 3H), 1.29–1.47 (m, 2H), 1.24 (t, *J* = 7.6 Hz, 3H); ^{13}C NMR ($CDCl_3$, 100 MHz) δ 201.0, 172.8, 148.0, 136.0, 128.6, 128.5, 119.5, 77.9, 60.4, 44.7, 31.8, 31.0, 26.5, 26.2, 25.2, 16.9, 14.2; EIMS *m*/*z* (relative intensity): 313 (1), 91 (100), 77 (6), 55 (7); HRMS–EI (*m*/*z*): $[M - C_2H_5O]^+$ calcd for $C_{18}H_{21}N_2O_3$, 313.1552; found, 313.1556.

Ethyl (*E*)-4-(2-((benzyloxy)imino)acetyl)-7-oxooctanoate (5h): IR (neat, ZnSe) ν_{max} (cm^{-1}): 3510, 2936, 1732, 1715, 1684; ^{1}H NMR ($CDCl_3$, 400 MHz) δ 7.49 (s, 1H), 7.38–7.26 (m, 5H), 5.25 (s, 2H), 4.12–4.07 (m, 2H), 3.39–3.35 (m, 1H), 2.40–2.27 (m, 2H), 2.27–2.20 (m, 2H), 2.06 (s, 3H), 2.00–1.85 (m, 2H), 1.82–1.73 (m, 2H), 1.25–1.22 (t, *J* = 7.2 Hz, 3H); ^{13}C NMR ($CDCl_3$, 100 MHz,) δ 207.7, 200.9, 172.9, 147.9, 136.0, 128.6, 128.6, 128.5, 78.0, 60.4, 44.3, 40.6, 31.7, 29.9, 26.5, 25.2, 14.2; EIMS *m*/*z* (relative intensity): 302 (2), 91 (100), HRMS–EI (*m*/*z*): $[M - C_2H_5O]^+$ calcd for $C_{17}H_{20}NO_4$, 302.1392; found, 302.1390.

Ethyl (*E*)-4-(2-((benzyloxy)imino)-2-cyanoacetyl)decanoate (5i): IR (neat, ZnSe) ν_{max} (cm^{-1}): 2930, 2857, 1733, 1698, 1455, 1035; ^{1}H NMR ($CDCl_3$, 500 MHz) δ 7.43–7.38 (m, 5H), 5.50 (s, 2H), 4.12–4.06 (m, 2H), 3.37–3.32 (m, 1H), 2.26–2.14 (m, 2H), 2.01–1.94 (m, 1H), 1.85–1.80 (m, 1H), 1.66–1.60 (m, 1H), 1.44–1.33 (m, 1H), 1.28–1.19 (m, 11H), 0.89–0.86 (t, *J* = 6.5 Hz, 3H); ^{13}C NMR ($CDCl_3$, 125 MHz) δ 195.4, 172.7, 134.4, 132.4, 129.2, 128.9, 128.8, 107.4, 80.6, 60.4, 45.4, 31.9 31.6, 31.5, 29.1, 27.0, 26.1, 22.5, 14.2, 14.1; EIMS *m*/*z* (relative intensity): 341 (2), 200 (6), 131 (8), 91 (100); HRMS–EI (*m*/*z*): $[M - C_2H_5O]^+$ calcd for $C_{20}H_{26}N_2O_3$, 341.1865; found, 341.1867.

Ethyl (*E*)-4-(2-((benzyloxy)imino)-2-cyanoacetyl)-7-((*tert*-butyldimethylsilyl)oxy)heptanoate (5j): IR (neat, ZnSe) ν_{max} (cm^{-1}): 2929, 2857, 1732, 1698, 1255; ^{1}H NMR ($CDCl_3$, 500 MHz) δ 7.34 (m, 5H), 5.47 (s, 2H), 4.12–4.05 (m, 2H), 3.53–3.48 (m, 2H), 3.39–3.36 (m, 1H), 2.28–2.18 (m, 2H), 2.06–1.93 (m, 1H), 1.85–1.78 (m, 1H), 1.72–1.61 (m, 1H), 1.59–1.50 (m, 1H), 1.41–1.38 (m, 2H), 1.26–1.21 (t, 3H), 0.88 (s, 9H), 0.02 (s, 6H); ^{13}C NMR ($CDCl_3$, 125 MHz) δ 195.2, 172.6, 134.3, 132.4, 129.2, 129.0, 128.8, 107.3, 80.7, 62.5, 60.5, 41.1, 31.5, 30.1, 28.0, 26.2, 25.9, 18.3, 14.2, −5.2; EIMS *m*/*z* (relative intensity): 417 (13), 215 (4), 131 (5), 91 (100); HRMS–EI (*m*/*z*): $[M - C_4H_9]^+$ calcd for $C_{21}H_{29}N_2O_5Si$, 417.1846; found, 417.1853.

Ethyl (*E*)-4-(2-((benzyloxy)imino)-2-cyanoacetyl)-12-chlorododecanoate (5k): IR (neat, ZnSe) ν_{max} (cm^{-1}): 2932, 2857, 1731, 1698, 1035; ^{1}H NMR ($CDCl_3$, 500 MHz) δ 7.40 (m, 5H), 5.48 (s, 2H), 4.12–4.07 (m, 2H), 3.55–3.53 (t, *J* = 6.5 Hz, 2H) 3.36–3.33 (m, 1H), 2.29–2.18 (m, 2H), 2.00–1.92 (m, 1H), 1.85–1.74 (m, 3H), 1.67–1.62 (m, 1H), 1.42–1.38 (m, 3H), 1.25–1.12 (m, 12H); ^{13}C NMR ($CDCl_3$, 125 MHz) δ 195.4, 172.7, 134.3, 132.4, 129.2, 129.0, 128.8, 107.3, 80.6, 60.4, 45.4, 45.1, 32.5, 31.8, 31.6, 29.3, 29.1, 28.7, 27.0, 26.7, 26.1, 14.2; EIMS *m*/*z* (relative intensity): 404 (1), 181 (16), 169 (14), 131 (23), 119 (17), 91 (100); HRMS–EI (*m*/*z*): $[M - C_2H_5O]^+$ calcd for $C_{22}H_{29}N_2O_3Cl$, 404.1867; found, 404.1858.

(*E*)-3-Cyclohexyl-2,6-dioxo-6-phenylhexanal *O*-benzyl oxime (5l): IR (neat, ZnSe) ν_{max} (cm^{-1}): 2926, 2852, 1682, 1449, 1208; ^{1}H NMR ($CDCl_3$, 400 MHz) δ 7.89–7.88 (m, 2H), 7.54–7.32 (m, 8H), 5.17 (s, 2H), 3.34–3.30 (m, 1H), 2.89–2.69 (m, 2H), 2.02–2.00 (m, 2H), 1.69–1.51 (m, 6H), 1.16–0.88 (m, 6H); ^{13}C NMR ($CDCl_3$, 100 MHz) 202.3, 199.5, 148.6, 136.7, 136.1, 132.9, 128.7, 128.5, 128.5, 128.4, 128.0, 77.8, 51.1, 40.2, 36.1, 31.4, 29.9, 26.3, 22.6; EIMS *m*/*z* (relative intensity): 300 (6), 284 (9), 257 (5), 91 (100); HRMS–EI (*m*/*z*): $[M - OCH_2Ph]^+$ calcd for $C_{18}H_{22}NO_2$, 284.1651; found, 284.1645.

Supporting Information

Supporting Information File 1

Copies of NMR spectra.
[https://www.beilstein-journals.org/bjoc/content/supplementary/1860-5397-15-176-S1.pdf]

Acknowledgements

This work was supported by a Grant-in-Aid for Scientific Research (B) (no. 19H02722) from the JSPS and Scientific Research on Innovative Areas 2707 Middle molecular strategy (no. JP15H05850) from the MEXT. AJ thanks the Région Aquitaine for a mobility grant. The French Agence Nationale de la Recherche (ANR-11-BS07-010-01), University of Bordeaux, CNRS, and the Hubert Curien Sakura program are gratefully acknowledged for financial support.

ORCID® iDs

Shuhei Sumino - https://orcid.org/0000-0002-7109-8995
Takahide Fukuyama - https://orcid.org/0000-0002-3098-2987
Frédéric Robert - https://orcid.org/0000-0003-2469-2067
Yannick Landais - https://orcid.org/0000-0001-6848-6703

References

1. Bienaymé, H.; Hulme, C.; Oddon, G.; Schmitt, P. *Chem. – Eur. J.* **2000,** *6,* 3321–3329. doi:10.1002/1521-3765(20000915)6:18<3321::aid-chem3321>3.0.co;2-a
2. Tojino, M.; Ryu, I. Free-Radical-Mediated Multicomponent Coupling Reactions. In *Multicomponent Reactions,* 1st ed.; Zhu, J.; Bienayme, H., Eds.; Wiley-VC: Weinheim, 2005; pp 169 ff. doi:10.1002/3527605118.ch6
3. Müller, T. J. J., Ed. *Science of Synthesis: Multicomponent Reactions 1 and 2;* Georg Thieme Verlag KG: Stuttgart.
4. Liautard, V.; Landais, Y. Free-Radical Multicomponent Processes. In *Multicomponent Reactions,* 2nd ed.; Zhu, J.; Wang, Q.; Wang, M. X., Eds.; Wiley-VCH: Weinheim. doi:10.1002/9783527678174.ch14
5. Fusano, A.; Ryu, I. In *Science of Synthesis: Multicomponent Reactions;* Müller, T. J. J., Ed.; Georg Thieme Verlag KG: Stuttgart, 2014; Vol. 2, pp 409 ff.
6. Ryu, I.; Sonoda, N.; Curran, D. P. *Chem. Rev.* **1996,** *96,* 177–194. doi:10.1021/cr9400626
7. Malacria, M. *Chem. Rev.* **1996,** *96,* 289–306. doi:10.1021/cr9500186
8. Godineau, E.; Landais, Y. *Chem. – Eur. J.* **2009,** *15,* 3044–3055. doi:10.1002/chem.200802415
9. Sumino, S.; Ui, T.; Hamada, Y.; Fukuyama, T.; Ryu, I. *Org. Lett.* **2015,** *17,* 4952–4955. doi:10.1021/acs.orglett.5b02302
10. Fukuyama, T.; Nakashima, N.; Okada, T.; Ryu, I. *J. Am. Chem. Soc.* **2013,** *135,* 1006–1008. doi:10.1021/ja312654q
11. Kippo, T.; Hamaoka, K.; Ryu, I. *J. Am. Chem. Soc.* **2013,** *135,* 632–635. doi:10.1021/ja311821h
12. Kawamoto, T.; Fukuyama, T.; Ryu, I. *J. Am. Chem. Soc.* **2012,** *134,* 875–877. doi:10.1021/ja210585n
13. Sumino, S.; Fusano, A.; Fukuyama, T.; Ryu, I. *Acc. Chem. Res.* **2014,** *47,* 1563–1574. doi:10.1021/ar500035q
14. Zhang, B.; Studer, A. *Chem. Soc. Rev.* **2015,** *44,* 3505–3521. doi:10.1039/c5cs00083a
15. Lei, J.; Li, D.; Zhu, Q. *Top. Heterocycl. Chem.* **2018,** *54,* 285–320. doi:10.1007/7081_2017_9
16. Kim, S.; Lee, I. Y.; Yoon, J.-Y.; Oh, D. H. *J. Am. Chem. Soc.* **1996,** *118,* 5138–5139. doi:10.1021/ja9600993
17. Kim, S.; Kim, S. *Bull. Chem. Soc. Jpn.* **2007,** *80,* 809–822. doi:10.1246/bcsj.80.809
18. Bertrand, F.; Le Guyader, F.; Liguori, L.; Ouvry, G.; Quiclet-Sire, B.; Seguin, S.; Zard, S. Z. *C. R. Acad. Sci., Ser. IIc: Chim.* **2001,** *4,* 547–555. doi:10.1016/s1387-1609(01)01270-1
19. Ovadia, B.; Robert, F.; Landais, Y. *Chimia* **2016,** *70,* 34–42. doi:10.2533/chimia.2016.34
20. Kim, S.; Song, H.-J.; Choi, T.-L.; Yoon, J.-Y. *Angew. Chem., Int. Ed.* **2001,** *40,* 2524–2526. doi:10.1002/1521-3773(20010702)40:13<2524::aid-anie2524>3.3.co;2-w
21. Godineau, E.; Landais, Y. *J. Am. Chem. Soc.* **2007,** *129,* 12662–12663. doi:10.1021/ja075755l
22. Landais, Y.; Robert, F.; Godineau, E.; Huet, L.; Likhite, N. *Tetrahedron* **2013,** *69,* 10073–10080. doi:10.1016/j.tet.2013.09.051
23. Ryu, I.; Kuriyama, H.; Minakata, S.; Komatsu, M.; Yoon, J.-Y.; Kim, S. *J. Am. Chem. Soc.* **1999,** *121,* 12190–12191. doi:10.1021/ja992125d
24. Ryu, I.; Kuriyama, H.; Miyazato, H.; Minakata, S.; Komatsu, M.; Yoon, J.-Y.; Kim, S. *Bull. Chem. Soc. Jpn.* **2004,** *77,* 1407–1408. doi:10.1246/bcsj.77.1407
25. Kim, S.; Lim, K.-C.; Kim, S.; Ryu, I. *Adv. Synth. Catal.* **2007,** *349,* 527–530. doi:10.1002/adsc.200600500
26. Ryu, I.; Yamazaki, H.; Ogawa, A.; Kambe, N.; Sonoda, N. *J. Am. Chem. Soc.* **1993,** *115,* 1187–1189. doi:10.1021/ja00056a076
27. Miura, K.; Tojino, M.; Fujisawa, N.; Hosomi, A.; Ryu, I. *Angew. Chem., Int. Ed.* **2004,** *43,* 2423–2425. doi:10.1002/anie.200453702
28. Uenoyama, Y.; Fukuyama, T.; Ryu, I. *Synlett* **2006,** 2342–2344. doi:10.1055/s-2006-949643
29. Quiclet-Sire, B.; Zard, S. Z. *Top. Curr. Chem.* **2006,** *264,* 201–236. doi:10.1007/128_029
30. Bosiak, M. J.; Pakulski, M. M. *Synthesis* **2011,** 316–324. doi:10.1055/s-0030-1258355
31. Stensbøl, T. B.; Uhlmann, P.; Morel, S.; Eriksen, B. L.; Felding, J.; Kromann, H.; Hermit, M. B.; Greenwood, J. R.; Braüner-Osborne, H.; Madsen, U.; Junager, F.; Krogsgaard-Larsen, P.; Begtrup, M.; Vedsø, P. *J. Med. Chem.* **2002,** *45,* 19–31. doi:10.1021/jm010303j
32. Renaud, P.; Ollivier, C.; Panchaud, P. *Angew. Chem., Int. Ed.* **2002,** *41,* 3460–3462. doi:10.1002/1521-3773(20020916)41:18<3460::aid-anie3460>3.0.co;2-6
33. Panchaud, P.; Chabaud, L.; Landais, Y.; Ollivier, C.; Renaud, P.; Zigmantas, S. *Chem. – Eur. J.* **2004,** *10,* 3606–3614. doi:10.1002/chem.200400027
34. Beniazza, R.; Liautard, V.; Poittevin, C.; Ovadia, B.; Mohammed, S.; Robert, F.; Landais, Y. *Chem. – Eur. J.* **2017,** *23,* 2439–2447. doi:10.1002/chem.201605043
35. Chatgilialoglu, C.; Crich, D.; Komatsu, M.; Ryu, I. *Chem. Rev.* **1999,** *99,* 1991–2070. doi:10.1021/cr9601425
36. Liautard, V.; Robert, F.; Landais, Y. *Org. Lett.* **2011,** *13,* 2658–2661. doi:10.1021/ol2007633
37. Tasker, S. Z.; Gutierrez, A. C.; Jamison, T. F. *Angew. Chem., Int. Ed.* **2014,** *53,* 1858–1861. doi:10.1002/anie.201308391

License and Terms